

**Synthetic protein scaffold-mediated
manipulation of LOX-1 scavenger receptor
in cell function, vascular physiology and
disease**

Gary Andrew Cuthbert

Submitted in accordance with the requirements for the
degree of Doctor of Medicine

The University of Leeds
Faculty of Medicine and Health

2020

The candidate confirms that the work submitted is his own, except where work which has formed part of jointly-authored publications has been included. The candidate confirms that the appropriate credit has been given within the thesis where reference has been made to the work of others.

This copy has been supplied on the understanding that it is copyright material and that no quotation from the thesis may be published without proper acknowledgement.

© 2020 The University of Leeds and Gary Andrew Cuthbert.

The right of Gary Andrew Cuthbert to be identified as Author of this work has been asserted by him in accordance with the Copyright, Designs and Patents Act 1988.

Acknowledgements

This work would not have been possible without the help and support I received from a few very talented and hard-working individuals. I will always be grateful for Professor Homer-Vanniasinkam “rescuing me from the surgical scrap heap”, rebuilding my confidence and giving me the mentorship I needed to get back on track. In giving me this opportunity, Prof has introduced me to so many incredible scientists and clinicians. My co-supervisor, Dr. Vas Ponnambalam has had the strenuous task of guiding me through the world of biological science and I will always be grateful for his approachability, friendliness and good sense of humour. Dr. Nadira Yuldasheva contributed enormously to this project. Nadira trained me in all the elements of animal work from the basics of husbandry to surgery and histopathology. Owing to the expertise required to perform femoral artery wire injury in mice, I thank Nadira for performing this procedure on all mice within the study while I observed and assisted. I must also thank Anna Skromna and Natalia Makava for all their guidance and support during my time in the animal house and the histopathology lab. It has been a great pleasure to work with fellow lab members, past and present, who have passed on their knowledge and have been there to offer sound practical advice, particularly when experiments were not going to plan. Lab members include Jon DeSiquiera, Faheem Shaik, Joanna Mitchell, Will Critchley, Barney Roper, Areej Alzahrani and Hala Ahmed.

This work was undertaken on a part-time basis and I must acknowledge the support I received from the vascular surgery department at Leeds General Infirmary, where I spent the rest of my time working on the registrar rota. It really was a “baptism-by- fire” in to the world of vascular and trauma surgery, however the friendliness and approachability of everyone in the department allowed me to settle in quickly and start developing my knowledge and skills. Special thanks to Deborah Armstrong and Jodi Lancaster for cheering me up on tough days and keeping my in-tray overflowing with a steady stream of paperwork!

Without the support from my wife, Upasana, it would have been impossible for me to achieve any of this and I thank her for continuing to put up with me.

Abstract

Binding and internalization of oxidized low-density lipoprotein (oxLDL) by immune cells within the arterial sub-intimal layer is a key step in the initiation and progression of atherosclerosis. Scavenger receptors (SRs) are a “super-family” of cell surface receptors expressed by immune cells which promote the removal of harmful non-self or altered-self targets, including oxidatively modified ligands such as oxLDL. Lectin-like oxidized LDL receptor-1 (LOX-1) is a member of the SR-E family of scavenger receptors. LOX-1 – oxLDL binding has been shown to exert significant pro-atherogenic effects. In this study, we used *in vitro* and *in vivo* models of atherosclerosis to explore the effectiveness of LOX-1 targeting in the inhibition of oxLDL binding and the amelioration of atherosclerosis and neointimal hyperplasia. LOX-1 was targeted using novel non-antibody artificial binding proteins, known as Affimers. Immunofluorescence studies using a tetracycline-inducible cell line expressing LOX-1 demonstrate the binding efficiency of fluorescent-labelled LOX-1 Affimers to LOX-1 in live cells. In same cell line, we co-incubated fluorescent-labelled oxLDL with increasing concentrations of LOX-1 Affimers. The findings show that LOX-1 Affimers inhibit LOX-1 – oxLDL binding. ELISA studies were carried out to identify LOX-1 affimers with comparable affinity for both human and murine LOX-1. The most cross-reactive LOX-1 Affimer was taken forward in to a transgenic mouse model of diet-induced atherosclerosis. This model used *APO-E* null and *APO-E/LOX-1* null mice to compare the effects of *LOX-1* knockout with LOX-1 targeting using LOX-1 affimers. *LOX-1* knockout resulted in a reduction in aortic and peripheral arterial atherosclerosis, and neointimal hyperplasia. LOX-1 targeting with affimers produced promising results. Treatment with LOX-1 affimers reduced atherosclerosis and NIH, but to a lesser extent compared with *LOX-1* knockout. Treatment with LOX-1 affimer exerted additional metabolic benefits including protective effects against diet-induced obesity and insulin resistance. The results from these studies suggest that LOX-1 is an attractive target in the development of novel therapeutics in atherosclerosis. Targeted LOX-1 inhibition potentially offers protective benefits in associated metabolic disorders such as obesity and insulin resistance.

Table of contents

Acknowledgements	iii
Abstract	iv
Table of contents	v
List of tables	ix
List of figures	x
Abbreviations	xii
CHAPTER 1	1
INTRODUCTION	1
1.1 Atherosclerosis and cardiovascular disease	1
1.1.1 The national burden of cardiovascular disease	1
1.1.2 The pathophysiology of atherosclerosis	3
1.1.2.1 Lesion initiation and progression	3
1.1.2.2 The role of lipoprotein particles in atherosclerosis	5
1.1.2.3 Vascular oxidative stress.....	8
1.1.2.4 The inflammatory component of atherosclerosis.....	10
1.1.2.5. Apoptosis, necroptosis and defective efferocytosis.....	11
1.1.3 Neointimal hyperplasia	12
1.1.3.1 Clinical perspective of NIH	12
1.1.3.2 Pathology of NIH	12
1.2 Scavenger Receptors	13
1.2.1 Background	13
1.2.2 Targeting SRs in cardiovascular disease	16
1.2.3 SRs as Biomarkers.....	16
1.2.4 Therapeutic strategies in atherosclerosis	18
1.2.4.1 Clinically approved treatments	18
1.2.4.2 Herbal and traditional medicine therapies	20
1.2.4.3 Novel therapeutics.....	21
1.3 Structure and function of the LOX-1 SR	25
1.3.1 Genetics and expression of LOX-1.....	25
1.3.2 Structure of LOX-1.....	25
1.3.3 LOX-1-mediated signal transduction	26
1.4 LOX-1 in the pathology of cardiovascular disease	28
1.4.1 Endothelial dysfunction.....	28

1.4.2 Smooth muscle cell migration and proliferation	29
1.4.3 Macrophage foam cell formation	29
1.4.4 Platelet activation and thrombosis	30
1.4.5 Hypertension	30
1.5 LOX-1 as a biomarker in cardiovascular disease	31
1.6 LOX-1 in cardiovascular disease therapeutics	32
1.6.1 Clinically approved treatments	32
1.6.2 Herbal and traditional medicine therapies	33
1.6.3 Novel therapeutics	33
1.7 LOX-1 linkage to other disease states	35
1.7.1 Diabetes Mellitus	35
1.7.2 Neoplasia	35
1.7.3 Sepsis and inflammation	36
1.8 Non-antibody artificial binding proteins	37
1.8.1 Introduction	37
1.8.2 Non-antibody artificial binding proteins: general principles	39
1.8.2.1 Scaffold design and consensus sequence	39
1.8.2.2 Phage display	40
1.8.3 Affimers	41
1.9 Hypothesis, aims and objectives	42
CHAPTER 2	44
MATERIALS AND METHODS	44
2.1 Materials	44
2.1.1 Chemical reagents and antibodies	44
2.1.2 Antibodies	44
2.1.3 Cell lines	44
2.1.4 Transgenic mice	45
2.1.5 Surgical equipment	45
2.2 Experimental methods	46
2.2.1 Protein chemistry and analysis	46
2.2.1.1 Preparation of competent <i>E.coli</i> cells	46
2.2.1.2 Transformation into competent <i>E.coli</i> cells	46
2.2.1.3 Small scale DNA purification	46
2.2.1.4 Affimer expression in competent <i>E.coli</i> cells	47
2.2.1.4.1 Inducing Affimer expression with isopropyl β -D-1-thiogalactopyranoside (IPTG)	47
2.2.1.4.2 Affimer purification	47

2.2.1.5 Biotinylation of Affimers	48
2.2.1.6 Labelling Affimers with Alexafluor-488 maleimide	48
2.2.1.7 Preparation of oxLDL.....	49
2.2.1.7.1 Preparation of LDL	49
2.2.1.7.2 Oxidation and analysis of LDL and oxLDL	50
2.2.1.8 DiI-labeling of oxLDL	51
2.2.2 Protein analysis	51
2.2.2.1 Preparation of cell lysates	51
2.2.2.2 BCA assay.....	51
2.2.2.3 SDS-PAGE electrophoresis.....	52
2.2.2.4 Western blotting.....	53
2.2.2.5 Cross-reactivity ELISA using Affimers.....	54
2.2.3 Cellular studies	55
2.2.3.1 Cell culture.....	55
2.2.3.2 Immunofluorescence analysis	56
2.2.3.3 Cell immunofluorescence using Affimers	56
2.2.4 Animal studies	57
2.2.4.1 Animal husbandry.....	57
2.2.4.2 DNA extraction for genotyping.....	57
2.2.4.3 Genotype analysis using polymerase chain reaction (PCR)	58
2.2.5 Animal experimental procedures	58
2.2.5.1 Glucose tolerance test.....	58
2.2.5.2 Insulin tolerance test.....	59
2.2.5.3 Induction and maintenance of anaesthesia	59
2.2.5.4 Femoral artery wire injury	59
2.2.5.5 Osmotic pump implantation	60
2.2.5.6 Tissue harvesting	62
2.2.5.7 Vascular harvest.....	62
2.2.6 Histological preparation	63
2.2.6.1 Processing.....	63
2.2.6.2 Embedding	63
2.2.6.3 Microtomy	64
2.2.7 Histological staining.....	67
2.2.7.1 Oil red O staining.....	67
2.2.7.2 Elastin staining with Miller and counter staining with Van Gieson.....	67
2.2.7.3 Haematoxylin and Eosin staining	68
2.3 Histological analysis	70
2.4 Statistical analysis	70
2.5 Home Office License and ethical approval for animal studies	70

CHAPTER 3	72
CELLULAR STUDIES ON LOX-1 FUNCTION	72
3.1 Introduction.....	72
3.2 Results.....	73
3.2.1 Expression, purification of LOX-1-specific Affimers.....	73
3.2.2 Labelling of LOX-1 Affimer	74
3.2.3 Affinity and cross reactivity studies using biotinylated LOX-1 Affimers	78
3.2.4 LOX-1 Affimers bind to LOX-1 <i>in vitro</i>	81
3.2.4.1 Validation of tetracycline-inducible LOX-1 expression in HEK-293T cells.....	81
3.2.4.2 Immunofluorescence studies using alexafluor-488 tagged LOX-1 Affimers.....	83
3.2.5 LOX-1 Affimers inhibit oxLDL uptake <i>in vitro</i>	85
3.2.5.1 Extraction and oxidation of low-density lipoprotein.....	85
3.2.5.2 Inhibition of oxLDL uptake in LOX-1 expressing HEK-293T cells	87
3.3 Discussion	89
CHAPTER 4	93
LOX-1 GENOTYPE INFLUENCE ON DISEASE STATES	93
4.1 Introduction.....	93
4.2 Study design and mouse genotyping.....	95
4.3 Results.....	99
4.3.1 Influence of LOX-1 on body mass	99
4.3.2 Effects of LOX-1 on insulin resistance.....	101
4.3.3 Effects of LOX-1 on hepatic steatosis	105
4.3.4 LOX-1 influence on atherogenesis	107
4.3.5 The influence of LOX-1 on neointimal hyperplasia in the femoral artery...	112
4.3.6 LOX-1 affimer biodistribution studies.....	113
4.4 Discussion	116
CHAPTER 5	124
OVERVIEW AND CONCLUDING REMARKS.....	124
5.1 Discussion	124
5.1.1 LOX-1 and disease states	124
5.1.2 Affimer-based LOX-1 targeting.....	125
5.2 General limitations	126
5.3 Future Perspectives	126
References	128

Appendix A: Publications and conference proceedings	169
Appendix B: Supplementary figures	170

List of tables

Table 1.1 Structure and function of SRs	14
Table 1.2. Synthetic or artificial protein technologies	38
Table 2.1. Primer sequences for DNA genotyping	58

List of figures

Figure 1.1. Prevalence of the three main clinical subtypes of cardiovascular disease	2
Figure 1.2. Formation of the atherosclerotic plaque	4
Figure 1.3. Structure of the low-density lipoprotein (LDL) particle	7
Figure 1.4. Lipoprotein particle subdivision into classes	8
Figure 1.5. Structure of human (A) and mouse (B) LOX-1.....	27
Figure 1.6. LOX-1 binding to LDL.....	28
Figure 1.7. The basic concepts of phage display	41
Figure 1.8. Basic structure of the affimer protein	43
Figure 2.1. Surgical instruments for animal and histological work	45
Figure 2.2. Preparation and oxidation of LDL.....	50
Figure 2.3. Anatomy of femoral artery wire injury.....	61
Figure 2.4. Orientation of specimen in embedding paraffin.....	65
Figure 2.5. Microtomy of carotid and femoral arteries: anatomical landmarks ..	66
Figure. 2.6. Measuring atherosclerotic plaque area	71
Figure 3.1. Expression and purification of LOX-1-specific Affimer H1	75
Figure 3.2. Fluorescent labelling of LOX-1-specific H1 Affimer.....	76
Figure 3.3. Biotinylation of LOX-1-specific H1 Affimer	77
Figure 3.4. Cross-reactivity of LOX-1-specific Affimers for human and mouse soluble LOX-1 proteins.....	79
Figure 3.5. Relative affinity of LOX-1-specific Affimers for human and mouse soluble LOX-1.....	80
Figure 3.6. LOX-1-FLAG expression in tetracycline-inducible HEK293T cell line	82

Figure 3.7. Fluorescent labelled LOX-1-specific Affimer binding to LOX-1-expressing cells	84
Figure 3.8. Purification and oxidation of low-density lipoprotein particles	86
Figure 3.9. LOX-1-specific H1 Affimer inhibits oxLDL uptake in LOX-1-expressing HEK293T cells	88
Figure 3.10. Quantification of LOX-1-specific H1 Affimer inhibition of cellular oxLDL uptake	89
Figure 4.1. Schematic of mouse studies	97
Figure 4.2. Genotyping transgenic mouse lines	98
Figure 4.3 Weight of transgenic mice upon Western diet treatment and LOX-1-specific Affimer treatment.....	100
Figure 4.4. Fasting glucose effects in transgenic mice after Western diet	102
Figure 4.5. Glucose tolerance test (GTT) of transgenic mice after Western diet	103
Figure 4.6. Insulin tolerance test (ITT) of transgenic mice after Western diet.	104
Figure 4.7. Effect of LOX-1 on hepatic fat deposition.....	106
Figure 4.8. LOX-1 allele influences atherosclerotic plaque incidence in APO-E null mice	109
Figure 4.9. LOX-1-specific Affimer effect on carotid atherosclerosis	110
Figure 4.10 LOX-1-specific Affimer effects on femoral atherosclerosis	111
Figure 4.11 LOX-1 knockout reduces neointimal hyperplasia in APO-E null mice	114
Figure 4.12. Detection of biotinylated LOX-1 affimers in mouse serum	115
Figure 4.13 Schematic of in vivo role for LOX-1 in lipid metabolism and atherosclerosis	123

Abbreviations

5-LOX	5-lipoxygenase
12/15 LOX	12/15 lipoxygenase
AM	Amphiphilic macromolecules
APO-B100	Apolipoprotein-B100
APO-E	Apolipoprotein-E
APS	Ammonium persulfate
AT1R	Angiotensin 2 receptor type 1
Bcl-2	B-cell lymphoma -2
BSA	Bovine serum albumin
BHT	Butylated hydroxytolunene
CAD	Coronary artery disease
CLP	Caecal ligation and puncture
CHOP	CCAAT enhancer- binding protein homologous protein
CVD	Cardiovascular disease
Cys	Cysteine
DAPI	4',6-diamidino-2-phenylindole
DARPs	Ankyrin repeat proteins
Dil	1,1 dioctadecyl-3,3,3',3' tetramethylindocarbocyanine perchlorate
DMEM	Dulbecco's Modified Eagle Medium
eNOS	Endothelial nitric oxide synthase

EDTA	Ethylene-diaminetetra acetic acid
ER	Endoplasmic reticulum
ERK1/2	Extracellular signal-regulated kinases ½
GTT	Glucose tolerance test
GWAS	Genome-wide association studies
HBS	Hepes buffered saline
HCAEC	Human coronary artery endothelial cells
HEK-293T	Human embryonic kidney -293T cells
HRP	Horseradish peroxidase
ICAM-1	Inter-cellular adhesion molecule 1
IDL	Intermediate-density lipoprotein
IL	Interleukin
IPTG	Isopropyl β -D-1-thiogalactopyranoside
ITT	Insulin tolerance test
LDL	Low-density lipoprotein
LDLR	Low-density lipoprotein receptor
LOX-1	Lectin-like oxidized ¹⁶ LDL receptor 1
LP _(a)	Lipoprotein-a
MAPK	p38 mitogen-activated protein kinase C
MCP-1	Monocyte chemoattractant protein-1
MMP	Matrix-metalloproteinases
MPO	Myeloperoxidase
NASH	Non-alcoholic steatohepatitis

NFκB	nuclear factor kappa-light-chain-enhancer of activated B cells
NIH	Neointimal hyperplasia
Ni-NTA	Nickel-nitrilotriacetic acid
NO	Nitric oxide
NOX	NADPH oxidase
OLR-1	Oxidized LDL receptor 1
OxLDL	Oxidized LDL
PBS	Phosphate buffered saline
PCOS	Polycystic ovarian syndrome
PCR	Polymerase chain reaction
PCSK9	Proprotein convertase subtilisin/kexin type 9
PEG	Polyethylene glycol
PFA	Paraformaldehyde
PPAR-γ	Peroxisome proliferator-activated receptor-γ
RIPA	Radio-immunoprecipitation assay
RAGE	Receptor for advanced glycation end-products
RAS	Renin-angiotensin system
ROS	Reactive oxygen species
SDS	Sodium dodecyl sulfate
scFv	Single-chain variable fragment
SNP	Single-nucleotide polymorphism
SR	Scavenger receptor
T2DM	Type 2 diabetes mellitus

TBS	Tris-buffered saline
TCEP	Tris (2-carboxyethyl)phosphine
TEMED	Tetramethylethylenediamine
Th-1	T-helper 1 cell
TMB	3,3',5,5'-tetramethylbenzidine
VCAM	Vascular cell adhesion molecule 1
VLDL	Very-low-density lipoprotein
VSMC	Vascular smooth muscle cell
WD	Western diet
XO	Xanthine oxidase
Yeast-SUMO	Yeast-small ubiquitin-like modifier protein

CHAPTER 1

INTRODUCTION

1.1 Atherosclerosis and cardiovascular disease

1.1.1 The national burden of cardiovascular disease

Cardiovascular disease (CVD) is a widely-accepted umbrella term which includes coronary artery, cerebrovascular and peripheral artery disease. An international multicentre registry study of 67888 patients from 44 countries found that coronary artery disease (CAD) was the most prevalent of the three major disease states (Figure 1.1) (Bhatt *et al.*, 2006). CVD is the leading cause of death worldwide, accounting for 30% of all deaths ('Global, regional, and national age-sex specific all-cause and cause-specific mortality for 240 causes of death, 1990-2013: a systematic analysis for the Global Burden of Disease Study 2013,' 2015). In the United Kingdom, CVD accounts for a quarter of all deaths and costs the health service 9 billion pounds annually (Cardiovascular disease statistics 2017., 2017). It is the leading cause of death in women in the UK (28%) and the second most common cause of death in men (29%), behind cancer (32%). In England, prescriptions for the treatment of CVD increased six-fold between 1981 and 2013 (Bhatnagar *et al.*, 2015). The total number of operations and invasive procedures performed to treat CVD has risen steadily over the same time period (Bhatnagar *et al.*, 2015). Large UK population studies have demonstrated that mortality rates from coronary artery and cerebrovascular disease have decreased significantly over the past 4 decades (Smolina *et al.*, 2012; Lee, Shafe and Cowie, 2011). Improvements in mortality have been primarily attributed to risk factor modification, particularly smoking cessation and dietary changes (Unal, Critchley Julia and Capewell, 2004).

Atherosclerosis is by far the leading pathophysiological process behind the development of CVD (Falk, 2006). Atherosclerosis is a systemic multifocal disease affecting medium and large sized arteries and is characterized macroscopically by the formation of plaque within the sub-intimal layer. Arterial

thrombosis associated with atherosclerotic plaque manifests clinically as ischaemic heart disease, stroke and peripheral arterial disease.

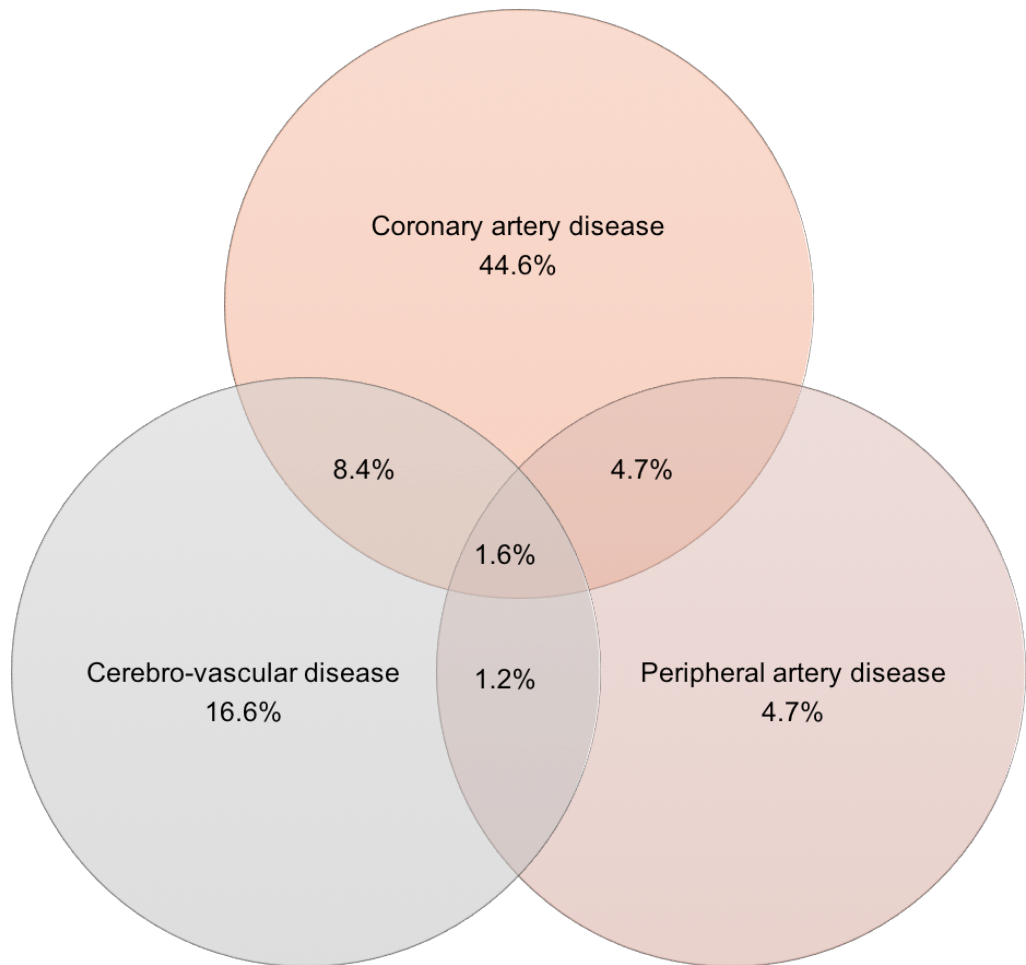


Figure 1.1. Prevalence of the three main clinical subtypes of cardiovascular disease. Coronary artery disease is the most prevalent, followed by cerebrovascular disease and peripheral artery disease. Figure adapted from Bhatt *et al.* (Bhatt *et al.*, 2006).

1.1.2 The pathophysiology of atherosclerosis

1.1.2.1 Lesion initiation and progression

Atherosclerosis is a complex, progressive, chronic inflammatory process characterized by the accumulation of lipid and fibrous elements within the arterial wall, manifesting macroscopically as atherosclerotic plaque (Figure 1.2). Abnormally high serum low-density lipoprotein (LDL) concentrations leads to the infiltration of LDL into the subendothelial space, where it becomes chemically modified by oxidation due to free radicals produced by cellular respiration. The process of atherosclerosis is widely understood to be initiated by the abnormal accumulation of this oxidized low-density lipoprotein (oxLDL) within the sub-endothelial matrix (Lusis, 2000). An inflammatory cascade within the endothelium simultaneously leads to the production of adhesion molecules and chemotactic factors. Monocytes attach to the endothelium via the adhesion molecules and penetrate to the subendothelial space, where they differentiate and mature into macrophages. The recruited macrophages bind and internalize oxLDL rapidly to form lipid-laden foam cells, promoting pro-atherosclerotic events i.e. atherogenesis (Gistera and Hansson, 2017). Vascular smooth muscle cells (VSMCs) within the blood vessel media layer are affected by growth factors being secreted by the endothelium in response to the accumulation of oxLDL (Katakami, 2018). VSMCs transform and migrate into the intima and begin to actively produce extracellular matrix leading to sclerosis and intimal thickening. VSMCs also take up oxLDL and form foam cells, contributing to the formation of the atherosclerotic plaque (Katakami, 2018).

In normal physiology, acute inflammation is followed by a resolution phase where tissue repair and restoration of homeostasis occurs (Nathan and Ding, 2010). In chronic inflammatory states where there is a persistent inflammatory stimulus, the resolution phase becomes defective due to the impaired synthesis and increased degradation of resolution mediators (Tabas and Lichtman, 2017). Atherosclerosis is such a chronic inflammatory process. Failure of the inflammatory process to resolve leads to an amplification cycle of ongoing inflammation and tissue injury, contributing to the clinical progression of plaque. The clinical consequences of atherosclerosis relate principally to acute thrombo-

occlusive events at the site of plaque disease. Plaques become most dangerous in this regard when they exhibit features which increase the likelihood of rupture; such as large areas of necrosis and thinning of the overlying fibro-collagenous cap (Virmani *et al.*, 2002). Plaque rupture exposes underlying thrombogenic material to circulating blood, leading to thrombus formation.

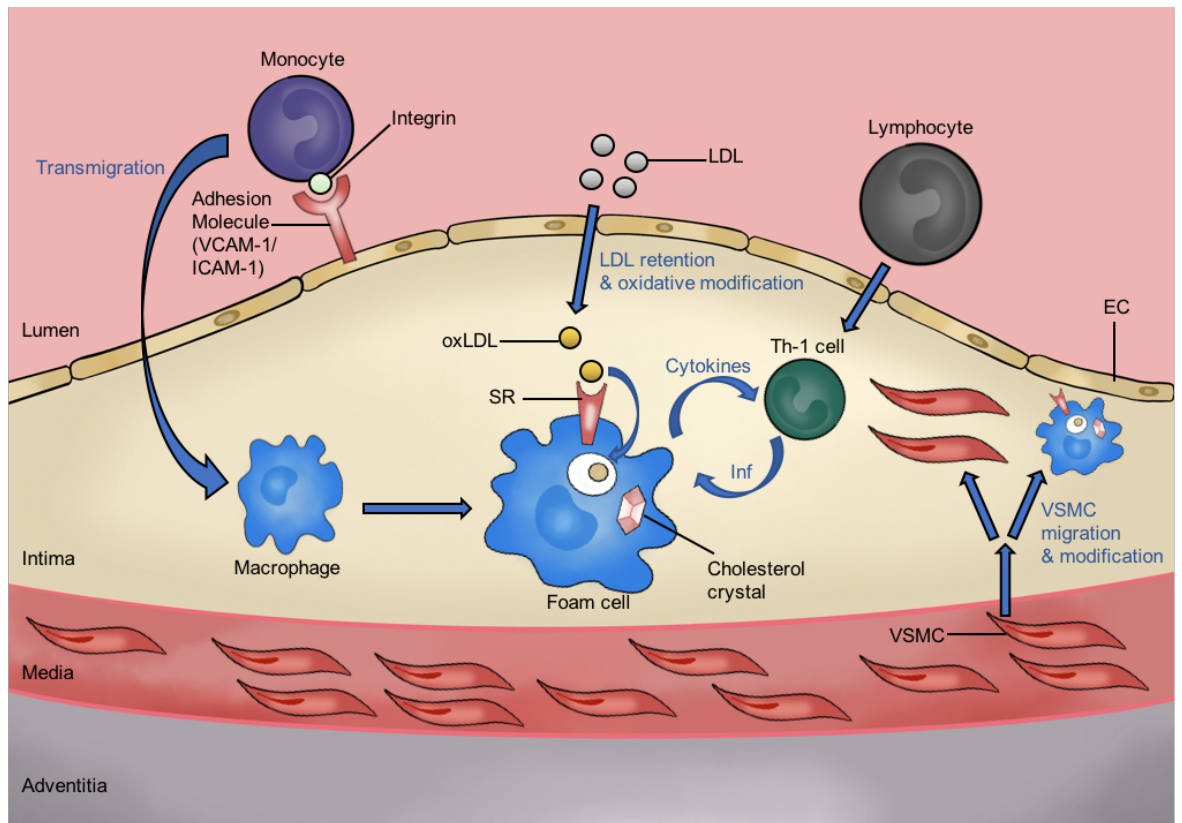


Figure 1.2. Formation of the atherosclerotic plaque. Within the blood vessel intima, LDL accumulation leads to a chronic inflammatory process leading to the transmigration of immune cells and the formation of foam cells. EC; endothelial cell. ICAM; intercellular adhesion molecule -1. Inf; interferon- gamma. LDL; low-density lipoprotein. oxLDL; oxidized low-density lipoprotein. SR; scavenger receptor. Th-1; T-helper 1 cell. VCAM; vascular cell adhesion molecule -1. VSMC; vascular smooth muscle cell.

1.1.2.2 The role of lipoprotein particles in atherosclerosis

Anitschkow first reported the relationship between cholesterol and atherogenesis in 1913 by demonstrating the development of atheroma in oil-fed rabbits (Anitschkow, 1913). Later, large human epidemiological studies have confirmed the association between raised serum cholesterol and LDL-cholesterol and the risk of cardiovascular events (Stamler, Wentworth and Neaton, 1986; Castelli *et al.*, 1986). Lipids such as cholesterol and triglycerides are essential components of the human diet, however they are insoluble in water and must be transported within the blood circulation bound to proteins; thus, the formation of lipoprotein particles. Lipoprotein particles are involved in the absorption and transport of dietary lipids from the small intestine to the liver, followed by peripheral tissues, and from the peripheral tissues back to the liver and intestine (reverse cholesterol transport). Lipoprotein particles are complex substances consisting of a central hydrophobic core of non-polar lipids, primarily cholesterol esters and triglycerides, which is surrounded by a hydrophilic membrane consisting of phospholipids, free cholesterol, and apolipoproteins (Figure 1.3). Lipoprotein particles can be subdivided into 7 classes based on their molecular weight, lipid composition and apolipoproteins (Figure 1.4). Of the seven classes of lipoprotein particles, LDL is widely considered to be the most pro-atherogenic owing to the following properties:

- LDL particles have a reduced affinity to the LDL receptor (LDLR) and is therefore retained in the circulation for longer.
- LDL particles enter the arterial wall more easily compared with larger lipoproteins.
- LDL particles contain apolipoprotein-B100 (APO-B100), which binds avidly to intra-arterial proteoglycans leading to trapping within the arterial wall.
- LDL particles are more susceptible to oxidative modification, with oxLDL being rapidly taken up by macrophages.

APO-B100 is the major structural component of very-low-density lipoprotein (VLDL), intermediate-density lipoprotein (IDL) and LDL. There is a single molecule of apo-B100 per VLDL, IDL or LDL particle. Ionic bonds between positively charged intra-arterial proteoglycans and negatively charged APO-B100 lead to the retention of LDL within the arterial wall. Transgenic mouse studies

have shown that single point mutations in APO-B100 impairs proteoglycan-LDL binding and reduces APO-B100 retention and atherosclerosis in the arterial wall, strengthening the hypothesis that the presence of APO-B100 and its interaction with proteoglycans is a key initiator in atherogenesis (Borén *et al.*, 1998; Skalen *et al.*, 2002). Retained LDL particles are susceptible to oxidative modification, forming oxLDL, due to structural changes in the APO-B100 molecule and lipid modification, brought about primarily by the interaction between LDL and proteoglycans.

Several oxidases and peroxidases are known to oxidize LDL both *in vitro* and *in vivo*. Known agents include myeloperoxidase (MPO), xanthine oxidase, nicotinamide adenine dinucleotide phosphate oxidase, inducible nitric oxide synthase and lipoxygenases such as 5-lipoxygenase (5-LOX) and 12/15 lipoxygenase (12/15-LOX) (Linton, Yancey and Davies, Jan 2019). Whilst the extent to which each agent is involved is not yet fully understood, we do know from transgenic mouse models and human studies that MPO and the lipoxygenases are pro-atherogenic and may be useful as biomarkers for cardiovascular disease states (Michowitz *et al.*, 2008; Brennan *et al.*, 2001; Dobrian *et al.*, 2011).

MPO and the lipoxygenases are the most closely linked to LDL oxidation. *In vitro* and *ex vivo* models have identified that the release of MPO is primarily from activated immune cells (primarily neutrophils) within the subintimal layer (Baldus *et al.*, 2001). The mechanisms behind the release of MPO from degranulating immune cells is not fully understood, however evidence suggests that reactive oxygen species (ROS) activity and the activation of Src and p38 mitogen activated protein kinase signaling pathways play important roles (Khan, Alsahli and Rahmani, 2018). 5-LOX and 12/15-LOX is expressed in vascular cells, such as endothelial cells and VSMCs, as well as in immune cells and adipose tissue (Dobrian *et al.*, 2011). The stimulus for the release of lipoxygenase is also not fully understood, however similar to MPO, ROS activity is thought to play a role (Mashima and Okuyama, 2015). Whilst native LDL does not interact with immune cells, oxLDL does. Following oxidative modification, oxLDL is recognized by tissue macrophages, leading to (a) oxLDL uptake and the formation of foam cells, and (b) a chronic inflammatory cascade which further perpetuates atherogenesis.

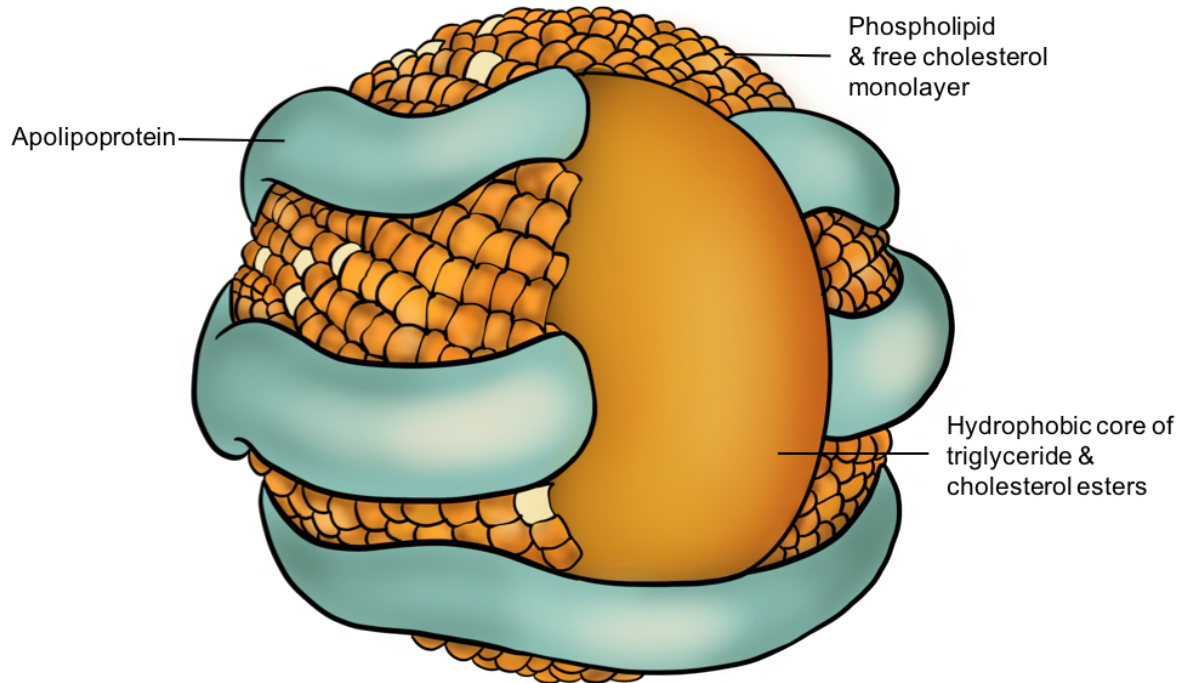


Figure 1.3. Structure of the low-density lipoprotein (LDL) particle. Lipoprotein particles consist primarily of a central hydrophobic core of non-polar lipids, largely cholesterol esters and triglycerides, which is surrounded by an amphipathic lipid monolayer consisting of phospholipids, free cholesterol, and apolipoproteins. Figure adapted from Feingold *et al.* (Feingold and Grunfeld, 2018).

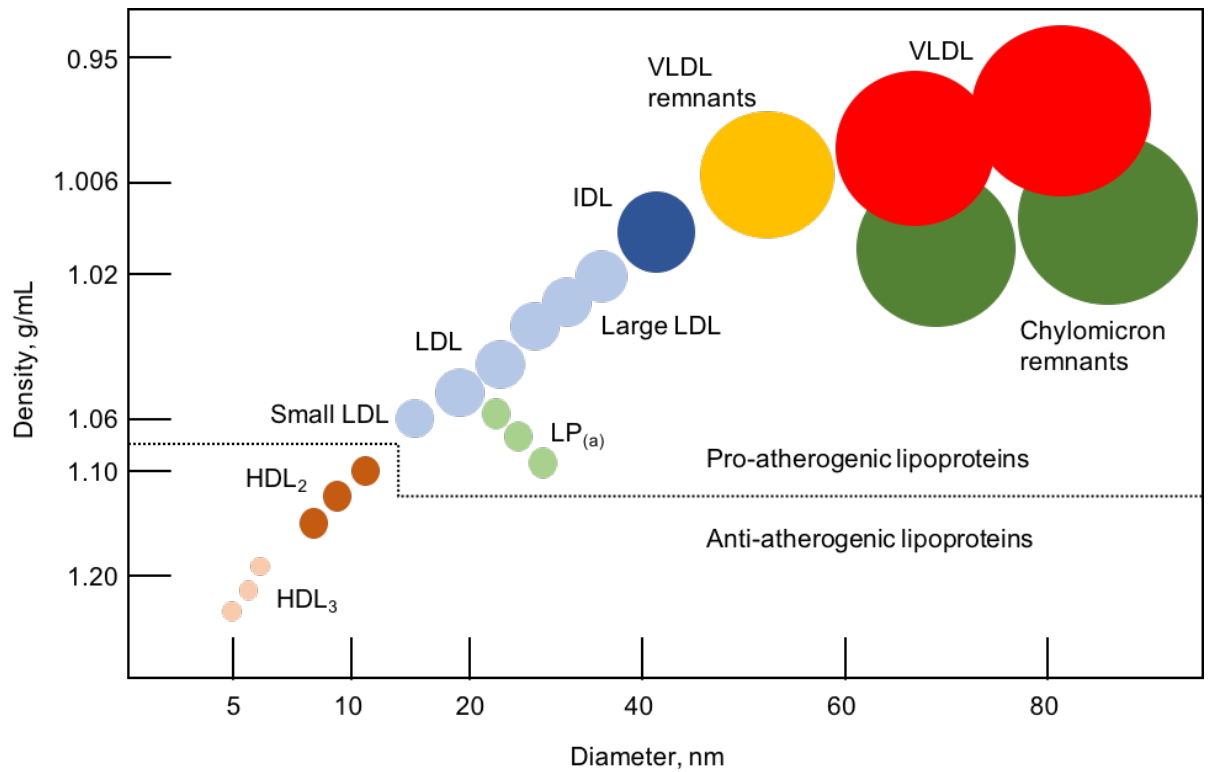


Figure 1.4. Lipoprotein particle subdivision into classes. HDL particles are understood to be anti-atherogenic, whilst LDL, IDL and VLDL particles are pro-atherogenic. HDL; high-density lipoprotein. LDL; low density lipoprotein. LP_(a); lipoprotein-a. IDL; intermediate-density lipoprotein. VLDL; very low-density lipoprotein. Figure adapted from Feingold *et al.* (Feingold and Grunfeld, 2018).

1.1.2.3 Vascular oxidative stress

Oxidative stress is known to play a role in atherogenesis, while endothelial nitric oxide (NO) production inhibits it. Reactive oxygen species (ROS) are oxygen-derived small molecules, including oxygen radicals, hydroxyl, peroxy, alkoxy and certain non-radicals that are either oxidizing agents and/or are easily converted into radicals, such as hypochlorous acid, ozone, singlet oxygen, and hydrogen peroxide (Bedard and Krause, 2007a). ROS avidly interact with a wide range of molecules such as proteins, lipids, carbohydrates, and nucleic acids. Through such interactions, ROS promotes the oxidative modification of molecules

associated with atherosclerosis, most importantly LDL (Bedard and Krause, 2007b). Regions of increased arterial wall shear stress and disturbed blood flow such as bifurcations and branches are associated with the greatest burden of atherosclerosis. Increased concentrations of ROS and reduced production of endothelial NO are understood to contribute significantly to this phenomenon (Forstermann, Xia and Li, 2017).

Sources of increased ROS include the NOX family of NADPH oxidases, xanthine oxidase (XO), mitochondria, and uncoupled endothelial nitric oxide synthase (eNOS). Crosstalk between these pro-oxidant systems maintains a cycle of increasing ROS production (Forstermann, Xia and Li, 2017). The primary function of NOX is the transmembrane transfer of electrons. The electrons are usually accepted by an oxygen molecule, leading to the reduction of oxygen to superoxide. There are 7 known isoforms of NOX, 4 of which are expressed in immune and vascular cells (NOX-1, NOX-2, NOX-4, NOX-5) (Bedard and Krause, 2007b). Not all isoforms are pro-atherogenic. NOX-1 and -2 have been shown to play a pro-atherogenic role in animal and human studies, while similar studies have found NOX-4 to be protective (Fulton and Barman, 2016). XO is found both in the circulation and in vascular cells (White *et al.*, 1996). XO expression is also increased in human atherosclerotic plaques and its activity is enhanced by vascular shear stress, suggesting a role for XO-derived superoxide molecules in atherosclerosis (Patetsios *et al.*, 2001; McNally *et al.*, 2003). Furthermore, XO inhibition in *APO-E* null mice leads to the attenuation of atherosclerosis (Nomura *et al.*, 2014).

eNOS promotes endothelial NO production under normal conditions, but becomes dysfunctional under oxidative stress. NO undergoes rapid oxidative deactivation under oxidative stress, leading to endothelial cell dysfunction. Ongoing endothelial oxidative stress renders eNOS “uncoupled”, whereby oxygen reduction in the synthesis of NO is uncoupled from the reaction and preferentially produces superoxide, at the expense of NO production (Forstermann, Xia and Li, 2017). This mechanism has been found in association with atherosclerosis in transgenic mouse models of atherosclerosis and human studies (Wohlfart *et al.*, 2008; Xia *et al.*, 2010; Antoniades *et al.*, 2007). Under normal conditions, mitochondria generate a physiological amount of superoxide.

Mitochondrial oxidative stress results from excessive ROS production or insufficient ROS detoxification in the cytoplasm. Mitochondrial oxidative stress has been found in association with human atherosclerotic plaque and to exert a pro-atherogenic effect in transgenic knockout studies (Corral-Debrinski *et al.*, 1992; Ballinger *et al.*, 2002).

1.1.2.4 The inflammatory component of atherosclerosis

Atherosclerosis is a chronic inflammatory process. Inflammation is initiated by exposure of the endothelium to noxious stimuli such as dyslipidaemia / oxLDL (Raggi *et al.*, 2018). Endothelial cells respond by upregulating the transcriptional messenger protein “nuclear factor kappa-light-chain-enhancer of activated B cells” (NFkB) and releasing a series of substances that enhance leukocyte adhesion including E-selectin and vascular and inter-cellular adhesion molecules (VCAM-1 and ICAM-1) (Raggi *et al.*, 2018). Circulating leucocytes thus adhere to the endothelium and migrate to the sub-intimal space, where along with resident tissue macrophages, begin to engulf oxLDL particles. Non-classical patrolling monocytes also engulf oxLDL early in atherogenesis through the expression of scavenger receptor (SR) CD36 (Marcovecchio *et al.*, 2017). The initial immune cell activity generates more adhesion molecules, promoting the recruitment of bone marrow-derived monocytes from the circulation to the intima. Once within the intimal layer, monocytes differentiate to macrophages and engulf oxLDL, leading to the formation of foam cells (Raggi *et al.*, 2018).

The presence of cytoplasmic cholesterol crystals within foam cells and the subsequent activation of SRs leads to the release of activated cytokines interleukin-1A (IL-1A), interleukin-1B (IL-1B) and interleukin-18 (IL-18) into the extracellular space (Sheedy *et al.*, 2013). Interactions between cytokines and their receptors result in the release of ROS and matrix degrading enzymes, and the activation and proliferation of pro-atherogenic T-helper 1 (Th1) cells. It is worth noting that not all T-helper cells are pro-atherogenic. For example, regulatory T-lymphocytes and T-helper 17 cells act to stem atherosclerosis by secreting transforming growth factor-beta / IL-10 and IL-17 respectively (Libby, Ridker and Hansson, 2009; Gistera *et al.*, 2013).

VSMCs contribute to the inflammatory process and do form foam cells, albeit to a lesser degree than the primary immune cells. The activation of VSMCs in response to the exposure to oxLDL, cytokines and growth factors leads to a phenotypic transition from a contractile, non-proliferative phenotype to a “macrophage-like” phenotype with proliferating, migratory and matrix-secreting properties, as well as the ability to express cell-surface macrophage markers and develop phagocytic activity (Raggi *et al.*, 2018).

1.1.2.5. Apoptosis, necroptosis and defective efferocytosis

Macrophages undergo endoplasmic reticulum (ER) stress, apoptosis and necroptosis due to the uptake of toxic non-esterified cholesterol within oxLDL (Raggi *et al.*, 2018). Apoptosis results from the activation of the unfolded-protein response (UPR) within the ER following exposure to cholesterol (Rayner, 2017). The resulting ER stress stimulates the production of CCAAT enhancer-binding protein homologous protein (CHOP) and initiates the release of Ca^{2+} from the ER, release of cytochrome C from the mitochondria and activation of caspase-dependent apoptosis (Gonzalez and Trigatti, 2017). Early in atherogenesis, apoptosis is protective as it allows the clearance of lipid-engorged cells and reduced lesion cellularity. Efferocytosis (the phagocytosis and clearance of apoptotic cells) is initially efficient, but becomes defective leading to the accumulation of dead foam cells and apoptotic debris within the lesion. Secondary necrosis of apoptotic cells occurs, causing rupture and release of toxins (Raggi *et al.*, 2018). Impairment of MerTK activity (macrophage cell surface receptor primarily responsible for efferocytosis) may have a role in the failure of efferocytosis, but the exact mechanism remains unclear (Kojima, Weissman and Leeper, 2017).

Necroptosis is an alternative form of programmed cell death observed in macrophages after prolonged exposure to oxLDL (Karunakaran *et al.*, 2016). Necroptosis unlike apoptosis, stimulates an innate inflammatory response due to the unregulated release of intracellular compounds. Necroptotic cells feature more predominantly in advanced atherosclerotic lesions, particularly those with a necrotic core. Defective efferocytosis of necroptotic cells gives rise to more

inflammation and the expansion of the necrotic core rendering the lesion more prone to rupture.

1.1.3 Neointimal hyperplasia

1.1.3.1 Clinical perspective of NIH

Minimally invasive and surgical treatment modalities for symptomatic cardiovascular disease generally aim to restore blood flow to areas of ischaemia by recanalising stenotic or occluded arteries. The techniques used in current practice include angioplasty, stenting, surgical endarterectomy and surgical bypass. Advances in such interventions have greatly improved clinical outcomes for our patients, however their long-term durability is an area of concern. Vessel re-stenosis and / or occlusion is clinically more challenging compared with native vessel disease and the outcomes of re-intervention are less promising. The main pathological process underlying re-stenosis related to vascular intervention is neointimal hyperplasia (NIH).

1.1.3.2 Pathology of NIH

NIH is a complex inflammatory process defined by thickening of the intimal layer due to the proliferation of VSMCs and the production of extra-cellular matrix (Kijani *et al.*, 2017). Intimal thickening leads to luminal narrowing, restenosis and potentially arterial / graft occlusion. NIH is initiated by endothelial denudation and the accumulation and activation of platelets (McMonagle, 2020). Endothelial cell and platelet activation leads to the release of growth factors such as platelet-derived growth factor and fibroblast growth factor-2, which stimulates VSMC to proliferate and migrate from the tunica media to the tunica intima (McMonagle, 2020). Additionally, VSMCs undergo a phenotypic change from their normal contractile function to a secretory one, leading to the production and deposition of extracellular matrix in the neointima (Jain *et al.*, 2020). Oxidative stress and downstream inflammatory signaling in the injured artery leads to ongoing migration and proliferation, and lesion progression (Li *et al.*, 2018a).

1.2 Scavenger Receptors

1.2.1 Background

Goldstein and co-workers first described scavenger receptors (SRs) in 1979 whilst investigating the involvement of LDL in the formation of foam cells in atherosclerosis (Goldstein *et al.*, 1979; Brown *et al.*, 1980). The authors found that macrophages exhibited high affinity binding sites recognizing negatively charged modified LDL, resulting in rapid internalization and the formation of foam cells (Brown *et al.*, 1980). SRs are defined as cell surface receptors which typically bind multiple ligands and promote the removal of harmful non-self or altered-self targets. They often function by mechanisms that include endocytosis, phagocytosis, adhesion, and signaling that ultimately lead to the elimination of degraded or harmful substances (Prabhudas *et al.*, 2014). They share the ability to recognize common ligands including lipoproteins, phospholipids, apoptotic cells, carbohydrates and cholesterol ester, however the primary amino acid sequences of proteins within each class bear little or no resemblance (Zani *et al.*, 2015).

Most SRs are primarily expressed in immune cells, particularly macrophages under conditions of oxidative stress, commonly in association with atherosclerosis. Expression of SRs has been identified in other cell types and processes contributing to a wide range of diseases such as degenerative brain disease (Wilkinson and El Khoury, 2012; Singh *et al.*, 2010), malignancy (Bachli *et al.*, 2006) and systemic inflammatory states such as sepsis (Leelahavanichkul *et al.*, 2012), rheumatoid arthritis (Matsushita *et al.*, 2002), and renal vasculitis (Nagai *et al.*, 2016).

Table 1.1 Structure and function of SRs

SR class	No. Isoforms	Nomenclature	Structure	Expression	Function
SR-A	5	Macrophage SR	Cytoplasmic tail. Transmembrane domain. Spacer region. α helical coiled coil domain. Collagenous domain. C-terminal cysteine-rich domain. (Prabhudas <i>et al.</i> , 2014; Matsumoto <i>et al.</i> , 1990)	Macrophages & subtypes e.g. Kupffer cells, medullary thymic macrophages. Vascular smooth muscle cells. Endothelial cells. Microglia. (Hughes, Fraser and Gordon, 1995; Plüddemann, Neyen and Gordon, 2007; Gough <i>et al.</i> , 1999)	Internalization of oxLDL in atherosclerosis. Bacterial cell recognition in innate immunity. Involved in beta-amyloid clearance in the brain. (Kelley <i>et al.</i> , 2014; Plüddemann, Mukhopadhyay and Gordon, 2011; Christie, Freeman and Hyman, 1996; El Khoury <i>et al.</i> , 1996; Wilkinson and El Khoury, 2012)
SR-B	3	SR-B1 SR-B2 (CD36) SR-B3 (LIMP2)	2 transmembrane domains flanking an extracellular loop with both the N and C termini located within the cytoplasm. (Prabhudas <i>et al.</i> , 2014; Febbraio, Hajjar and Silverstein, 2001)	Macrophages. Endothelial cells. Adipocytes. Renal tubular cells. Podocytes. (Talle <i>et al.</i> , 1983; Yokoi and Yanagita, 2016)	Internalization of oxLDL in atherosclerosis. Bacterial cell adhesion, internalization and lysosomal sequestration. May participate in systemic inflammation associated with sepsis. (Nicholson <i>et al.</i> , 2001; Stewart <i>et al.</i> , 2010; Leelahavanichkul <i>et al.</i> , 2012)
SR-C	Expressed in insects only therefore not discussed				
SR-D	1	CD68	Heavily glycosylated type 1 transmembrane glycoprotein strongly associated with the lysosomal/endosomal compartment. (Holness and Simmons, 1993)	Macrophages. Monocytes. Microglia. Osteoclasts. Myeloid dendritic cells. (Greaves and Gordon, 2002)	May play a role in internalization of oxLDL. This remains unclear. (Yoshida <i>et al.</i> , 1998b; de Beer <i>et al.</i> , 2003; Song, Lee and Schindler, 2011)
SR-E	3	SR-E1 (LOX-1) SR-E1.1 (LOXIN) SR-E2 (Dectin-1)	Type-II membrane protein. Short N-terminal cytoplasmic domain. Transmembrane domain. Connecting neck.	Macrophages. Neutrophils. Endothelial cells. Smooth muscle cells.	Internalization of oxLDL in atherosclerosis. Bacterial and fungal cell recognition in innate immunity. LOXIN is an alternatively spliced

			Lectin-like domain at the C terminus. (Sawamura <i>et al.</i> , 1997)	Platelets. (Herre <i>et al.</i> , 2004)	form of SR-E1 which lacks part of LOX-1's functional domain and demonstrates no known scavenger receptor activity, but has been shown to exert a dominant negative effect on LOX-1 function. (Herre <i>et al.</i> , 2004; Mango <i>et al.</i> , 2011)
SR-F	3	SR-F1 (SREC-1, SCARF-1) SR-F2 (SREC-2, SCARF-2) MEGF10	Extended extracellular domain comprised of epidermal growth factor like cysteine rich motifs (EGF repeats). Long intracellular domain containing a serine-proline rich region. (Suzuki and Nakayama, 2007)	Neuronal cells. Endothelial cells. (Zani <i>et al.</i> , 2015; Ishii <i>et al.</i> , 2002)	SR-F1 binds and internalizes oxLDL, while formation of heterodimer with SR-F2 suppresses oxLDL binding activity. MEGF10 is involved in beta-amyloid clearance in the brain. (Adachi and Tsujimoto, 1999; Ishii <i>et al.</i> , 2002; Singh <i>et al.</i> , 2010)
SR-G	1	SR-G1 (CXCL16, SR-PSOX)	Extracellular chemokine domain fused to a transmembrane mucin stalk. (Matloubian <i>et al.</i> , 2000)	Macrophages. Smooth muscle cells. (Hofnagel <i>et al.</i> , 2002; Wågsäter <i>et al.</i> , 2004)	Adhesion of cells expressing the CXCR6 receptor such as natural killer T cells and polarized T helper cells. Internalization of oxLDL in atherosclerosis. Bacterial cell recognition in innate immunity. (Ma <i>et al.</i> , 2016; Hu <i>et al.</i> , 2016; Zhou <i>et al.</i> , 2016)
SR-H	2	SR-H1 (FEEL-1, Stabilin-1, Clever-1) SR-H2 (FEEL-2, Stabilin-2)	Type I transmembrane protein. Short cytoplasmic tail. Transmembrane region. Large extracellular region containing seven fasciclin domains, multiple epidermal growth factor-like domains, and a single C-type lectin-like hyaluronan-binding link domain. (Politz <i>et al.</i> , 2002)	Macrophages. Splenic, hepatic and lymphatic endothelial cells. Monocytes. (Adachi and Tsujimoto, 2002; Zhou <i>et al.</i> , 2000)	Internalization of oxLDL in atherosclerosis. Bacterial cell recognition in innate immunity. Binding of advanced glycation end-products (AGEs). Potential role in the adhesion of metastatic tumour cells to lymphatic endothelial cells. (Adachi and Tsujimoto, 2002; Irjala <i>et al.</i> , 2003b; Irjala <i>et al.</i> , 2003a)
SR-I	2	SR-I1 (CD163, heamoglobin SR) SR-I2 (CD163B)	Type I transmembrane Glycoprotein. Extracellular domain is composed of nine	Circulating and tissue specific macrophages and monocytes.	Mediates haptoglobin-haemoglobin complex endocytosis during intravascular haemolysis.

			scavenger receptor cysteine-rich domains in tandem. Transmembrane region. Short intracellular cytoplasmic tail. (Nielsen <i>et al.</i> , 2006)	Leukaemic blasts. (Etzerodt <i>et al.</i> , 2012; Kristiansen <i>et al.</i> , 2001)	(Kristiansen <i>et al.</i> , 2001)
SR-J	1	RAGE	Extracellular variable-type domain. Single transmembrane spinning helix that connects the short C-terminal cytosolic domain and two C-type domains. (Zani <i>et al.</i> , 2015)	Endothelial cells. Hepatocytes. Smooth muscle cells. Monocytes. (Ramasamy, Yan and Schmidt, 2009)	Binds AGEs. Activated by pro-inflammatory ligands such as β -amyloid, and S100/calgranulin leading to amplification of immune and inflammatory responses, cell mobility, arterial injury, and atherogenesis via sustained post-receptor signaling. (Ramasamy, Yan and Schmidt, 2005)

1.2.2 Targeting SRs in cardiovascular disease

SRs are multi-ligand receptors, each class with a unique structure, but all receptors sharing a common function; the scavenging of harmful substances. Many SRs are expressed in cells involved in the development of atherosclerosis which is the main contributor to cardiovascular disease. Research to date has identified the main players: SR-A; CD36; lectin-like oxidized LDL receptor-1 (LOX-1); CXCL16; Receptor for advanced glycation end-products (RAGE). Each of receptor shows promise in future applications as biomarkers for disease and novel therapeutics. The applications of SR-A, CD36, CXCL16 and RAGE are discussed here. LOX-1 is the primary focus of this research and will be discussed in more detail, separately.

1.2.3 SRs as Biomarkers

SRs have been identified as having potential roles in genetic screening or as diagnostic and prognostic biomarkers in cardiovascular disease. Screening for patients with a genetic predisposition to cardiovascular disease has potentially far reaching benefits in disease prevention and early management. Polymorphisms in genes encoding both CD36 have been associated with

increased overall cardiovascular risk (Che, Shao and Li, 2014; Jayewardene *et al.*, 2014; Morini *et al.*, 2016). Cohort studies of both healthy and known coronary artery disease patients have shown an association between CD36 genotype and increased lipid oxidation, overall cardiovascular risk and specifically the development of premature coronary artery disease (Che, Shao and Li, 2014; Jayewardene *et al.*, 2014).

Much has been done to investigate the diagnostic value of quantifying SR levels in acute coronary syndrome. Both serum concentrations of soluble protein and levels of protein expression in immune cells have been studied. Using an “SR-A index” which quantifies monocyte SR-A expression in peripheral blood smears from patients with coronary artery disease, investigations demonstrate that an increase in SR-A index is associated with atherosclerotic plaque complications (disruption, fissure, erosion) (Nakayama *et al.*, 2008). Furthermore the SR-A index may be useful in determining plaque morphology which in turn may help guide therapy in coronary artery disease (Emura *et al.*, 2011; Emura *et al.*, 2007). Similar studies have shown an association between circulating monocyte CD36 expression and atheroma burden in coronary artery disease patients (Teupser *et al.*, 2008). Promising results from a study using CD36 specific nanovesicles in detecting and quantifying atherosclerosis in LDLR-null mice indicate their potential application as a tool in non-invasive imaging of atherosclerosis (Nie *et al.*, 2015).

CXCL16 acts both as a scavenger receptor which binds oxLDL and as an inflammatory chemokine, establishing it as a molecule of interest in atherosclerosis (Aslanian Ara and Charo Israel, 2006). Serum soluble CXCL16 has been evaluated as a potential biomarker in carotid artery disease, coronary artery disease and inflammatory cardiomyopathy. In 118 patient presenting with an acute ischaemic stroke, serum CXCL16 concentrations were significantly higher in those with vulnerable carotid plaque, a higher degree of luminal stenosis and increased intima-media thickness (Jin, 2017). A number of small clinical studies have also shown that measuring serum CXCL16 concentration can improve diagnostic accuracy when combined with troponins and soluble LOX-1 in acute coronary syndrome, and that it may be of particular benefit in those with type 2 diabetes (Mitsuoka *et al.*, 2009; Zhou *et al.*, 2016). As a prognostic

biomarker, a study of 1351 patients presenting with acute coronary syndrome found that a single measurement of raised serum CXCL16 within 24 hours of admission to hospital was associated with higher long term mortality, owing presumably to its role in promoting a pro-atherogenic inflammatory response (Jansson *et al.*, 2009). CXCL16 has also been proposed as a prognostic biomarker in inflammatory cardiomyopathy and heart failure. In 174 patients with heart failure, myocardial biopsy samples stained for CXCL16 showed significantly enhanced expression in inflammatory cardiomyopathy compared with non-inflammatory cardiomyopathy (Borst *et al.*, 2014). The same study found that increased CXCL16 expression was an independent predictor of death in both inflammatory and non-inflammatory cardiomyopathy patients.

Like other SRs, RAGE undergoes proteolytic cleavage to form a circulating soluble form (sRAGE). sRAGE has been proposed as a novel diagnostic and prognostic biomarker for cardiovascular disease particularly in patients with diabetes mellitus. Multiple cohort studies have found that an increasing serum concentration of sRAGE is predictive for coronary artery disease and future cardiovascular events (Nakamura *et al.*, 2007; Nin *et al.*, 2010; Colhoun *et al.*, 2011; Fujisawa *et al.*, 2013). The relationship is not entirely straightforward, evidenced by a study of sRAGE levels in 127 consecutive patients with non-acute coronary artery disease (Basta *et al.*, 2012). Using computed tomography angiography, the authors found that higher concentrations of sRAGE were inversely related to overall plaque burden. A study of 328 non-diabetic males found the same inverse relationship (Falcone *et al.*, 2005). Certainly to-date it appears that sRAGE has a potential future role as a biomarker in patients with diabetes mellitus, however its utility in non-diabetic patients is probably less promising.

1.2.4 Therapeutic strategies in atherosclerosis

1.2.4.1 Clinically approved treatments

HMG Co-A reductase inhibitors, otherwise known as statins, are widely utilised cholesterol-lowering agents used in the treatment and prevention of

cardiovascular disease (Hawkes, 2017). Statins not only reduce total serum cholesterol, but also exhibit pleiotropic effects on the vessel wall including improved endothelial function, a reduction in vascular inflammation and enhanced plaque stability (Liao, 2002). The effect of statin therapy on scavenger receptor function is not yet understood. An *in vitro* study of atorvastatin therapy in oxLDL exposed immortalized human monocytes (THP-1 cells) found that atorvastatin attenuated SR-A expression and monocyte chemoattractant protein-1 in a dose-dependent manner (Zhu *et al.*, 2007). Atorvastatin therapy also reduced overall foam cell formation, indicating a possible association between cholesterol levels and plaque formation. Using cultured murine and human macrophages, incubation with pitavastatin was associated with significantly increased expression of SR-B1: this expression is known to be protective against atherogenesis (Han *et al.*, 2004; Arai *et al.*, 1999). Statins also increase production of endothelium-protective nitric oxide *in vitro* in a rapid, dose dependent manner via the activation of SR-B1 (Arai *et al.*, 1999).

Statin therapy may also interact with the pro-atherogenic SR RAGE. RAGE expression is down-regulated in atherosclerotic plaques from diabetic patients treated with simvastatin (Cuccurullo *et al.*, 2006). Atorvastatin was also found to increase the production of sRAGE *in vitro*. The soluble isoforms of RAGE are thought to act as a decoy and inhibit the pro-atherogenic effects of advanced glycation endproducts (Santilli *et al.*, 2007). Whilst the results of this study are convincing, it does raise the issue of the range of actions of structurally different statins on SR activity. While the mentioned effects were seen with atorvastatin therapy, the same effects were not detected when pravastatin was used.

Monoclonal antibody proprotein convertase subtilisin/kexin type 9 (PCSK9) inhibitors are relatively novel LDL-lowering agents which have recently been approved for clinical use. PCSK9 is a protease required for the degradation of the LDL-receptor (LDLR) (Wang and Liu, 2019). PCSK9 inhibitors work by inhibiting PCSK9-LDLR interaction leading to decreased LDLR degradation and ultimately a reduction in serum LDL-cholesterol. Studies by Ding *et al* investigating the possibility of interactions between PCSK9 and LOX-1 suggest that cross-talk between PCSK9 and LOX-1 exists in the form of positive feedback (Ding *et al.*, 2015). The authors demonstrate LOX-1 ablation in cellular and

transgenic mouse experiments results in reduced PCSK9 expression and *vice versa* with PCSK9 ablation. The effects of monoclonal PCSK9 inhibitors on LOX-1 expression in humans is not known, however it is conceivable that LOX-1 downregulation as a result of PCSK9 inhibition could be providing additional anti-atherogenic benefit.

Peroxisome proliferator-activated receptor- γ (PPAR- γ) exhibits anti-inflammatory and anti-diabetic properties. Pioglitazone is a PPAR- γ agonist which is commonly prescribed as a glucose-lowering agent in type 2 diabetes mellitus (T2DM). Human and animal studies have described the effect of pioglitazone on SR expression and function in the context of diabetes and metabolic syndrome. In a study of 30 patients with polycystic ovarian syndrome (PCOS) combined with either increased fasting glucose or obesity, the concentration of serum soluble CD36 was significantly raised compared to healthy controls (n=14) (Glintborg *et al.*, 2008). Further, it was found that treatment with pioglitazone significantly reduced the concentrations of soluble CD36 and the inflammatory marker C-reactive protein while improving insulin sensitivity. The authors conclude that the evidence strengthens the basis for an association between sCD36 and insulin resistance in PCOS. Pioglitazone may in addition have potential in reducing overall cardiovascular risk in this cohort. A further study investigates the effects of pioglitazone on atherosclerosis in diabetic APO-E null mice and found that atherosclerosis was attenuated via RAGE signaling pathways (Gao *et al.*, 2017). The authors demonstrated that pioglitazone administration reduced atherosclerotic load in harvested aortae, inhibited RAGE expression in harvested tissues and in cultured murine vascular smooth muscle cells.

1.2.4.2 Herbal and traditional medicine therapies

Herbal and traditional medicines have attracted some interest in scavenger receptor research relating to atherosclerosis. *Ginkgo biloba* root is used in traditional Chinese medicine for a variety of illnesses. Its extract and its biologically active molecules “ginkgolides” have demonstrated anti-oxidant and anti-inflammatory properties when applied to endothelial cells (Tsai *et al.*, 2010). SR-A expression and oxLDL uptake was significantly reduced in the presence of *Ginkgo biloba* extract *in vitro*, and moreover SR-A expression and aortic

atherosclerotic load was significantly reduced in *APO-E* null mice treated with *Ginkgo biloba* extract (Tsai *et al.*, 2010). Similar results have been obtained in rat models demonstrating a significant reduction in circulating inflammatory factors and aortic SR-A expression compared with controls (Zhu *et al.*, 2016).

Lowbush blueberries have been shown to reduce atherosclerosis in *APO-E* null mice (Xie *et al.*, 2011). The mechanisms for this effect are not yet fully understood, however the effects on SR-A and CD36 expression has been evaluated. Investigators found that *APO-E* null mice fed diet containing 1% lowbush blueberry had significantly reduced expression of SR-A and CD36 and significantly reduced foam cell formation (Xie *et al.*, 2011).

1.2.4.3 Novel therapeutics

Transgenic mouse studies have demonstrated that SR-A deletion leads to a significant reduction in aortic atherosclerotic load, leading to numerous studies aiming to identify novel therapeutics based on SR-A inhibition (Babaev *et al.*, 2000). Amphiphilic macromolecules (AM) selected for SR-A binding affinity have shown promising results in atherosclerosis attenuation (Hehir *et al.*, 2012; Iverson *et al.*, 2011). SR-A specific AMs reduced both oxLDL uptake in SR-A expressing human embryonic kidney cells and pro-inflammatory signaling in activated THP-1 macrophages (Iverson *et al.*, 2011). The authors also demonstrated a reduction in intimal cholesterol accumulation and macrophage retention post carotid artery injury in rats fed a high fat diet.

Higher serum levels of the anti-inflammatory cytokine interleukin-10 (IL-10) has been associated with superior outcomes in patients with acute coronary syndromes, however the mechanisms at the time were not fully understood (Fichtlscherer *et al.*, 2004; Anguera *et al.*, 2002). It has since been shown that incubation with IL-10 reduces oxLDL uptake and SR-A expression in activated THP-1 macrophages, providing further support for IL-10 as a potential treatment in atherosclerosis, particularly acute coronary syndrome (Yang *et al.*, 2011).

SR-A expression in macrophages is also reduced leading to attenuation of atherosclerosis in *APO-E* null mice by intermedin; a novel member of the calcitonin gene-related peptide family (Dai *et al.*, 2012). Intermedin has been

previously implicated in the maintenance of vascular homeostasis and has been shown to contribute to the reduction of calcium deposition in atherosclerotic plaque (Cai *et al.*, 2009). The authors found that levels and stability of phosphatase and tensin homolog (PTEN) were associated with reduced SR-A expression leading to the conclusion that intermedin attenuates atherosclerosis via PTEN mediated SR-A inhibition and this has potential in the treatment of atherosclerotic disease. SR-A has also been identified as a potential target in diabetic nephropathy, although no agent has been identified thus far. In SR-A null mice with streptozotocin-induced diabetes mellitus, there is a significant reduction in markers of nephropathy including albuminuria, glomerular hypertrophy, mesangial matrix expansion, parenchymal macrophage infiltration and overexpression of transforming growth factor- β compared with *SR-A*^{+/+} controls (Usui *et al.*, 2007).

The use of RNA interference mediated silencing to downregulate SR-A and CD36 is effective in reducing oxLDL uptake *in vitro* and atherosclerotic load *in vivo* when one receptor is targeted alone, however interestingly when both receptors are targeted, there is no change observed against controls (Mäkinen *et al.*, 2010). The authors also found that the downregulation of either SR-A or CD36 resulted in a reciprocal upregulation of the other. Crosstalk between two scavenger receptors may explain why the inhibition of multiple receptors could be less effective than inhibiting a single receptor. The results from studies of both SR-A and CD36 in tandem do conflict. Monoclonal antibody mediated inhibition of either SR-A or CD36 reduces foam cell formation *in vitro*; however, the authors did not block both receptors simultaneously (Seizer *et al.*, 2010). Double knockout of *SR-A* and *CD36* in *APO-E* null mice did not reduce aortic root atherosclerosis compared with *APO-E* null mice, however the authors did not study *SR-A* or *CD36* knockout in isolation (Manning-Tobin *et al.*, 2009). Isolated and double knockout has been studied by a different group, who found that *CD36* knockout significantly reduced aortic atherosclerotic load compared with controls, however *SR-A* knockout was less effective in isolation, and double knockout was similar in efficacy to *CD36* knockout alone (Kuchibhotla *et al.*, 2008).

CD36 is a multi-ligand and multifunctional scavenger receptor which plays a complex role in cardio- and cerebrovascular disease states (Cho and Kim, 2009).

It has been shown to exhibit both pro-atherogenic and anti-angiogenic properties both *in vitro* and *in vivo* (Cho, 2012; Mwaikambo *et al.*, 2008). Investigators studying CD36 in cerebrovascular disease have demonstrated that CD36 null mice benefit from significantly improved angiogenesis after acute stroke (Qin *et al.*, 2011). The same group have found that treatment with a cell-permeable antioxidant peptide (SS31) reduces cerebral oxidative stress and infarct size in mice subjected to transient middle cerebral artery occlusion (Cho *et al.*, 2007). The effect was not seen in CD36 null controls, leading the authors to conclude that SS31 is producing the desired effects via CD36.

Nanoparticles such as AMs and nanovesicles have been identified which bind to CD36 and inhibit oxLDL uptake *in vitro* (Chnari *et al.*, 2006; Nie *et al.*, 2015). CD36-targeted liposome-like nanovesicles show impressive binding affinities to CD36 *in vitro* and *in vivo* in atherosclerotic *LDLR* null mice. Atherosclerosis attenuation was not studied here, however the therapeutic potential of CD36-targeted nanovesicles is clear, given the results previously discussed from transgenic models studying the effects of *CD36* knockout on atherosclerotic load. Synthetic proteins such as EP 80317; a CD36 selective ligand have been shown to reduce macrophage oxLDL uptake and atherosclerotic load in *APO-E* null mice (Marleau *et al.*, 2005). Furthermore, investigators have demonstrated that treatment with this protein promotes reverse transport of cholesterol in macrophages and increases the excretion of cholesterol in faeces via the modulation of various receptors in the gut ($LXR\alpha$, NPC1L1) (Bujold *et al.*, 2013).

The relationship between CXCL16 and atherogenesis is not as well established compared with SR-A, CD36 and LOX-1. As previously discussed, a soluble CXCL16 isoform has been identified as a potential novel biomarker in coronary artery disease. It has been shown that CXCL16 is highly expressed in human carotid and coronary artery atheroma (Minami *et al.*, 2001). Hofnagel *et al.* have investigated the role of CXCL16 in atherosclerosis and found that CXCL16 was expressed primarily in endothelium at sites predisposed to atherosclerosis in harvested rabbit aorta (Hofnagel *et al.*, 2011). The authors treated human umbilical vein endothelial cells with anti-CXCL16 antibody and demonstrated a significant reduction in monocyte adhesion. To date the efficacy of anti-CXCL16 monoclonal antibody in animal model of atherosclerosis is untested. Interestingly

a transgenic mouse found that *LDLR/CXCL16* double null were more atherosclerotic compared with *LDLR* null alone (Aslanian and Charo, 2006). This is not the first time that knockout of a SR gene has produced contradictory results. As previously discussed, double knockout of *SR-A/CD36* had no effect on the formation of atherosclerosis in *APO-E* null mice, while knockout of each gene in isolation reduced atherosclerosis compared with controls (Manning-Tobin *et al.*, 2009; Kuchibhotla *et al.*, 2008). In contrast, the *CXCL16* null mice are single SR knockout and it therefore remains that the role of *CXCL16* in atherogenesis and its potential in therapeutics is less clear.

Advanced glycation end-products (AGEs) are understood to be pro-atherogenic and are of interest in vascular disease associated with diabetes mellitus. Therapeutics aimed at the inhibition of advanced glycation with agents such as aminoguanidine-HCl, which inhibits crosslinking necessary to form AGEs has produced a range of beneficial cardiovascular effects *in vivo* (Bierhaus *et al.*, 1998). RAGE recognizes and internalizes oxLDL; RAGE expression is upregulated when exposed to AGEs which leads to an increase in oxLDL accumulation *in vitro* (Xu *et al.*, 2016). The authors found that anti-RAGE antibody reversed this effect. A study investigating the role of RAGE in cardiovascular disease associated with obstructive sleep apnoea found that RAGE-targeted RNAi therapy reduced monocyte adhesion in HUVECs (Zhou *et al.*, 2018). *In vivo*, diabetic *APO-E/RAGE* double null mice had a statistically non-significant reduction in aortic atherosclerotic load and reduced leucocyte adhesion and expression of pro-inflammatory mediators (Soro-Paavonen *et al.*, 2008). Interestingly, recombinant sRAGE administration in diabetic *APO-E* null mice suppressed aortic atherosclerosis while having no effect on plasma lipid profile or serum glucose concentration (Park *et al.*, 1998). Immunohistochemical analysis of aortic atherosclerotic plaque showed reduced AGE and RAGE levels in mice treated with sRAGE, leading the authors to hypothesize that sRAGE acts as a “sponge” for AGEs thus reducing the expression of RAGE in vascular tissue, in turn reducing downstream signaling responsible for plaque development.

1.3 Structure and function of the LOX-1 SR

1.3.1 Genetics and expression of LOX-1

LOX-1 is a member of the SR-E family of scavenger receptors first described by Sawamura and co-workers in 1997 (Sawamura *et al.*, 1997). With the premise that vascular endothelial cells both *in vitro* and *in vivo* internalize and degrade oxLDL via a receptor pathway unrelated to macrophage scavenger receptors, LOX-1 was cloned from bovine endothelial cells using expression cloning. LOX-1 is encoded by the oxidized LDL receptor 1 (*OLR1*) gene locus located within of the short arm of human chromosome 12 which is also enriched with genes involved in innate immunity (Yamanaka *et al.*, 1998). LOX-1 is predominantly expressed in endothelial cells, but subsequently been detected in macrophages, smooth muscle cells and platelets (Yoshida *et al.*, 1998a; Draude, Hrboticky and Lorenz, 1999; Chen *et al.*, 2001b). Furthermore, LOX-1 is over-expressed in human and animal atherosclerotic lesions *in vivo* (Kataoka *et al.*, 1999). Expression of LOX-1 is induced by a number of stimuli including oxLDL, angiotensin 2, shear stress and tumour necrosis factor α (Li *et al.*, 1999; Murase *et al.*, 1998; Kume *et al.*, 1998).

1.3.2 Structure of LOX-1

LOX-1 is a type II integral membrane glycoprotein with a short N-terminal cytoplasmic domain, a single transmembrane domain, a short neck region and an extracellular C-type lectin-like fold (Figure 1.5). This C-type lectin-like fold is critically required for LOX-1 binding activity and is highly conserved within LOX-1 mammalian orthologues, notably at six cysteine residues which underpin the lectin-like fold by forming three intramolecular disulfide bonds (Shi *et al.*, 2001). N-glycosylation of LOX-1 regulates protein folding within the endoplasmic reticulum, secretory transport to the plasma membrane and ligand recognition (Kataoka *et al.*, 2000). It is likely that LOX-1 improves the efficiency of oxLDL binding by undergoing multimerization via inter-chain disulphide bonds between cysteine¹⁴⁰ (Cys¹⁴⁰) residues (Ishigaki *et al.*, 2007) (Figure 1.6).

1.3.3 LOX-1-mediated signal transduction

The cellular effect of oxLDL is mainly dependent on specific binding to LOX-1, hence multiple signal transduction pathways involved in the development of atherosclerosis are affected by LOX-1 activation (Xu *et al.*, 2013). When oxLDL binds to LOX-1, it induces rapid RhoA and Rac1 activation via MT1-MMP, which results in NADPH oxidase activation and eNOS downregulation (Sugimoto *et al.*, 2009). The resulting imbalance of NO and oxidative stress likely leads to endothelial cell dysfunction. The following pathways have also been implicated in the activation of LOX-1: p38 mitogen-activated protein kinase C (MAPK), p44/42MAPK, protein kinase C, protein kinase B, extracellular signal-regulated kinases 1/2 (ERK1/2), protein tyrosine kinase (Ogura *et al.*, 2009).

Adhesion molecules and chemokines such as E- and P- selectins, ICAM-1, VCAM-1 which mediate monocyte adhesion to endothelial cells, are overexpressed following LOX-1-mediated NF- κ B activation by oxLDL (Ogura *et al.*, 2009). Reactive oxygen species generated by LOX-1-oxLDL binding in the endothelial cell activate NF- κ B (Cominacini *et al.*, 2000). NF- κ B activation can induce upregulation of pro-inflammatory mediators as well as LOX-1 itself which in turn increase LOX-1-mediated oxLDL uptake, thus amplifying the effects of atherogenic oxLDL (Nagase *et al.*, 1998). Additionally, LOX-1 activation changes endothelial cells and smooth muscle cells prone to apoptosis by increasing the B-cell lymphoma – 2 (Bcl-2) -associated X protein (Bax)/Bcl-2 ratio (Kataoka *et al.*, 2001).

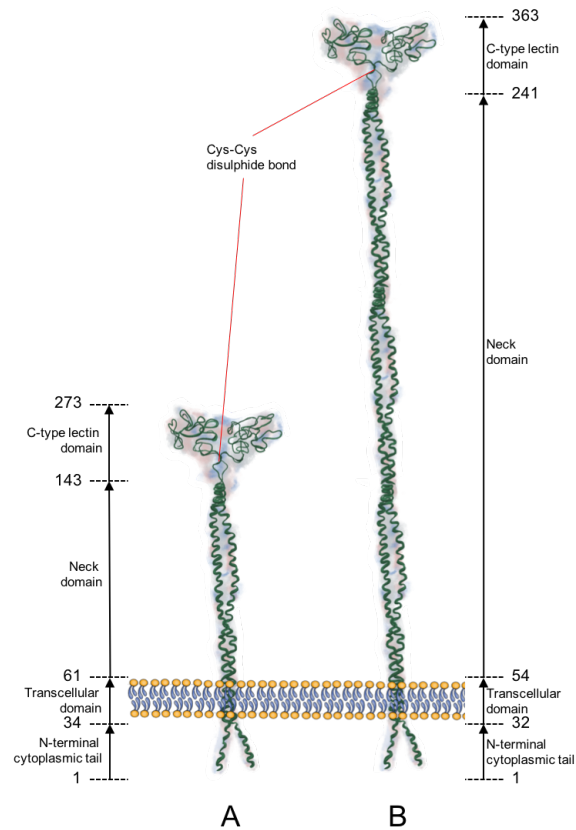


Figure 1.5. Structure of human (A) and mouse (B) LOX-1. The molecule exists as a homodimer and has four domains: an extracellular C-terminal C-type lectin domain, a connecting neck domain, a single transcellular domain and a short N-terminal cytoplasmic tail. A disulphide bond exists between cysteine 140 in each of the C-type lectin domains. The C-type lectin domain sequence is highly conserved in mammals. Mouse LOX-1 is structurally similar, but contains triple repeats of the extracellular neck domain.

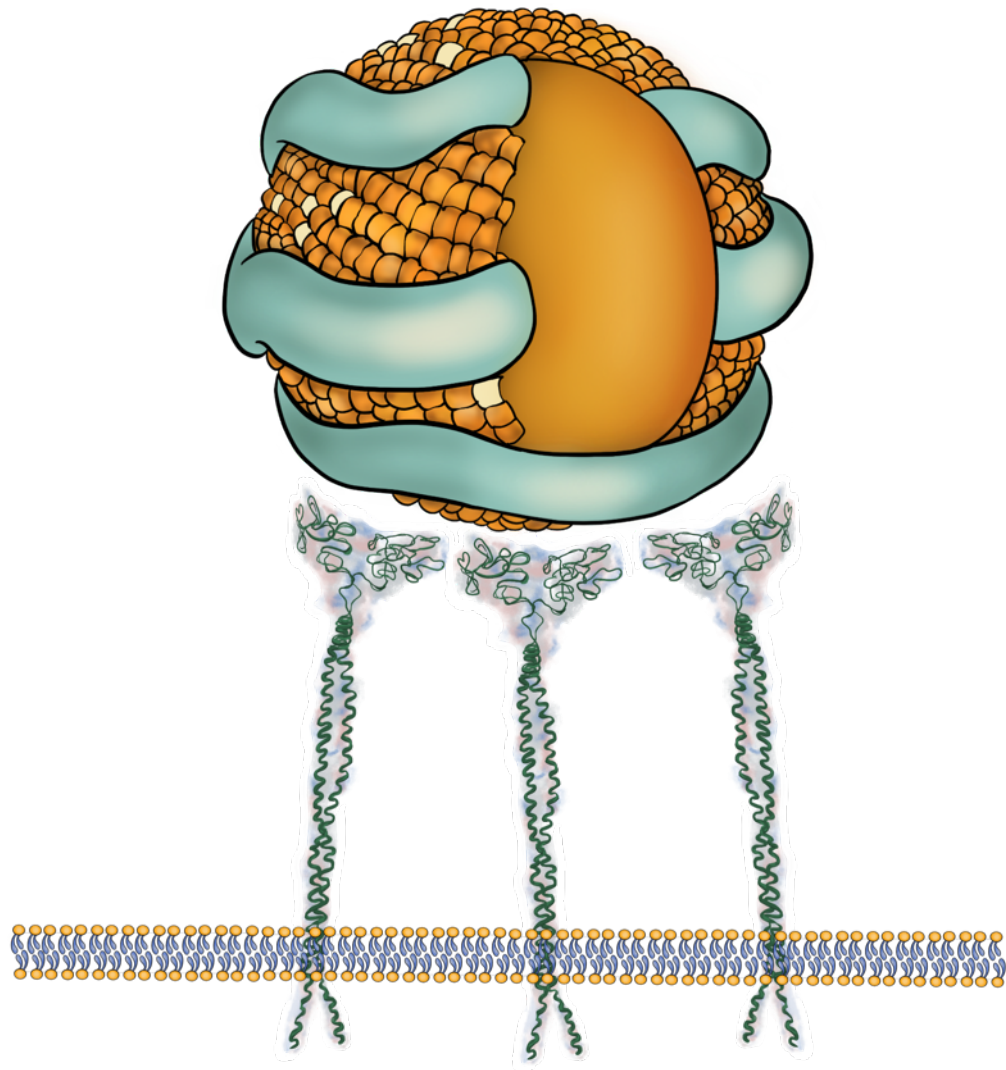


Figure 1.6. LOX-1 binding to LDL. It is likely that LOX-1 improves the efficiency of oxLDL binding by undergoing multimerization via inter-chain disulphide bonds between Cys¹⁴⁰ residues.

1.4 LOX-1 in the pathology of cardiovascular disease

1.4.1 Endothelial dysfunction

Activation of LOX-1 by oxLDL results in endothelial activation and dysfunction, characterized by reduced endothelium-dependent relaxation, increased monocyte adhesion to endothelial cells, as well as endothelial cell apoptosis (Xu

et al., 2013). OxLDL-LOX-1 binding activates arginase II leading to down-regulated nitric oxide production in endothelial cells, a main contributor to vascular relaxation (Ryoo *et al.*, 2011). In addition, LOX-1 mediates oxLDL uptake by endothelial cells and impairs endothelium-dependent NO-mediated dilation of coronary arterioles by activation of a signaling cascade involving LOX-1 and NADPH oxidase (Shi *et al.*, 2011). Anti-LOX-1 antibodies have been shown to restore nitric oxide-mediated coronary dilation in atherosclerotic APO-E null mice, but do not affect the endothelium-dependent vasodilation in wild-type mice (Xu *et al.*, 2007).

Recruitment of inflammatory cells to the endothelium is crucial in the development of atherosclerosis. Li and co-workers incubated human coronary artery endothelial cells (HCAEC) with oxLDL and demonstrated increased monocyte chemoattractant protein-1 (MCP-1) production as well as monocyte adhesion to HCAEC (Li and Mehta, 2000). This response was inhibited by human LOX-1 antisense RNA, suggesting that LOX-1 is a key factor in oxLDL-mediated monocyte adhesion in atherosclerosis.

1.4.2 Smooth muscle cell migration and proliferation

VSMC migration and proliferation is an important characteristic in atherosclerosis. OxLDL-induced LOX-1 expression stimulates VSMC growth and proliferation via NF- κ B- and JNK-signaling; a process which has been inhibited by LOX-1 antisense mRNA *in vitro* (Xu *et al.*, 2013). The link between VSMC proliferation and LOX-1 has been demonstrated in *APO-E/LOX-1* double knockout mouse models of atherosclerosis (Mehta Jawahar *et al.*, 2007) and in animal models of neointimal hyperplasia following balloon injury (Hinagata *et al.*, 2006). Hinagata and co-workers found that in rats administered anti-LOX-1 antibody intravenously every 3 days after balloon injury, intimal hyperplasia, oxidative stress, and leukocyte infiltration were markedly suppressed.

1.4.3 Macrophage foam cell formation

As previously discussed macrophages express a wide range of SRs which bind and internalize oxLDL resulting in the formation of atherosclerotic foam cells (Li

and Mehta, 2009). LOX-1 mediated uptake of oxLDL in macrophages stimulated by oxLDL and lysophosphatidylcholine, palmitic acids and hyperglycaemia (Schaeffer *et al.*, 2009).

1.4.4 Platelet activation and thrombosis

The role of platelet activation in thrombosis is well described. Platelets have been found to internalize oxLDL, leading to down-regulation of platelet nitric oxide synthase activity and platelet aggregation (Chen, Mehta and Mehta, 1996). The LOX-1 receptor is expressed in platelets and has been shown to accumulate at the site of thrombus within the atherosclerotic plaque of patients with unstable angina pectoris (Chen *et al.*, 2001b). Blocking LOX-1 with anti-LOX-1 antibody has been shown to diminish the formation of arterial thrombus in an animal model (Kakutani *et al.*, 2000). Furthermore, it has been shown that variations in LOX-1 polymorphisms within platelets affect platelet activation by oxLDL (Puccetti *et al.*, 2007).

1.4.5 Hypertension

The involvement of the renin-angiotensin system (RAS) in blood pressure homeostasis and the development of hypertension is well documented. It has been proposed that an interaction between LDL, especially oxLDL, and RAS activation is an important determinant of hypertension (Chen and Mehta, 2006). High levels of oxLDL upregulate angiotensin 2 receptor type 1 (AT1R), and angiotensin 2 via AT1R induces the transcription of LOX-1. Cross-talk between oxLDL and RAS activation has been shown in laboratory animals (Chen *et al.*, 2006). *APO-E* null mice fed a high cholesterol diet showed limitation of atherosclerosis when simultaneously treated with the AT1R blocker candesartan or the HMG-CoA reductase inhibitor rosuvastatin, or both. In addition, the expression of LOX-1 as well as other pro-inflammatory and redox signals was completely blocked in the mice given the drug combination.

Furthermore, Nagase and co-workers found that expression of LOX-1 mRNA in the aorta was up-regulated in hypertensive rats compared to normal healthy rats (Nagase *et al.*, 1997). An *in vitro* study supported this hypothesis, which detected

a marked increase in LOX-1 mRNA levels in cultured human coronary artery endothelial cells upon activation of AT1R (Li *et al.*, 1999).

1.5 LOX-1 as a biomarker in cardiovascular disease

The association between SRs and cardiovascular disease is well established and multiple subtypes have been identified as having potential roles in genetic screening or as diagnostic and prognostic biomarkers. Screening for patients with a genetic predisposition to cardiovascular disease has potentially far reaching benefits in disease prevention and early management. Polymorphisms in genes encoding both CD36 and LOX-1 have been associated with increased overall cardiovascular risk (Che, Shao and Li, 2014; Jayewardene *et al.*, 2014; Morini *et al.*, 2016). A single-nucleotide polymorphism (SNP) of the OLR1 gene has been shown to improve the efficiency of LOX-1 expression in-vitro, suggesting that this may contribute to overall cardiovascular risk and may be useful in risk stratification (Morini *et al.*, 2016). Moreover, a study of 150 patients with acute myocardial infarction versus 103 healthy controls identified SNPs in OLR1 associated with increased risk of myocardial infarction (Mango *et al.*, 2003).

Measuring the concentration of circulating soluble biomarkers in serum is widely used in clinical practice to aid the diagnosis of acute coronary syndrome (Shah *et al.*, 2018). SRs such as LOX-1 and CXCL16 have been identified as potential novel biomarkers in a range of cardiovascular disease states including acute coronary syndrome, cardiac failure, cardiomyopathy and carotid disease. A small clinical study of 67 patients found that serum soluble LOX-1 concentrations were significantly increased in acute coronary syndrome patients compared to those with stable angina pectoris (Misaka *et al.*, 2014). The combination of serum soluble LOX-1 with troponin concentration improved diagnostic accuracy in acute coronary syndrome compared with each protein in isolation. The same study also found that soluble LOX-1 was comparable in accuracy in the diagnosis of acute coronary syndrome (Kobayashi *et al.*, 2011). A study of 107 patients undergoing coronary stenting found that soluble LOX-1 was more accurate compared with troponin in the diagnosis of acute coronary syndrome and that combining both

biomarkers improved accuracy above that of soluble LOX-1 in isolation (Kume *et al.*, 2010).

In vitro and *in vivo* animal models of heart failure have shown that LOX-1 is released by cardiac myocytes and promotes apoptosis (Iwai-Kanai *et al.*, 2001; Kobayashi *et al.*, 2006). To evaluate LOX-1 as a biomarker for systolic heart failure, serum soluble LOX-1 concentrations were measured in 55 patients with systolic heart failure and compared to concentration in 25 control subjects. Serum soluble LOX-1 concentrations were negatively correlated with left ventricular ejection fraction particularly in patients with ischaemia-related Aetiology (Besli *et al.*, 2016).

1.6 LOX-1 in cardiovascular disease therapeutics

1.6.1 Clinically approved treatments

Owing to their central role in the key pathways leading to atherosclerotic plaque formation, scavenger receptor inhibition or downregulation is an area of great interest in therapy for cardiovascular disease. Multiple avenues have been explored in drug discovery research including the efficacy of existing drugs, herbal medicines and novel therapeutics such as gene therapy and nanoparticles.

Statin exposure reduces LOX-1 expression and its ability to bind oxLDL *in vitro* (Biocca *et al.*, 2015). Additional studies demonstrating the reduction in LOX-1 expression during statin therapy found additional benefits including increased NO production and reduced production of adhesion molecules (Mehta *et al.*, 2001; Li *et al.*, 2002a). The importance of the relationship between LOX-1 and statins is further highlighted by a cohort study of 751 patients with hypercholesterolaemia receiving statin therapy which found that LOX-1 genetic variations negatively influenced LDL reduction and cardiac risk (Puccetti *et al.*, 2007).

Other additional existing drugs have been shown to interact with LOX-1 including ursolic acid, histamine, spironolactone and ACE inhibitors. Ursolic acid was found to inhibit LOX-1 expression *in vitro* and significantly reduce both LOX-1 expression and aortic atherosclerotic load in *APO-E* null mice (Li *et al.*, 2018b).

Similar results were obtained from a study of the same design when histamine was administered (Song *et al.*, 2011). Anti-hypertensive medications such as the potassium sparing diuretic spironolactone and the ACE-inhibitor losartan have been shown to suppress LOX-1 expression and activity and thus hold potential in the prevention of atherosclerotic disease (Taye, Sawamura and Morawietz, 2010; Morawietz *et al.*, 1999).

1.6.2 Herbal and traditional medicine therapies

Herbal and traditional medicines have attracted some interest in scavenger receptor research relating to atherosclerosis. *Ginkgo biloba* extract also reduces LOX-1 expression both in combination and without aspirin, protecting against the oxidative effects of both oxLDL and activated platelets in cultured endothelial cells (Ma *et al.*, 2013; Zhu *et al.*, 2013). Cryptotanshinone, which occurs naturally in the herb *Danshen* has also been shown to attenuate atherosclerosis in *APO-E* null mice whilst significantly reducing LOX-1 expression and the production of adhesion molecules (Liu *et al.*, 2015).

1.6.3 Novel therapeutics

LOX-1 targeting in atherosclerosis is an area of ongoing interest, owing to its well established role in multiple stages of the formation of atherosclerotic plaque (De Siqueira *et al.*, 2015). Blocking LOX-1 in vitro has been shown to reduce the apoptotic effects of oxLDL co-incubation while transgenic animal studies have shown that LOX-1 knockout attenuates the development of atherosclerosis (Mehta Jawahar *et al.*, 2007; Li *et al.*, 2003). Studies investigating the use of anti-LOX-1 antibody in vivo report significant reductions in neointimal hyperplasia post balloon carotid artery injury and myocardial infarct size post coronary artery ligation (Hinagata *et al.*, 2006; Li *et al.*, 2002b). Additional reported effects of anti-LOX-1 antibody include reduced mesenteric artery lipid deposition in hypertensive rats and the attenuation of renal vascular fibrosis in obese diabetic hypertensive rats (Nakano *et al.*, 2010; Dominguez *et al.*, 2008).

The role of microRNA (miRNA) in atherosclerosis is a relatively novel area of ongoing research aiming to identify potential new therapies. MiRNAs are tissue

specific, small (~22 nucleotides) non-coding RNAs which regulate expression of protein coding genes within cells involved in a wide range of pathological processes, including atherosclerosis (McDonald *et al.*, 2012). Yao Dai *et al.* identified the LOX-1 targeting miRNA-98 using bio-informatics databases and demonstrated that administration of miRNA-98 affected a reduction in both lipid accumulation *in vitro*, and LOX-1 expression and aortic plaque accumulation in *APO-E* null mice (Dai *et al.*, 2018). A similar study identifies miRNA let-7g in LOX-1 targeting and attenuation of atherosclerosis (Liu *et al.*, 2017). The potential for miRNA to produce unwanted side effects due to off-target effects is concerning, however in the case of miRNA-98 this was addressed to some degree within the groups animal work and no obvious side effects or toxicity were detected (Dai *et al.*, 2018).

Using the high resolution crystal structure of LOX-1 to screen chemical libraries, novel molecules with potential LOX-1 affinity and inhibitory actions have been identified (Thakkar *et al.*, 2015). Out of 5 screen-detected molecules, 2 produced the desired effect of reducing oxLDL uptake and monocyte adhesion to human endothelial cells. Chemical inhibitors have the potential advantage of producing less immunogenic side effects in comparison with antibody therapy, however their pharmacokinetics and effects in animal studies have yet to be determined.

Single-chain variable fragment (scFv) antibodies targeting LOX-1 have only very recently been proposed as having therapeutic potential. According to recent reports, scFvs exhibit specific binding affinity, enhanced biodistribution and low immunogenicity compared with antibodies, while being potentially much cheaper to produce given that they can be expressed in bacterial cell culture (Fan *et al.*, 2014). Anti-LOX-1 scFvs are in the early stages of development and various methods have been employed aiming to improve binding affinity, thermostability and serum half-life including fusion with LOX-1 binding peptides and multimerization (Hu, Xie and Xiang, 2017; Hu *et al.*, 2018). Small interfering RNAs (siRNA) developed to target LOX-1 mRNA inhibit downstream LOX-1/oxLDL mediated pathways *in vitro* (Arjuman and Chandra, 2017). The results are promising, however further evaluation in animal studies is needed to assess their ability to attenuate atherosclerosis. The challenges facing the development of interference RNA technology are similar to that of other previously discussed

alternatives to traditional antibodies, including off-target effects and the need for an effective delivery strategy (Gavrilov and Saltzman, 2012).

1.7 LOX-1 linkage to other disease states

1.7.1 Diabetes Mellitus

Endothelial dysfunction leading to accelerated atherosclerosis occurs in diabetes mellitus, hence the potential link between LOX-1 activity and diabetes mellitus has been investigated. In 2001, Chen and co-workers examined vascular LOX-1 expression in streptozotocin-induced diabetic rats, finding that LOX-1 expression was significantly increased in diabetic rat aorta compared with controls (Chen *et al.*, 2001c). In a human study, serum sLOX-1 concentration was found to be significantly higher in patients with diabetes compared with those without and reduced in response to improved glycaemic control (Tan *et al.*, 2008). Serum sLOX-1 has been proposed as a marker for peripheral arterial disease in patients with type 2 diabetes mellitus. The authors demonstrated a significant inverse correlation between serum sLOX-1 and ankle-brachial pressure index in a group of 27 patients with known T2DM and peripheral arterial disease (Fukui *et al.*, 2013).

1.7.2 Neoplasia

OxLDL and LOX-1 are involved in mechanisms linked to tumour genesis such as cell transformation state in diverse cancer cell lines and in tumour growth (Lu *et al.*, 2011). Moreover, individuals with atherosclerotic plaques and high levels of circulating ox-LDL and LOX-1 expression seem to be more prone to develop cancer, implying a mechanistic overlap in the pathobiology of atherogenesis and tumorigenesis which most likely involves the generation of reactive oxygen species secondary to LOX-1 - oxLDL binding and subsequent oxidative DNA damage (Balzan and Lubrano, 2018).

The depletion of LOX-1 protects against tumour-genicity, motility and growth of cancer cells. The beneficial effects exerted by LOX-1 depletion are common among several lineages, such as hepatocellular carcinoma, breast and cervical

cancers (Hirsch *et al.*, 2010). Furthermore, LOX-1 was shown to be upregulated in 57% of bladder and cervix cancer cells, 11% of mammary gland cancer cells, 10% of lung cancer cells and in 20% of colorectal cancer cells in a meta-analysis of gene expression profiles of about 950 cancer cell lines (Murdocca *et al.*, 2016). Further studies have found the expression of LOX-1 is significant in gastric, colorectal, pancreatic and hepatocellular carcinoma (Balzan and Lubrano, 2018).

1.7.3 Sepsis and inflammation

The role of oxLDL and LOX-1 in leukocyte activation and microvascular perfusion disturbances has been demonstrated in an experimental endotoxaemia model in rats (Landsberger *et al.*, 2010). OxLDL and LOX-1 may play a role in the increased inflammation and capillary leakage, two factors associated with disturbances in the microcirculation in sepsis. *LOX-1* null mice had improved survival in a caecal ligation and puncture (CLP) sepsis model. *LOX-1* null mice also had lower inflammatory response to CLP, in terms of pro-inflammatory cytokine levels (e.g., TNF-alpha) in the serum and the extent of lung oedema. These mice were also able to clear the bacteria from peritoneum, blood, and lungs more than wild mice (Wu *et al.*, 2011).

The destruction of articular cartilage in rheumatoid arthritis is mediated by a series of proteinases (Burrage, Mix and Brinckerhoff, 2006). Matrix-metalloproteinases (MMP), namely MMP-1 and MMP-3 play pivotal roles and are potent biomarkers for joint destruction (Ribbens *et al.*, 2002). Kakinuma and co-workers found an increase in MMP-3 synthesis in articular cartilage cells upon activation of LOX-1 by oxLDL (Kakinuma *et al.*, 2004). Ishikawa and co-workers demonstrated that oxidative modification of LDL in the synovium human rheumatoid joints is increased. The authors blocked the production of MMP-3 by inhibiting the interaction between LOX-1 and oxLDL with LOX-1 specific antibody (Ishikawa *et al.*, 2012). This suggests that LOX-1 is a potential target in the treatment of rheumatoid arthritis in the future.

1.8 Non-antibody artificial binding proteins

1.8.1 Introduction

The utility of antibodies in therapeutics is well documented. Research and development in antibody therapy in cardiovascular and most other disease states continues (Nakagami, 2017; Ohta *et al.*, 2017; Akaishi and Nakashima, 2017; Levy, 2000; Wang and Weiner, 2008). As therapeutic agents, there are several advantages in the use of antibodies. Antibodies can be quickly generated against a wide range of target proteins and exhibit levels of affinity (in the low nanomolar or picomolar range) and specificity to their targets which surpass most chemical drugs (Gebauer and Skerra, 2009). With the wide acceptance and increasing application of antibody therapy, significant limitations have emerged. They are large multimeric proteins that require disulphide bonds and glycosylation for stability, thus their manufacture involves eukaryotic expression systems and transfection of mammalian cell lines – the optimization and fermentation of which is a lengthy and costly process (Gebauer and Skerra, 2009). Antibodies are often highly sensitive to higher temperatures, potentially impacting on clinical efficacy while increasing transportation and storage costs (Tiede *et al.*, 2014).

A variety of non-antibody artificial binding proteins have been developed to overcome the limitations of antibodies while mimicking their molecular recognition properties. In contrast to antibodies, artificial binding proteins are generally small, monomeric, thermostable and easily expressed in bacterial cell culture (Tiede *et al.*, 2014). In general, artificial binding proteins structurally comprise of a highly stable protein scaffold and a variable binding region. To name a few, these include ankyrin repeat proteins (DARPin), Repebodies, Anticalins, Fibronectins, Affibodies and engineered Kunitz domains (Table 2.1) (Binz *et al.*, 2003; Lee *et al.*, 2012; Schlehuber and Skerra, 2005; Koide *et al.*, 1998; Nord *et al.*, 1995; Nixon and Wood, 2006).

Table 1.2. Synthetic or artificial protein technologies

Adapted from cited references (Skerra, 2007; Škrlec, Štrukelj and Berlec, 2015; Martin *et al.*, 2018).

Name	Parent protein	Structure	Residues / S-S bridges	Variable regions	Selection method
Bacterial / micro-organism protein species					
ABD	Albumin binding domain	3 x α -helices	46/0	15 surface residues	Phage display, ribosome display
Affibody	Z-domain of staphylococcal protein A	3 x α -helices	58/0	13 residues in 2 helices	Phage display, ribosome display
Affitin/Nanofitin	DNA-binding protein Sac7d	5-stranded incomplete β -barrel	66/0	14 residues in β -sheet	Ribosome display
Obody/OB-fold	OB-fold of the aspartyl tRNA synthetase	5-stranded β -barrel	111/0	17 residues	Phage display
Peptide aptamer	Thioredoxin	5 β -strands surrounded by 4 α -helices	108/1	20-30 residues	Yeast two-hybrid
Human protein species					
AdNectin/Monobody	¹⁰ Fn3 (fibronectin III)	β -sandwich of 7 x β -sheets	94/0	Residues in BC, DE, and FG loops	Phage display, mRNA display, yeast two-hybrid
Affilin	γ B-crystallin/Ubiquitin	β -sheet (γ B) α/β (Ub)	176/0 (γ B) 76/0 (Ub)	8 residues (γ B) 6 residues (Ub)	Phage display (γ B) Ribosome display (Ub)
Anticalin	Lipocalin	8-stranded β -barrel	160–180/0-2	4 loops (up to 20 residues)	Phage display
Atrimer/Tetranectin	C-type lectin domain-3	5 flexible loops	40 / 3	11 residues	Phage display
Avimer/Maxibody	Multimerised LDLR-A module	4 loops	43/3	28 residues	Phage display
Centyrin	Fn3 domains of h-Tenascin C	β -sheet	89/0	13 residues	CIS display, Phage display
DARPin	Ankyrin repeat	3 x α/β	166/0	7-13 residues	Ribosome display, phage display
Fynomer	SH3 domain of the human Fyn tyrosine kinase	β -sandwich	63/0	6 residues in two loops	Phage display, DNA display
Kunitz domain	BPTI/LACI-D1/ITI-D2	α -helices, β -sheets	58/3	1-2 loops	Phage display
Microbody/Knottin	EETI-III/AGRP	3 x β -sheets	28-34/3-4	1 loop	Phage display
Pronectin	¹⁴ Fn3	2 x β -sheets and 3 surface exposed loops	90-95/0	3 loops	Phage display
Artificial / Other					
Affimer / Adhiron	Phytocystatin (plant species)	Four-strand anti-parallel β – sheet core with a central helix	100/0	2 variable peptide regions	Phage display

Alphabody	Triple antiparallel helices (artificial, <i>de novo</i> design)	3 x α -helices	70-100/0	11 residues (A and C helices)	Phage display
Armadillo repeat proteins	Armadillo (homologous to β -catenin) (artificial, consensus design)	3 x α -helices	40/0	6 residues in each repeat	Ribosome display
Repebody	Leucine-rich repeat modules of variable lymphocyte receptors (jawless vertebrates, artificial)	β -strand turn, α -helix	20-29/0	5 residues in each repeat	Phage display

1.8.2 Non-antibody artificial binding proteins: general principles

1.8.2.1 Scaffold design and consensus sequence

Enhanced thermostability of therapeutic compounds broadens the range of processes suitable for purification (e.g. heat purification), and the options available for storage and administration. One design-approach to improve thermostability in artificial protein scaffolds is the use of consensus sequence design. The consensus sequence approach to protein stabilization is based on the hypothesis that random mutations which lead to protein destabilization have a high probability of occurring during natural and in vitro evolution processes, but do not cause the stability of the protein to fall below a level that renders it inactive, therefore remaining functionally neutral. Random mutations that increase the protein stability are assumed to be much less probable due to a lack of positive selection for such increases in stability. Thus, amino acid positions in homologs that have a strongly conserved consensus residue are thought to contribute more to the stability than those positions without a clear consensus (Jacobs *et al.*, 2012). In basic terms, consensus design aims to identify frequently occurring residues at a given position (consensus residues), as they are likely to optimize stability in this position. By averaging over many residue sequences that share the same structure and function, a consensus sequence of residues is formulated (Sternke, Tripp and Barrick, 2019). Scaffold stability is particularly important in artificial binding proteins given that the insertion of variable binding regions can reduce stability (Skerra, 2007). In the affimer scaffold sequence, the inhibitory sequences within 2 loops are each replaced with a randomized sequence of 9 amino acids (Tiede *et al.*, 2014).

1.8.2.2 Phage display

The randomized amino acid sequences within the variable binding region of the protein offer the possibility of generating binding proteins to a wide range of molecular targets. Affimers use phage display technology to generate binding proteins specific to molecular targets. Alternative techniques exist in this field, including ribosome display, mRNA display, CIS display, DNA display and yeast two-hybrid system, which are not discussed. In basic terms, the phage display technique is performed in the following stages (Figure 1.7):

- Recombinant DNA coding for the artificial binding protein is amplified by PCR. PCR primers are designed to introduce a sequence of degenerate trimers (NNN), corresponding to the variable binding regions.
- The recombinant DNA is cloned in to a phagemid vector which is then transformed in to competent E. Coli cells.
- Phage expression by E. Coli cells is induced. During transcription, the degenerate sequence gives rise to mutagenesis and thus coding for random amino acid sequences within the variable binding regions of the protein.
- The phages are extracted from the E. Coli cells and suspended in solution. Each phage expresses a binding protein with a specific binding region on its surface. The solution will contain populations of phages, each population expressing on its surface a binding protein with a different binding region – the phage display library.
- The target protein is purified and immobilised in wells. The phage library is added to the wells and binders with affinity to the target protein isolated by washing and elution steps. Eluted phage is transfected in to E. Coli cells and the process is repeated in a series of panning steps.
- Highly specific high-affinity binding proteins are thus isolated from the library. Following phagemid DNA sequencing, a plasmid DNA vector encoding the isolated binding protein is created using recombinant DNA techniques.
- Plasmid DNA can then be transformed in to competent bacterial cells, allowing inducible protein expression and the extraction and purification of binding protein.

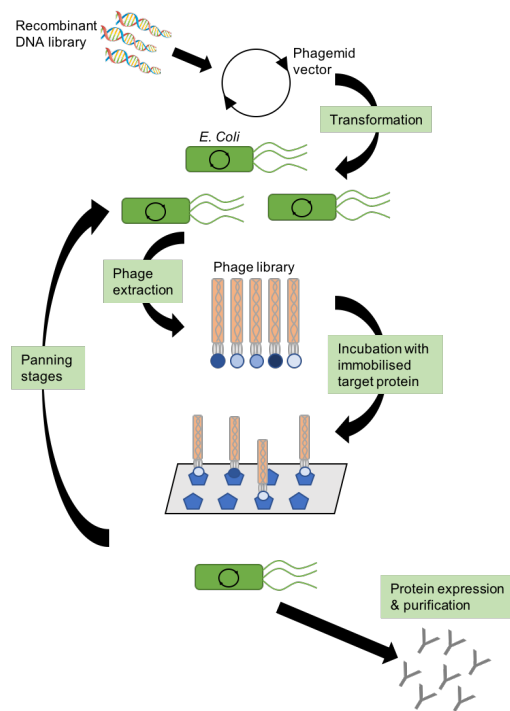


Figure 1.7. The basic concepts of phage display. A phage display library is incubated with immobilised target protein to isolate phages expressing specific binding proteins. DNA coding for specific binding proteins can be expressed in bacterial cells and purified for use as an affinity agent.

1.8.3 Affimers

At the University of Leeds M. McPherson and D. Tomlinson have developed and patented a non-antibody artificial protein scaffold named “Affimer” (Tiede *et al.*, 2014; Tiede *et al.*, 2017). Affimers are synthetic proteins based on a consensus sequence of plant-derived phytocystatins which are easily expressed in bacterial cell culture and highly thermostable ($T_m = 101^\circ\text{C}$) (Tiede *et al.*, 2014). The Affimer protein comprises the characteristic cystatin family fold of a four-strand anti-parallel β -sheet core with a central helix and contains two variable binding regions (Figure 1.8) (Tiede *et al.*, 2014). A phage-display library of variable proteins has the potential to generate distinct binding proteins to a wide range of ligands (Tiede *et al.*, 2014). To-date, affimers specific to multiple target proteins

have been generated and tested in a range of applications with translational potential (Tiede *et al.*, 2017):

- The development of MRI reagent (trivalent Gd-DOTA reagents).
- Affinity histochemistry (anti-tenascin C affimer, anti-VEGFR2 affimer).
- In-vivo imaging (anti-tenascin C affimer).
- Biosensor technology (anti-myc affimer, anti-IL8 affimer).
- Modulators of protein function (anti-p85 affimer, anti-VEGFR2 affimer, anti-TRPV1 affimer).

1.9 Hypothesis, aims and objectives

My scientific hypothesis is that LOX-1 is a key mediator of the pro-atherogenic response *in vitro* and *in vivo*. The long-term aim or goal is to develop therapeutics that could be clinically useful for vascular disease treatments. Specific experimental objectives to answer the hypothesis are:

- Test Affimers specific for LOX-1 using a tightly regulated cell expression system.
- Investigate whether LOX-1 is required for atherosclerosis *in vivo*.
- Investigate whether targeting LOX-1 *in vivo* modulates neointimal hyperplasia.

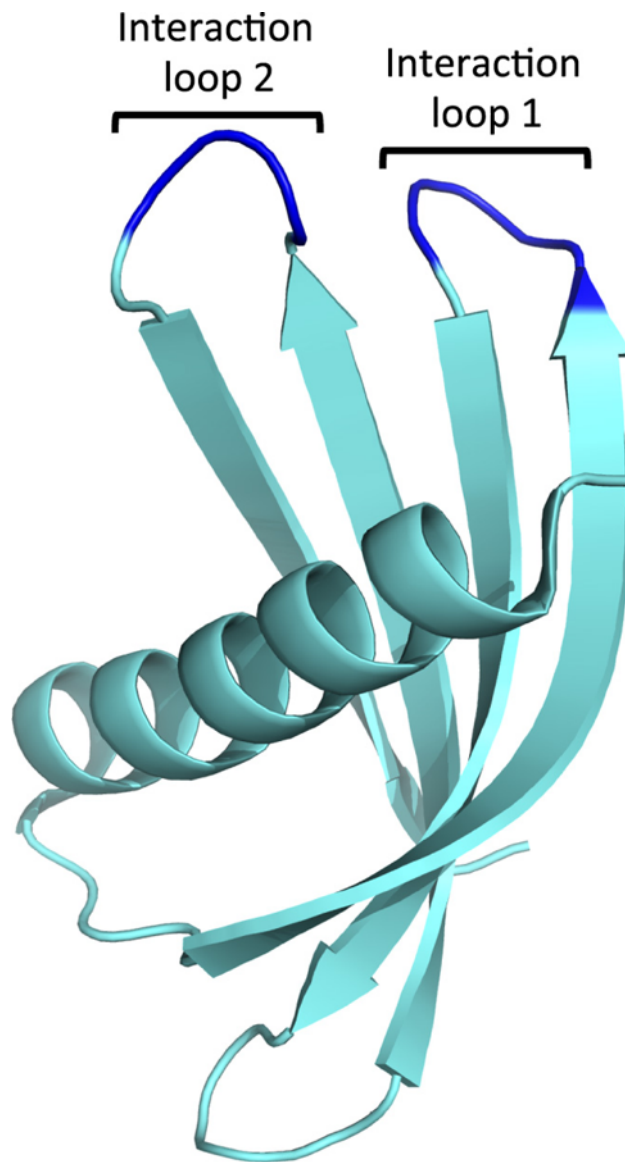


Figure 1.8. Basic structure of the affimer protein. The affimer protein comprises the characteristic cystatin family fold of a four-strand anti-parallel β -sheet core with a central helix and contains two variable binding regions (interaction loop 1 & 2).

CHAPTER 2

MATERIALS AND METHODS

2.1 Materials

2.1.1 Chemical reagents and antibodies

All chemicals were purchased from VWR, Sigma or Melford Laboratories unless stated otherwise. Bicinchoninic acid assay (BCA assay) was from ThermoFisher (Cramlington, UK) or Pierce (Rockford, USA). Enhanced chemiluminescence (ECL) reagents for Western blotting were from ThermoFisher (Cramlington, UK). Oligonucleotide primers were from Sigma-Aldrich (Poole, UK) or Integrated DNA Technologies (Coralville, USA). Cell culture media and reagents were from Invitrogen (Amsterdam, Netherlands). Isofluorane was purchased from Central Business Services at the University of Leeds.

2.1.2 Antibodies

The following antibodies were purchased: mouse anti-FLAG (Sigma-Aldrich, Poole, UK), goat polyclonal anti-LOX-1 (R+D Systems, Minneapolis, USA), horseradish peroxidase (HRP)-conjugated secondary antibody (Thermo Fisher, Cramlington, UK), AlexaFluor-488, -594 conjugated secondary antibodies (Invitrogen, Amsterdam, Netherlands). The following antibodies were produced by the Ponnambalam laboratory: sheep anti-LOX-1 (Diagnostics Scotland, Edinburgh, UK), rabbit anti-LOX-1 (Eurogentec, Seraing, Belgium).

2.1.3 Cell lines

The XL-10 gold *Escherichia coli* (*E.coli*) strain (*Tetr* Δ (*mcrA*)183 Δ (*mcrCB-hsdSMR-mrr*)173 *endA1 supE44 thi-1 recA1 gyrA1 gyrA96 relA1 lac Hte* [*F'* *proAB lacIqZDM15 Tn10 (Tetr) Amy Camr*) was from Stratagene (CA, USA). The XL-10 gold strain was used for plasmid propagation and cloning. Tetracycline-inducible LOX-1 expressing and empty vector human embryonic kidney -

HEK293T cells were kindly provided by Dr. Izma Abdul Zani (University of Leeds, UK).

2.1.4 Transgenic mice

LOX-1 knockout mice on the C56BL/6 background were kindly gifted by Professor Tatsuya Sawamura (National Cerebral and Cardiovascular Centre, Osaka, Japan). *APO-E* knockout and wild-type (C57Bl/6J) mice were purchased from Charles River (Charles River Laboratories, Margate, UK). Mice were housed in a custom-built transgenic animal facility run by Central Biomedical Services at the University of Leeds.

2.1.5 Surgical equipment

All dissections were performed using instruments purchased from World Precision Instruments (Sarasota, USA) or InterFocus (Cambridge, UK) (Figure 2.1).



Figure 2.1. Surgical instruments for animal and histological work. (A) Micro-dissecting scissors, (B) Kuehne Coverglass/Specimen Forceps, (C) Fine tip handling forceps, (D) Curved handling forceps, (D) Various straight handling forceps, (E) Metzenbaum dissecting straight scissors, (F) Iris dissecting scissors, (G) No. 3 Scalpel handle.

2.2 Experimental methods

2.2.1 Protein chemistry and analysis

2.2.1.1 Preparation of competent *E.coli* cells

E.coli XL-10 Gold cells were grown on Luria-Bertani (LB) agar (1% (w/v) bacto-tryptone, 0.5% (w/v) bacto-yeast extract, 1% (w/v) NaCl and 1.5% (w/v) agar (pH 7.0) overnight at 37°C. A single colony was then inoculated into 50 ml of LB media (1% (w/v) bacto-tryptone, 0.5% (w/v) bacto-yeast extract and 1% (w/v) NaCl, pH 7.0) and grown for ~24 h at 37°C with shaking. The stationary phase bacteria was then diluted 1:20 in fresh LB and grown until an OD₅₅₀₋₆₀₀ of ~0.3-0.6 was reached. The culture was then chilled on ice for up to 15 min followed by centrifugation for 5 min at 3000 *g* at 4°C. Cells were then resuspended in a small amount of residual LB by vortexing. 20 ml of ice-cold Tfb I (30 mM potassium acetate, 100 mM RbCl₂, 50 mM MnCl₂, 10 mM CaCl₂ and 15% (v/v) glycerol, pH 5.8) was added per 50 ml of culture and cells resuspended in the buffer then incubated on ice for up to 45 min. Cells were centrifuged for 10 min at 3000 *g* at 4°C. The pelleted cells were then resuspended in 4 ml ice-cold Tfb II (10 mM MOPS, 75 mM CaCl₂, 10 mM RbCl₂ and 15% (v/v) glycerol, pH6.5) and incubated on ice for 30 min. Cells were aliquoted and snap frozen on dry ice before storage at -70°C.

2.2.1.2 Transformation into competent *E.coli* cells

10 µl of competent *E.coli* XL-10 Gold cells were added to the DNA and incubated on ice for 5 min. Cells were heat shocked at 42°C for 1 min, and returned to ice for 3 min. Cells were plated onto LB plates containing the appropriate antibiotic and incubated at 37°C overnight.

2.2.1.3 Small scale DNA purification

5 ml of LB plus appropriate antibiotic was inoculated with a single colony of XL10 *E. coli* cells and grown at 37°C for 16 h in a shaking incubator. 1.5 ml was pelleted by centrifugation at 16000 *g*. Plasmid DNA was then purified using the Qiagen miniprep kit (Hilden, Germany) according to the manufacturer's instructions.

2.2.1.4 Affimer expression in competent E.coli cells

BL21*DE3 cells were thawed on ice. 1.5 µl of plasmid DNA is incubated with 10 µl of BL21*DE3 cells for 30 min, followed by heat shock at 42°C for 45 sec. 450 µl of SOC medium was added and incubated at 37°C for 1 h at 180-200 rpm. Cells were centrifuged at 4000 rpm and most of media removed, with ~100 µl liquid remaining. The pellet was resuspended in the remaining supernatant and plated on to LB agar + ampicillin (50 µg/ml) and incubated overnight at 37°C.

2.2.1.4.1 Inducing Affimer expression with isopropyl β-D-1-thiogalactopyranoside (IPTG)

A chosen colony from the LB agar plate was added to 3ml of LB + 1:1000 ampicillin and incubated overnight at 37°C. 1ml of culture was added to 50ml of LB + 1:1000 ampicillin and grown until optical density at 600nm reaches 0.6-0.8. At this point affimer expression was induced by adding IPTG to a final concentration of 0.1nM (5µl) and incubated for 6 hours at 25°C at 150rpm.

2.2.1.4.2 Affimer purification

Buffers were prepared as follows:

- Lysis buffer: 50 mM NaH₂PO₄; 300 mM NaCl; 20 mM Imidazole; 10% (v/v) Glycerol; pH 7.4
- Wash buffer: 50 mM NaH₂PO₄; 500 mM NaCl; 20 mM Imidazole; pH 7.4
- Elution buffer: 50 mM NaH₂PO₄; 500 mM NaCl; 300 mM Imidazole; 10% (v/v) Glycerol; pH 7.4

5 µl of 20 mg/ml lysozyme (0.1 mg/ml), 10 µl Triton X-100, 0.4 µl Benzonase, and 10µl 100 mM PMSF (1 mM) were added to 1 ml of lysis buffer, mixed and subsequently added to the cell pellet and vortexed. This was then sonicated and placed on a rotator wheel at 4°C for 20 min. This was then placed in a water bath at 50°C for 20 min. The lysate was then centrifuged to remove cell debris. The supernatant was incubated for 2 h with pre-washed (with lysis buffer) Ni-NTA agarose slurry at 4°C, then centrifuged to remove unbound protein. The cell pellet / Ni-NTA agarose slurry was placed in a 5 ml Pierce centrifuge column and

washed with lysis buffer 5x, followed by wash buffer 10x, or until A280 reading was <0.01. 500 µl of elution buffer was added to the column, incubated for 5 mins and collected off the column. Affimers were either biotinylated, conjugated with Alexafluor-488 or dialysed into PBS. Affimers were analysed by BCA and SDS-PAGE and concentrations ranged from 0.1-5 mg/ml. Affimers were snap frozen and stored in 50 µl aliquots at -70°C. .

2.2.1.5 Biotinylation of Affimers

Affimers with C-terminal cysteine were biotinylated directly after elution from the nickel-agarose column. For each Affimer, 150 ml Tris (2-carboxyethyl)phosphine (TCEP) immobilised resin (ThermoFisher Scientific) was washed and incubated with 150 ml of 40 mM Affimer solution on a rocker for 1 h. The solution was centrifuged for 1 min at 1500 g and 120 ml of the supernatant was transferred into a fresh tube containing 6 ml of 2 mM biotin-maleimide (Sigma) and incubated for 2 h at room temperature. Excess biotin linker was removed by using a Zeba spin desalting column (ThermoScientific) according to the manufacturer's protocol.

2.2.1.6 Labelling Affimers with Alexafluor-488 maleimide

The C-terminal cysteine residues were labelled with Alexafluor-488 maleimide. Affimers in elution buffer was pre-treated with TCEP resin. A 10 mM stock solution of Alexafluor-488 was made up in DMSO. This stock solution was added to the protein solution dropwise while stirring to produce approximately 10-20 moles of reagent per mole of protein, and the reaction proceeds at room temperature for 2 h protected from light. Excess reagent was removed from solution using a Zeba spin desalting column (ThermoFisher Scientific) according to the manufacturer's protocol.

2.2.1.7 Preparation of oxLDL

Buffers and solutions are prepared as follows:

Hepes buffered saline (HBS):

- 16 g NaCl per litre
- 0.4 g $\text{Na}_2\text{HPO}_4 \cdot 7\text{H}_2\text{O}$ (can use dibasic salt as well; important thing is that final phosphate conc. is 1.5 mM)
- 13 g Hepes
- ddH₂O to final volume 1 L

Sudan black:

- Make 200 ml of 60% ethanol in glass beaker
- Place on stirring platform and heat to 37°C
- Place a magnetic stirrer in the beaker when temperature has reached 37°C
- Stir in Sudan black powder until saturated (about or less than 0.5g of Sudan black)
- Cool solution to room temperature
- Filter Sudan black using filter paper into 50 ml sterile plastic tube
- Into each 50 ml of Sudan black, add 0.1 ml of 25% (w/v) NaOH solution

2.2.1.7.1 Preparation of LDL

18 ml of blood (donated by human volunteers under University of Leeds local ethics approval #BIOSCI 15-007) was drawn and transferred to a 50 ml sterile plastic tube containing 2 ml of 3.8% (w/v) trisodium citrate (9:1 ratio). Whole blood was centrifuged at 3000 rpm for 10 min at 4°C and plasma (supernatant) was pipetted off and transferred to a new tube. OptiPrep (Sigma) was added at a 4:1 ratio. Using pipette-boy with sharp glass tip, plasma was transferred into Beckman centrifuge tubes containing 1 ml HBS, filling it to the top and placing black bungs and tube collars on all tubes. After balancing tubes, they were placed

in Beckman TL-110 rotor using a Beckman Optima-MAX centrifuge running at 100 000 g for 3 h at 16°C. Tubes were wrapped in cellotape and placed in clamps. A 25-gauge needle and 1 ml syringe was used to aspirate the LDL band, which appeared bright yellow/orange (Figure 2.2). The LDL was then dialysed against 1XPBS overnight at 4°C.

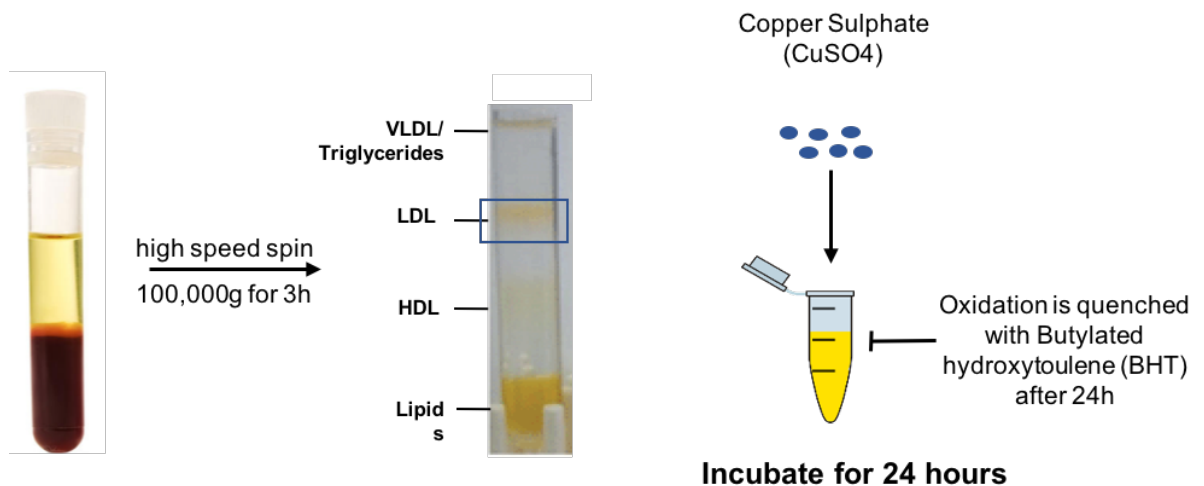


Figure 2.2. Preparation and oxidation of LDL. Plasma was extracted from whole blood and spun at 100,000 g for 3 h, separating the LDL from HDL, LDL and VLDL. LDL is then removed and oxidized by addition of CuSO_4 . HDL; high-density lipoprotein. LDL; low-density lipoprotein. VLDL; very low-density lipoprotein.

2.2.1.7.2 Oxidation and analysis of LDL and oxLDL

LDL fraction was transferred to tube and add 5 μM CuSO_4 was added and the mixture incubated at 37°C for 24 h, wrapped in tinfoil. After 24 h, 100 μM EDTA and 20 μM BHT was added and solution placed on ice. The oxLDL should have changed colour from yellow LDL to a clear solution. After dialysis against PBS, oxLDL concentration was determined by BCA assay, then LDL and oxLDL were subjected to agarose gel electrophoresis at quantity of 4 μg in each lane. The agarose gel was then added to container containing solution of 75% (v/v) ethanol

and 5% (v/v) acetic acid and incubated at room temperature for 15 min. The solution was then drained off and Sudan black stain was added to the gel and incubated at room temperature for 3 h, wrapped in foil. After draining off Sudan black, the gel is washed twice with 50% (v/v) ethanol and left overnight in 50% (v/v) ethanol, wrapped in tinfoil. The gel was then ready for imaging. Successful oxidation is demonstrated by increased electrophoretic migration of the oxLDL towards the positive anode (red) compared to LDL on the same gel.

2.2.1.8 Dil-labeling of oxLDL

OxLDL particles were labelled with the fluorescent compound 1,1 dioctadecyl-3,3,3',3'-tetramethylindocarbocyanine perchlorate (Dil; Sigma) in DMSO. 300 µg of Dil was added to each milligram of lipoprotein and incubated in the dark at 37°C for 18 h. The labelled oxLDL was then centrifuged at 13,000 rpm for 10 min before dialysing against PBS in the dark for 24 h at 4°C. The concentration of Dil-oxLDL was measured by BCA assay.

2.2.2 Protein analysis

2.2.2.1 Preparation of cell lysates

Media was aspirated from flasks and cells were washed twice in cold PBS. Cells were then lysed in 2% (w/v) SDS in PBS containing 1 mM PMSF and protease inhibitor cocktail (Roche) and scraped into microcentrifuge tubes. This was followed by incubating lysates at 95°C for 5 min and sonicated for 5 sec.

2.2.2.2 BCA assay

After preparing lysates, total protein concentration can be quantified by bicinchoninic acid (BCA) assay. On a 96-well plate, 10 µl of standard bovine serum albumin (BSA) controls at different concentration of 0, 0.2, 0.4, 0.6, 0.8, 1.0 mg/ml and 5 µl of protein samples were added in duplicates. Reagents A and B of Pierce BCA protein assay (ThermoFisher Scientific, Massachusetts, US) were mixed together in a 50:1 ratio, and 200 µl of the mixture was added into each well. The plate was then incubated at 37°C for 20 min, followed by reading at 562 nm using a Tecan plate reader connected to a PC running on Magellan

5% Stacking Gel Mix:

Can be made fresh each month and stored in the fridge at 4°C

For 200 ml:

Solution	Volume (ml)
30% Acryl	33.3
1 M Tris	25
10% SDS	2
ddH ₂ O	139.7

Protein samples were added to an equal volume of 2X SDS-PAGE sample buffer. Samples were briefly centrifuged (maximum speed, 10 sec) to collect all droplets. To separate proteins, 15% SDS-PAGE gels were made up and the gels were allowed to set for >15 min. Samples were loaded in a 5% stacking gel and subjected to electrophoresis in a discontinuous running buffer (25 mM Tris, 192 mM glycine, 0.1% (w/v) SDS) at 130V for ~2 h.

2.2.2.4 Western blotting

Buffers were prepared as follows:

Transfer buffer:

- 400 ml Methanol
- 1200 ml ddH₂O
- 200 ml 10x transfer buffer

TBS-T:

- 10 mM Tris, pH 7.5
- 150 mM NaCl
- 0.1% Tween-20

Four 6x16.5 cm strips of 3MM Whatman blotting paper and one 6x16.5 cm strip of nitrocellulose membrane per gel were pre-soaked in transfer buffer. A trimmed protein gel was inverted on to the 0.2 µm pore size nitrocellulose membrane (BioRad) and sandwiched between 2 strips of blotting paper either side. Air

bubbles are removed and the gel sandwich is placed in to a transfer cassette. The cassette was then placed in to a transfer tank filled with transfer buffer. Transfer was performed at 300 mA for 3 h or overnight (~16 h) at 30 mA at 4°C. To confirm transfer is complete, the nitrocellulose membrane was removed and placed in a glass dish containing enough Ponceau S solution to cover the membrane. Visible bands confirm successful transfer of proteins to the membrane. Ponceau S solution was poured back to its bottle for re-use. Remaining Ponceau S was rinsed off with ddH₂O followed by washes with TBS-T. The membrane was then incubated in 50 ml (or enough to cover the membrane) 1-5% (w/v) non-fat skimmed milk in TBS-T for ≥ 30-60 min, followed by rinsing with TBS-T. 1° antibody was diluted into 1% (w/v) non-fat skimmed milk in TBST to 1:1000-10 000 of serum final concentration. The nitrocellulose membrane was incubated on a rocker in 10 ml of 1° antibody overnight or over the weekend at 4°C in a sealed plastic bag. 1° antibody solution was then removed and membrane was washed 3 times with TBS-T. 2° antibody was diluted to 1:2500 in 10 ml TBS-T with 1% milk and then added to washed membrane blot and incubated on a rocker for 1 h at room temperature. The 2° antibody was removed and the membrane is washed 3 times for 10 min each time with TBS-T. A working concentration of enhanced chemiluminescence (ECL) solution was made up by mixing reagents A and B in a 1:1 ratio (500 µl total volume per membrane strip). The ECL solution was pipetted onto a sheet of plastic acetate covering an area that corresponds to the size of the membrane and the membrane blot was inverted a few times onto the ECL solution, ensuring no air bubbles are trapped between the membrane and acetate sheet. After leaving to stand for 1 min, the membrane blot was sandwiched with another plastic acetate sheet, and with protein-antibody sandwich facing upwards, placed inside the chemiluminescence workstation for digital imaging.

2.2.2.5 Cross-reactivity ELISA using Affimers

Buffers were prepared as follows:

Buffer A:

- 0.0025 M NaH₂PO₄·2H₂O
- 0.0075 M Na₂HPO₄·2H₂O

- 0.145 M NaCl
- pH 7.2

Buffer B:

- To 1 L of Buffer A, add:
 - 2 ml Tween-20
 - 20.75 g NaCl

Buffer E:

- 1.5 M H₂SO₄

An Immunosorp 96-well ELISA plate (Nunc) was coated with 100 µl triplicates of 0.1 and 1.0 µg/ml of human and mouse soluble LOX-1 protein in buffer A overnight. Plate was then washed and blocked with 1% (w/v) BSA. 100 µl of 1 µg/ml biotinylated Affimer in buffer B was added to each well and incubated for 2 h at room temperature on plate shaker. Streptavidin-HRP was then added to each well at 1 µg/ml in buffer B and incubated for 1 h at room temperature on plate shaker. 100 µl of TMB liquid substrate (Sigma-Aldrich) was then added to each well after washing and reaction stopped after 30 min with buffer E.

2.2.3 Cellular studies**2.2.3.1 Cell culture**

Epithelial human embryonic kidney 293 (HEK293) cell line and Flp-In™ T-Rex™ -293 cell line were cultured in Dulbecco's modified eagle medium (DMEM; Gibco, Cramlington, UK) containing 10 U/ml penicillin, 100 µg/ml streptomycin, 2 mM L-Glutamine, 1X non-essential amino acids and 10% (v/v) foetal calf serum (FCS; Life Technologies, Paisley, UK).

Cells were incubated at 37°C in a hydrated 5% CO₂ atmosphere and passaged every 2-3 days by incubation with PBS-EDTA. Cells were incubated with PBS-EDTA at 37°C for 3-5 min. PBS-EDTA solution was then carefully aspirated from

the plate. The plate was then tapped gently 5 times before cells were washed off using DMEM and split at the appropriate ratio. If plating on to coverslips, coverslips were coated with filter-sterilized poly-L-lysine (1 mg/ml) / pig skin gelatin (0.05% w/v) mixture in PBS for 1-2 h in a 24-well plate. The mixture was then aspirated from the coverslip and cells resuspended in DMEM were plated on to the coverslip in aliquots of 300 μ l at an appropriate confluence.

2.2.3.2 Immunofluorescence analysis

Media was aspirated from cells seeded on poly-L-lysine (Sigma-Aldrich, Poole, UK) coated coverslips in 24-well plates and cells were rinsed twice in PBS. Cells were fixed in 500 μ l 10% (v/v) formalin (Sigma-Aldrich, Poole, UK) for 5 min at 37°C. Fixative was aspirated and coverslips rinsed twice in PBS. Coverslips were then incubated in 0.5% (w/v) BSA in PBS to block non-specific antibody binding to cells, followed by washing twice in PBS. Coverslips were inverted onto a 25 μ l drop of primary antibody solution diluted in 0.1% (w/v) BSA in PBS (Table 2.1) in a moist staining chamber and incubated overnight at room temperature. Coverslips were washed 3 times with PBS and inverted onto a 25 μ l secondary antibody solution containing 4 μ g/ml donkey Alexa Fluor-conjugated secondary antibody (Invitrogen, Amsterdam, Netherlands), 2 μ g/ml 4,6-diamidino-2-phenylidole (DAPI) in 1% (w/v) BSA in PBS and incubated for 2 h at room temperature. Coverslips were washed 3 times with PBS and mounted onto slides using Fluoromount G (Southern Biotech, Alabama, US). Images were acquired either using a wide-field deconvolution microscope DeltaVision (Applied Precision Inc., Issaquah, US) or an EVOS-fl inverted digital microscope (Life technologies, Paisley, UK). Relative protein levels or co-distribution were analysed and quantified using Image J (NIH, Bethesda, US).

2.2.3.3 Cell immunofluorescence using Affimers

Non-permeabilised LOX-1 expressing HEK-293-T cells were incubated with increasing concentrations of Alexafluor-488 labelled Affimer in DMEM on ice for 2 h. To assess inhibition of oxLDL uptake, HEK293T cells pre-incubated with Affimer as described were then incubated with Dil labelled oxLDL. After washing

steps with PBS, cells were fixed with 3% (w/v) PFA and coverslips mounted as previously described.

2.2.4 Animal studies

2.2.4.1 Animal husbandry

All mice were housed in individually ventilated cages at no more than 5 per unit. Animals only shared a cage with siblings of the same sex. The complex lighting was on a 'fade up-fade down', 12 h light and 12 h dark cycle from 0630 to 1830. Room temperature was 21°C +/- 2°C. Standard chow feed (Rat and Mouse No.1 Maintenance; Special Diet Services, Essex, UK) and water were available *ad libitum*. Mice were checked upon daily. Breeding cages were set up with 1 male and 2 females over the age of 8 weeks. Pups were weaned at 18 days and ear notched for identification thereafter. Stringent records were kept of husbandry and experimental procedures. Any mice displaying stunted development or overly aggressive behaviour were excluded from experiments. Mice were fed with 0.2% cholesterol Western diet (Special Diet Services, Essex, UK) for 12 weeks from 8 weeks of age. Before 8 weeks old, they were fed standard chow (Special Diet Services, Essex, UK). Feed was available *ad libitum* and animals were weighed weekly.

2.2.4.2 DNA extraction for genotyping

Ear notches were taken from mice in accordance with Home Office regulations. DNA from ear notches were extracted using MyTaq Extract PCR kit (Bioline, London, UK) according to the manufacturer's instructions. Briefly, 20 µl of buffer A, 10 µl of buffer B and 20 µl deionized water were added and vortexed. The mixture was incubated at 75°C for 5 min followed by further incubation at 95°C for 10 min. The mixture was then spun down for 1 min at top speed. The extracted DNA in the supernatant was diluted 1:9 with deionized water and used for PCR analysis.

2.2.4.3 Genotype analysis using polymerase chain reaction (PCR)

PCR amplification of DNA was carried out using MyTaq HS Red mix (Bioline, London, UK) according to manufacturer's guidelines. For *LOX-1* and *APO-E* PCR, 1 µl of DNA was mixed on ice with 12.5 µl MyTaq HS Red mix, 0.5 µl of 20mM primers (table 2.3) and top it up to 25 µl with deionized water. PCR was carried out using a Biometra TProfessional thermocycler (Göttingen, Germany).

Table 2.1. Primer sequences for DNA genotyping

<i>LOX-1</i>	
Forward	5'- CGC CAA CCA TGG CTA TGG GAG AAT GG -3'
Reverse	5'- CAG CGA ACA CAG CTCCGT CTT GAA GG -3'
<i>APO-E</i>	
Common	5'- GCC TAG CCG AGG GAG AGC CG -3'
Wild-type reverse	5'- TGT GAC TTG GGA GCT CTG CAG C -3'
Mutant reverse	5'- GCC GCC CCG ACT GCA TCT -3'

Electrophoresis of DNA samples from PCR was carried out using 1-2.5% (w/v) agarose gels containing 1 µg/ml ethidium bromide in 0.5X TAE buffer (2 mM Tris, 1 mM acetic acid, 0.5 mM EDTA, pH 8) or 0.5X TBE buffer (45 mM Tris, 45 mM boric acid, 1 mM EDTA, pH 8). Gels were run in 0.5X TAE or 0.5X TBE buffer at 100 V for ~1 h. DNA was visualised in a G:BOX XT4 Chemi imaging workstation (Syngene, Cambridge, UK).

2.2.5 Animal experimental procedures

2.2.5.1 Glucose tolerance test

Mice were fasted from feeding for 16 h. A single tail wound was then created using a 20 gauge needle and a blood drop put onto a glucose test-strip (SD

Codefree glucose test strips, SD biosensor, South Korea) to obtain a baseline fasting glucose measurement using an Accu-Check Aviva Nano system (Hoffmann-La Roche, Basel, Switzerland). 1 mg per g total body weight of 10% sterile glucose solution was then injected intraperitoneally and further blood glucose measurements were obtained by expressing blood from the wound at 30, 60, 90 and 120 min. Mice were monitored for 1 h post procedure.

2.2.5.2 Insulin tolerance test

Mice were fasted from feed for 4 h and a baseline fasting glucose measurement was taken as described above. 0.75 IU/kg sterile actrapid insulin (0.1 IU/ml in 1XPBS) was then injected intraperitoneally and further blood glucose measurements were obtained by expressing blood from the tail wound at 30, 60, 90 and 120 min. During the procedure mice exhibiting signs of severe hypoglycaemia or giving blood glucose readings of <1.5 mmol/L were treated with 1 mg per g total body weight of 10% glucose solution intraperitoneally and excluded from the experiment. Mice were monitored for 1 h post procedure.

2.2.5.3 Induction and maintenance of anaesthesia

Mice were placed in an anaesthetic chamber. 2 L/min oxygen and 5 L/min isoflurane were administered to achieve full anaesthesia (unresponsive to stimulus, reduced respiratory rate). Mice were then transferred to a warmed operating table (37°C) and anaesthesia maintained by administering oxygen and isoflurane, both at 2L/min via a veterinary face mask throughout the procedure. On completion, mice were given 0.25 mg/kg of buprenorphine (Vetergesic, Reckitt Benckiser Healthcare, Hull, UK) and a 500 µl bolus of 0.9% saline intraperitoneally. The isoflurane was withdrawn and oxygen continued at 2 L/min for 1-2 min. Mice were then transferred to a pre-warmed (37°C) recovery cage and monitored every 30 minutes until full recovery from anaesthesia.

2.2.5.4 Femoral artery wire injury

At 16 weeks of age (8 weeks of Western diet), anaesthesia was induced and maintained as described above. The mice were placed supine with the legs extended, abducted and externally rotated. Positioning was secured using

surgical tape. The left leg and lower abdomen was initially shaved. To optimize hair removal, veet cream was then applied to the area and removed after 2 min using a cotton bud. Skin was then cleansed using 70% (v/v) ethanol solution. The procedure was performed with the aid of a surgical microscope (Carl Zeiss, Thornwood, USA) under the appropriate magnification (~X10 → X20). A longitudinal groin incision was made, crossing the inguinal ligament. The femoral vessels are exposed at two sites: immediately distal to the inguinal ligament and distal to the epigastric artery. The segment of femoral artery between the origins of the epigastric and saphenous arteries was dissected free from the neurovascular bundle and encircled with a loosely tied 8/0 vicryl suture (Ethicon, Somerville, USA) (Figure 2.3). The femoral artery was clamped immediately distal to the inguinal ligament and an arteriotomy is made 1 mm distal to the origin of the epigastric artery. A 0.25 mm diameter angioplasty guidewire was introduced via the arteriotomy and the clamp released. The guidewire was then advanced and withdrawn 3 times to the level of the aortic bifurcation. The wire was then removed and the arteriotomy site is ligated using the 8/0 vicryl suture. The skin incision was closed using a continuous 6/0 vicryl suture. Anaesthesia was then completed as described above and the mice are placed in a pre-warmed (37°C) recovery cage and monitored every 30 minutes until full recovery from anaesthesia.

2.2.5.5 Osmotic pump implantation

Alzet ® osmotic pumps (Model 1004, Charles River Laboratories, Wilmington, USA) were pre-loaded with 100 µl of 1mg/ml LOX-1 specific affimer in 1XPBS in accordance with manufacturer's instructions. At 12 and 16 weeks of age (4 weeks and 8 weeks of western diet), anaesthesia was induced and maintained as described above. At 12 weeks of age, mice were positioned prone and an area extending from the base 2cm caudally was shaved and cleansed. A 1 cm longitudinal incision was made in the midline, immediately caudal from the base of the skull. A closed artery forcep was advanced bluntly within the subcutaneous layer to create a tract extending to the right flank. An osmotic pump containing 1mg/ml LOX-1 specific affimer in 1 X PBS was advanced in to the tract to the right flank using the artery forcep. The wound was closed using a continuous 6/0

vicryl suture and the mice recovered as described above. At 16 weeks of age, the procedure was repeated by re-opening the same incision, but by placing the second osmotic pump in the contralateral flank. The skin incision was closed and the mouse recovered in the same fashion as before.

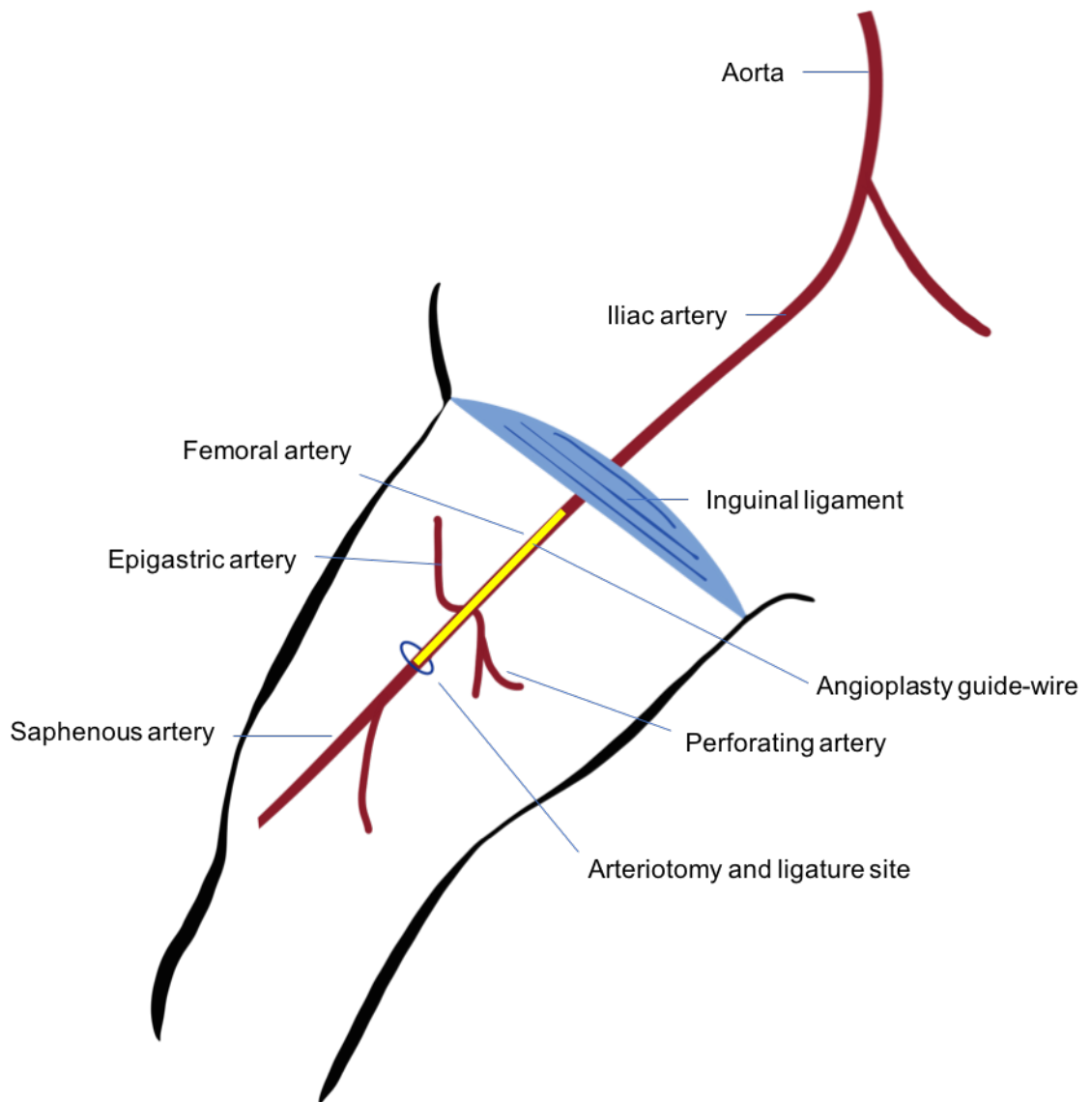


Figure 2.3. Anatomy of femoral artery wire injury. Demonstrating the basic anatomical landmarks for femoral artery wire injury.

2.2.5.6 Tissue harvesting

Isoflurane (CBS, University of Leeds) anaesthesia was induced and a cardiac puncture technique was performed to withdraw blood. Mice were laid on their back, and using a 1 ml syringe and a 22-gauge needle, needle was inserted perpendicular to chest wall, straight to the apex of the heart in the left ventricle. Blood was slowly withdrawn by gently pulling back on the plunger to obtain the maximum amount of blood available. Blood was transferred to heparin-coated tubes and immediately placed on ice. This was followed by performing a midline laparotomy. The abdominal contents were displaced to the right. 5 ml of PBS was slowly perfused into the left ventricle to flush out any remaining blood. Using the same needle, 10 ml of 4% (w/v) PFA was perfused to achieve fixation. Following fixation, organs were dissected out and placed in to cassettes in 4% (w/v) PFA for further processing.

2.2.5.7 Vascular harvest

Aorta

The aorta was exposed from the heart to the iliac bifurcation and carefully dissected from the surrounding tissue. Minor branching arteries were cut off and the adventitia is removed as much as possible *in situ*, being careful not to tear the aorta. The aorta was divided at its root and placed in a 1.5 ml Eppendorf tube on its side, half full with 4% (w/v) PFA, allowing the aorta to straighten and avoiding folding. The aorta was then prepared under microscopy by stripping away the residual fat and adventitia. It was then opened longitudinally along its ventral surface and following the inner curvature of the aortic arch. Oil red-O staining of the aorta was then carried out to visualize lipid- and fat-enriched plaques or lesions.

Carotid artery

The midline thoracotomy incision was extended to open the ventral surface of the neck, exposing the salivary glands. Glandular tissue and surrounding fat was moved laterally by blunt dissection and the trachea is dissected out to the level of the larynx to expose the oesophagus and common carotid arteries. The oesophagus and carotid arteries were taken *en-bloc* as high as possible to the

level of the jaw. If taken high at the level of the jaw, the carotid bifurcation should be within the distal third of the specimen.

Femoral artery

The iliac bifurcation was left intact after harvesting of the aorta. The hind-limbs were opened along their medial surface (anterior when mouse is in position as described in 2.2.7) from the pelvis to the level of the knee. The femoral vessels were dissected out along with surrounding musculature to the level of the iliac bifurcation, which was kept intact. The result should be a single specimen comprising of the iliac bifurcation and both femoral arteries to the level of both distal saphenous arteries.

2.2.6 Histological preparation

Histological preparation was carried out in the following steps:

- Fixation (Described in 2.2.7)
- Processing
- Embedding
- Microtomy
- Staining
- Analysis

2.2.6.1 Processing

Due to the hydrophobic nature of embedding paraffin, specimens must be chemically dehydrated and cleared of lipids to allow penetration of paraffin during the embedding process. Fixed harvested tissues within cassettes were sent for processing to the histopathology lab at St. James University Hospital (University of Leeds, UK). Processing was carried out and data collected by an automated imaging system.

2.2.6.2 Embedding

The embedding station was warmed and tissue cassettes were placed in a container of liquid paraffin for 30 min. Each organ / tissue element was placed an

appropriate mould in the desired orientation and the mould filled with liquid paraffin to half full. The mould was then placed on a cold (4°C) surface to solidify the paraffin and hold the specimen in the desired position. An embedding ring was then placed on top of the mould and the paraffin in poured in to reach the top of the ring. The mould was then placed on the cold surface for 20-30 min to allow the entire block to solidify. Once this has occurred, the ring can be gently removed from the mould along with the paraffin block for microtomy or storage. I recommend storage at room temperature as cutting the block in preparation for microtomy may lead to cracking and potential damage of the specimen if storage has been stored at 4°C. If this does happen, the block must be handled carefully and re-embedded.

2.2.6.3 Microtomy

A water bath of ddH₂O at 45-50°C was prepared. At room temperature, the block was cut on its distal surface in to a trapezium as shown in Figure 2.4. The block was then placed face-down in ice for 20-30 min. Instruments used for microtomy (fine forcep, small paint brush) should also be placed in the ice for this time. The ring was placed in the microtome (Leica Biosystems, Germany) and a microtome blade (S35: 80mm / 8mm / 35°, Feather, Japan) was loaded. 5 µm sections were cut. At intervals of 100 µm, a ribbon of 8-10 slices was placed in the water bath and transferred to an uncoated microscopy slide for viewing. Once the desired level was reached (carotid bifurcation, femoral bifurcation, femoral artery) (Figure 2.5), the process was repeated using a poly-l-lysine-coated microscopy slide. The slide was labelled and set aside in an upright position in a drying rack before storage at room temperature.

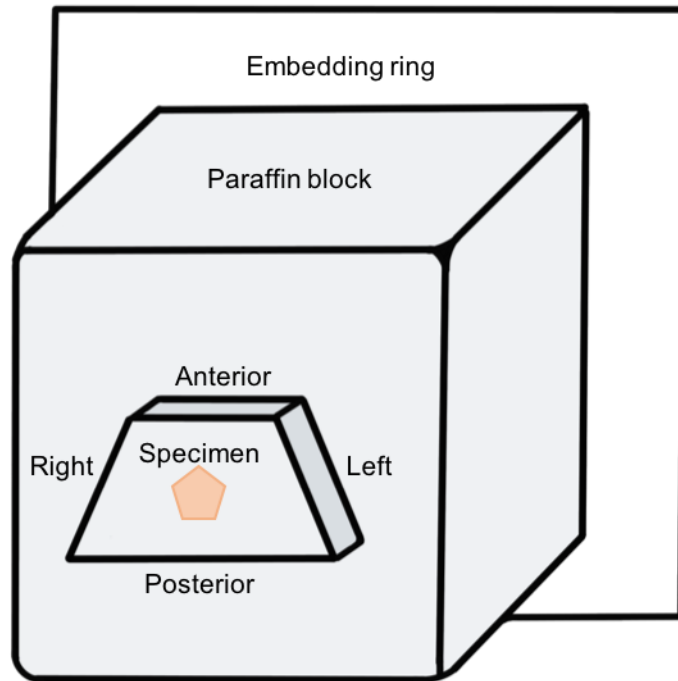


Figure 2.4. Orientation of specimen in embedding paraffin. The trapezium cut around the specimen is such that the short edge represents the anterior aspect of the specimen in the anatomical position.

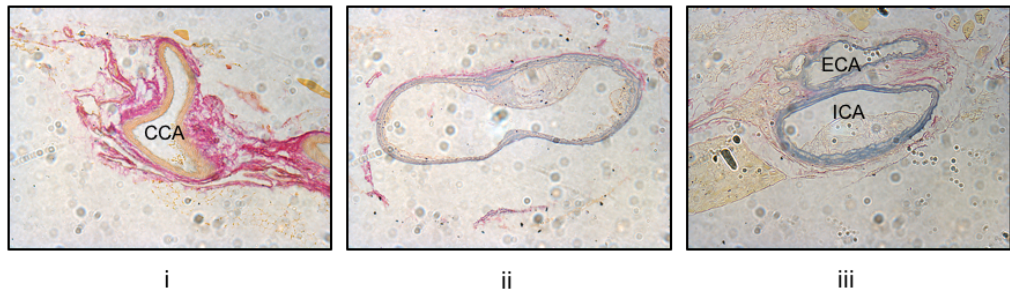
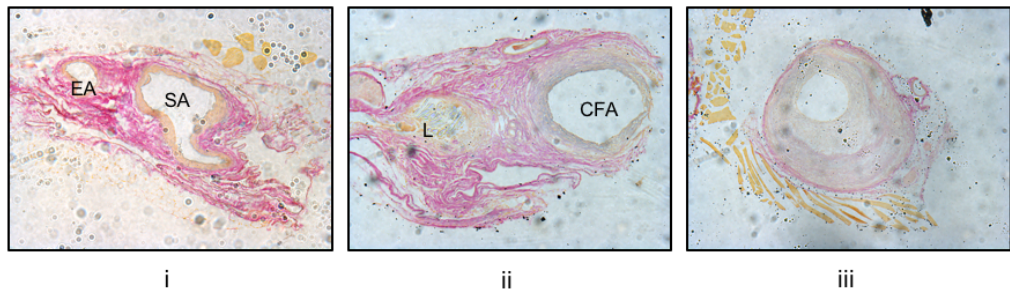
A**B**

Figure 2.5. Microtomy of carotid and femoral arteries: anatomical landmarks. (A) Carotid artery: (i) common carotid artery (CCA), (ii) bifurcation of common carotid artery, (iii) internal carotid artery with plaque (ICA), external carotid artery(ECA). (B) Femoral artery: (i) saphenous artery (SA) and epigastric artery (EA), (ii) ligature (L) and common femoral artery with degree of neointimal hyperplasia (CFA), (iii) common femoral artery with neointimal hyperplasia.

2.2.7 Histological staining

2.2.7.1 Oil red O staining

Stock oil red O stain was prepared by dissolving 0.5 g of oil red O in 100 ml of isopropanol while gently heating in a water bath. The solution was covered from light. Prior to use, 30 ml of stock stain was diluted in 20 ml of ddH₂O and allowed to stand for 10 min before being filtered. The prepared aorta was placed in 60% (v/v) isopropanol for 5 min. It was then placed in an Eppendorf tube containing oil red O and covered from light. The tube was then placed in a 50 ml falcon tube and put on a rotating platform for 1 h. The aorta was then removed from the oil red O and washed in 60% (v/v) isopropanol followed by ddH₂O. The stained aorta was then mounted on a 64 mm microscope slide for viewing and analysis.

2.2.7.2 Elastin staining with Miller and counter staining with Van Gieson

The following solutions are required:

- Xylene: 100% solvent (Sigma or ThermoFisher). NB: toxic, handle under fume hood.
- Ethanol 100% (Sigma).
- Potassium Permanganate KMnO₄ 0.5 % (Product Number: 223468, Sigma). Prepare by dissolving 2.5 g in 500 ml of ddH₂O. Store in bottle protected from light at room temperature. Prepare fresh when it changes colour from dark purple to brown.
- 2% Oxalic Acid (Product Number: 75688, Sigma). To prepare 2% solution dissolve 8 g of powder in 400 ml of ddH₂O. Store in bottle protected from light at room temperature. Prepare fresh once becoming non-clear (slightly brown from bleaching after KMnO₄).
- Miller stain 100% solution (Product number: RHS-235 500ml, Cell Path).
- Van Gieson stain made by diluting ready bought Van Gieson solution with picric acid to achieve bright orange/red coloured dye. Store in bottle protected from light at room temperature.
- DPX mountant (Product number: 06522, Sigma).

Before staining slides were dried in oven (37°C) overnight. Staining was carried out in fume hood to avoid inhalation of harmful solvents. Slides were placed in a rack for staining; each rack holding 25 slides. Chemicals and staining solutions were placed in jars designed for holding and submerging racks. Each rack was moved through 3 consecutive jars of deparaffinising xylene, for 3 min at a time, followed by 3 consecutive jars of 100% ethanol, also for 3 min each. The rack was then submerged briefly in a basin of tap-water to wash off ethanol. The rack was then washed briefly in ddH₂O before being placed in a covered jar of 0.5% (w/v) KMnO₄ for 10 min. The rack was washed in tap-water, followed by ddH₂O as before. The sections at this point were expected to turn brown in colour. The rack was then placed in a jar of 2% oxalic acid until sections turned translucent / white (1-2 min). The rack was then washed in tap-water, followed by ddH₂O and then placed in 100% ethanol for 5 sec before being placed in a covered jar of Miller stain. The racks were left in Miller stain for 1 h. They can be left for longer, however the time in Miller stain should remain consistent across all specimens throughout the experiment. Once Miller staining was complete, the rack is then placed in 6 consecutive jars of re-used 100% ethanol ranging from the most contaminated with Miller stain (dark blue) to the cleanest (colourless). The rack was then placed in tap-water followed by ddH₂O, followed by a covered jar of Van Gieson stain for 20 min. The rack was then washed in 2 consecutive jars of ddH₂O. The racks were then dried by tapping on tissue paper and placed in an oven at 70°C until completely dry (normally 20-30 min). The rack was then placed in 3 consecutive jars of xylene for 3 min each, leaving the rack in the final jar of xylene while each slide is individually mounted on 64 mm coverslips using DPX mounting solution. Slides were left to dry in the fume hood for 1-2 h before analysis or storage.

2.2.7.3 Haematoxylin and Eosin staining

The following solutions are required:

- Xylene: 100% solvent (Sigma or ThermoFisher). NB: toxic, handle under fume hood.
- Ethanol 100% (Sigma).

- Scott's tap water
 - In 1 L of deionised H₂O dissolve:
 - i. 2 g NaHCO₃
 - ii. 20 g MgSO₄
- 1% acid alcohol
- 1ml concentrated HCl in 99 ml 70% (v/v) ethanol
- Haematoxylin solution (Sigma).
- Eosin solution (Sigma)
- DPX mountant (Product number: 06522; Sigma).

Before staining slides were dried in oven (37°C) overnight. Staining was carried out in fume hood to avoid inhalation of harmful solvents. Slides were placed in a rack for staining; each rack holding 25 slides. Chemicals and staining solutions were placed in jars designed for holding and submerging racks. Each rack was moved through 3 consecutive jars of deparaffinising xylene, for 3 min at a time, followed by 3 consecutive jars of 100%, 95% and 95% ethanol respectively, also for 3 min each. The rack was then submerged briefly in a basin of tap-water to wash off ethanol. The rack was then placed in pre-filtered haematoxylin solution for 3-5 min, followed by tap-water and ddH₂O to wash. The rack is then dipped twice in 1% acid alcohol. At this point it is important to check under microscope that haematoxylin has not been washed out. The rack was then washed in tap-water for 1 min, followed by Scott's tap water for 1-3 min (until sections turn blue). The rack was then washed in tap-water followed by ddH₂O (removes alkali from Scott's tap water otherwise eosin will not stain). The rack was then placed in 5% eosin solution for 5 min, followed by tap-water for 5 min and finally washed in ddH₂O. The rack was then placed in 3 consecutive jars of 100% ethanol for 3 min each, followed by 3 consecutive jars of xylene also for 3 min each, leaving the rack in the final jar of xylene while each slide is individually mounted on 64mm coverslips using DPX mounting solution. Slides were left to dry in the fume hood for 1-2 h before analysis or storage.

2.3 Histological analysis

All histological analysis was performed using an Olympus BX41 microscope (Olympus, Japan) in conjunction with Image-Pro Plus software (Media Cybernetics, USA). To measure total aortic plaque, first a line was drawn around the aorta ensuring that arch and distal branches are not included. Total plaque area was divided over the aortic surface area for the final % value (figure 2.6). Cross-sectional plaque area at the carotid bifurcation and common femoral artery were measured as described in Figure 2.6. For the measurement of % neointimal hyperplasia (NIH), the adventitia was the most reliable landmark for the outermost layer of the artery and was used in a modified calculation to include the medial and neointimal layers:

$$\text{NIH \%} = (\text{adventitial area} - \text{lumen area}) / \text{adventitial area}$$

2.4 Statistical analysis

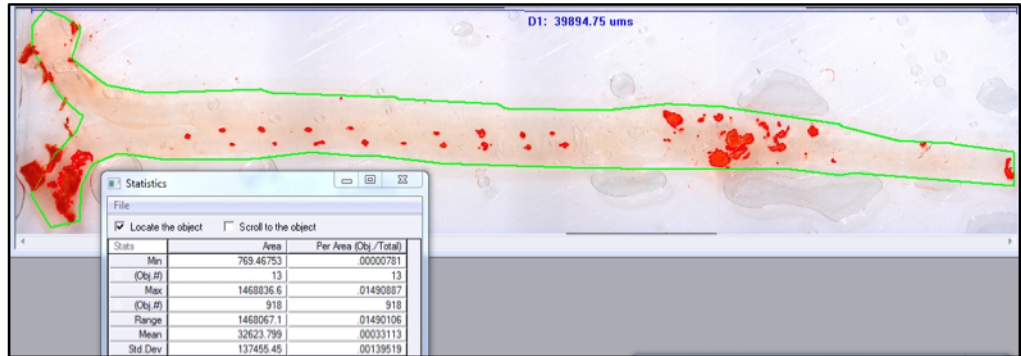
This was performed using the unpaired two-tailed Student's t-test for 2 groups or one-way analysis of variance (ANOVA) followed by Dunnett's post-hoc test for multiple comparisons using GraphPad Prism software (La Jolla, CA, US). Significant differences between control and test groups were evaluated with p values less than 0.05 (*), 0.01 (**), 0.001 (***) and 0.0001 (****) indicated on the graphs. Error bars in graphs denote \pm SEM (Standard error of mean).

2.5 Home Office License and ethical approval for animal studies

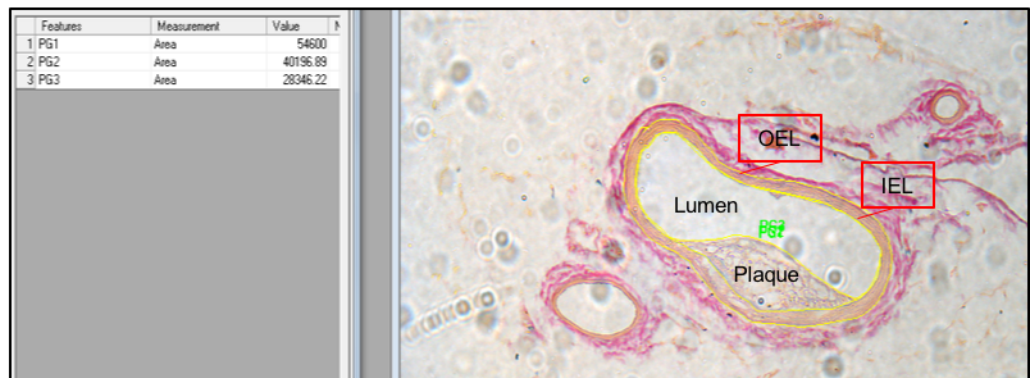
All animal studies were carried out by researchers holding a Home Office Personal License and under a Home Office Project License held by Professor Stephen Wheatcroft (Project License number: P144DD0D6). Ethical approval was granted by the University of Leeds Ethics Committee.

The severity of femoral artery wire injury and osmotic pump implantation were graded as moderate.

A



B



$$\text{Total plaque \%} = \frac{\text{IEL area} - \text{Lumen area}}{\text{OEL area}} \times 100$$

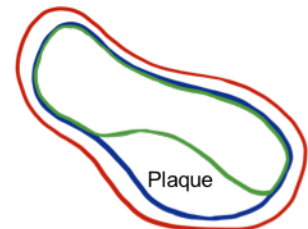


Figure. 2.6. Measuring atherosclerotic plaque area. (A) Total plaque area (%) is measured as plaque area (red) divided by total aortic surface area (area within green line). The measurement is repeated by 2 independent investigators and the final result is taken as the mean. (B) Total plaque / NIH area is calculated from a cross-section of the vessel. IEL; internal elastic lamina. OEL; outer elastic lamina. NIH; neointimal hyperplasia.

CHAPTER 3

CELLULAR STUDIES ON LOX-1 FUNCTION

3.1 Introduction

Monoclonal antibodies are the most commonly used affinity agents in biomedical research. They play an important role in the treatment of a range of pathologies including autoimmune, cardiovascular and infectious diseases, cancer and inflammation. Despite their widespread use, there are a number of known drawbacks including high molecular weight, limited tissue penetration, instability, high production cost, requirement for large doses, and potential immunogenicity (Chames *et al.*, 2009). Non-antibody synthetic protein scaffolds are low molecular weight molecules and affinity tools which mimic the molecular recognition properties of antibodies (Škrlec, Štrukelj and Berlec, 2015). They can be expressed in bacterial cell culture; reducing production costs, and are thermostable at a wide range of temperatures. The Affimer is a small (approximately 100 amino acid) synthetic protein scaffold which has been developed at the University of Leeds by McPherson and Tomlinson (Tiede *et al.*, 2014). Affimers are based on plant-derived phytocystatin sequence. They are monomeric, highly soluble, thermostable at temperatures up to 101°C and can be expressed in bacterial cell culture. Studies have demonstrated specific binding of Affimers to targets such as vascular endothelial growth factor receptor and tenascin C in cells, fixed tissue and *in vivo* (Tiede *et al.*, 2017). Affimers, as part of a wider spectrum of synthetic protein scaffolds, have potential as novel agents in diagnostics and therapeutics in cardiovascular disease, given their ability to bind a wide range of targets.

The LOX-1 scavenger receptor is implicated in the development of atherosclerosis partly due to its role in macrophage binding and internalization of oxLDL (Chistiakov, Orekhov and Bobryshev, 2016). This leads to the formation of foam cells which accumulate within the sub-endothelial layer, triggering an inflammatory cascade resulting in atherosclerotic plaque formation (Chistiakov,

Orekhov and Bobryshev, 2016). LOX-1 is a membrane protein consisting of 4 domains; a short N-terminal cytoplasmic, a transmembrane, a connecting neck, and a lectin-like domain at the C terminus which binds oxLDL (Zani *et al.*, 2015). Blocking LOX-1 *in vitro* has been shown to reduce the apoptotic effects of oxLDL co-incubation while transgenic animal studies have shown that LOX-1 knockout attenuates the development of atherosclerosis (Mehta Jawahar *et al.*, 2007; Li *et al.*, 2003). Studies investigating the use of anti-LOX-1 antibody *in vivo* report significant reductions in neointimal hyperplasia post balloon carotid artery injury and myocardial infarct size post coronary artery ligation (Hinagata *et al.*, 2006; Li *et al.*, 2002b). Additional reported effects of anti-LOX-1 antibody include reduced mesenteric artery lipid deposition in hypertensive rats and the attenuation of renal vascular fibrosis in obese diabetic hypertensive rats (Nakano *et al.*, 2010; Dominguez *et al.*, 2008).

Phage-display screening has identified 5 isoforms of LOX-1 specific Affimer. Affimer binding to the LOX-1 SR has the potential to attenuate the formation of atherosclerosis by interfering with the internalization of oxLDL in vascular cells. The aim of this chapter is to quantify Affimer-LOX-1 binding and investigate their effect on oxLDL internalization *in vitro*.

3.2 Results

3.2.1 Expression, purification of LOX-1-specific Affimers

As previously discussed, one potential advantage of using recombinant proteins as antibody mimetics is that they can be expressed in bacterial cell culture. The advantages of *Escherichia coli* (*E. coli*) as a host organism in recombinant protein technology include unparalleled fast growth kinetics, the ease at which high cell density cultures can be achieved, and the speed at which plasmid DNA transformation can be performed (Rosano and Ceccarelli, 2014). Affimer proteins which bind specifically to the LOX-1 SR have been isolated using phage display techniques prior to the undertaking of this research.

Plasmid DNA coding for 5 distinct LOX-1-specific Affimer isoforms were transfected in to competent *E. coli* cells (BL21*DE3) using a rapid transformation

protocol, following which the expression and purification of Affimer protein is carried out as per the protocol outlined in materials and methods. The Affimer scaffold includes a polyhistidine tag allowing for immobilised metal affinity chromatography to be carried out using immobilized nickel-nitrilotriacetic acid (Ni-NTA) agarose resin (Figure 3.1A). This method of protein purification is well described (Bornhorst and Falke, 2000). Briefly, the imidazole ring within the histidine residue readily forms coordination bonds with the immobilized Ni-NTA resin. The bacterial cell lysate is incubated with the immobilized Ni-NTA resin leading to the chelation of His-tagged Affimers to the resin. Unbound or weakly bound non-specific protein is washed from the resin in multiple repeated steps until the optical density at 280nm is undetectable. The desired Affimer protein is then eluted from the column by the addition of an imidazole-based elution buffer which competitively binds to the resin and cleaves off the his-tagged Affimers. The Affimer was eluted in low volume aliquots (100 μ l) to maintain protein concentration by avoiding dilution. The purity and concentration of the protein sample is then determined using SDS page electrophoresis against bovine serum albumin (BSA) controls (Figure 3.1A, B, C). A 50 ml culture volume would reliably yield at least 1 mg of purified Affimer protein.

3.2.2 Labelling of LOX-1 Affimer

Binding of fluorescent tags to molecules of interest to gain information from cells, fixed tissue and living organisms is a widely accepted and enormously important tool in biomedical research. The lack of disulphide bonds in the Affimer allows directed introduction of a cysteine (cys) residue for site specific chemical modification, including addition of a single biotin or fluorophore. Immediately following elution, Affimers were labelled with Alexafluor-488 or biotin at room temperature. Successful conjugation is determined by either biotinylation ELISA (Figure 3.2) or by absorbance at 488 nm following SDS-PAGE electrophoresis (Figure 3.3). An estimation of binding efficiency is calculated by comparing the internal density of a band at 11-14 kDa after excitation at 488 nm against the internal density of the same band stained with Coomassie blue. The binding efficiency of cys-tagged Affimers to Alexafluor-488 is approximately 1:1, showing maximal efficiency of labelling.

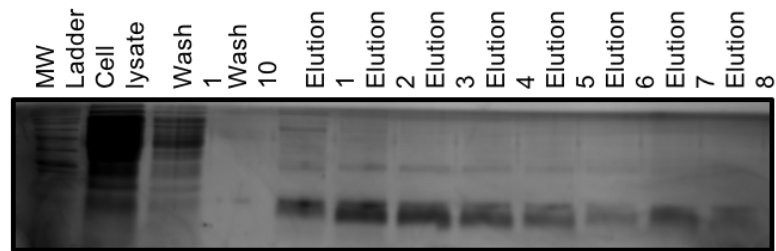
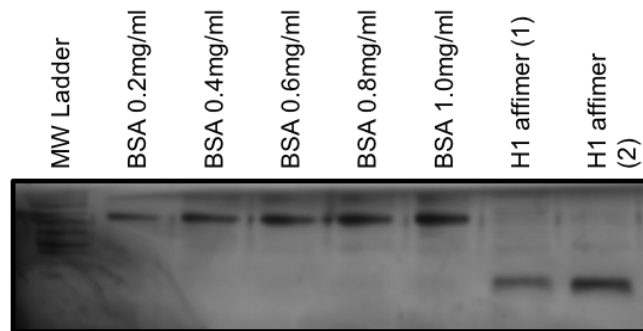
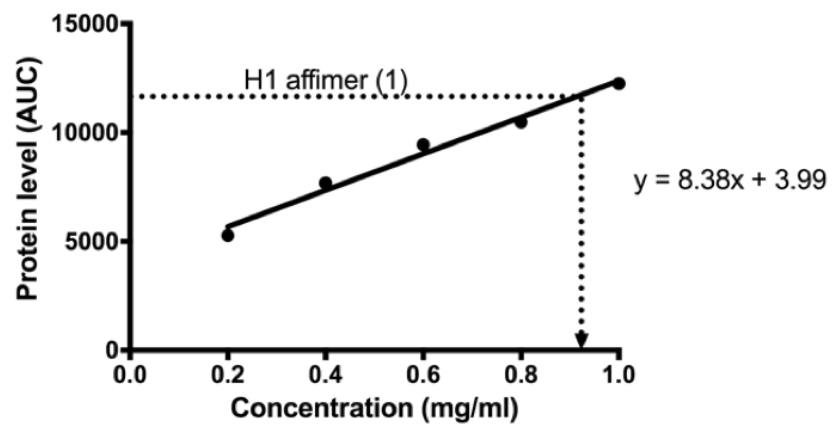
A**B****C**

Figure 3.1. Expression and purification of LOX-1-specific Affimer H1. (A) LOX-1-specific Affimers are expressed in *E. coli* BL21*DE3 cells. After cell lysis, and purification using Ni-NTA resin with washes and elution with imidazole (see Materials and Methods). Washing steps remove non-specifically bound proteins (Wash 1 and Wash 10), followed by elution using imidazole buffer (elutions 1-8). (B) Comparison of eluted H1 Affimer to BSA using SDS-PAGE and Coomassie staining. (C) The concentration of eluted H1 Affimer was compared to BSA standards (mg/ml) using densitometry. AUC; area under curve.

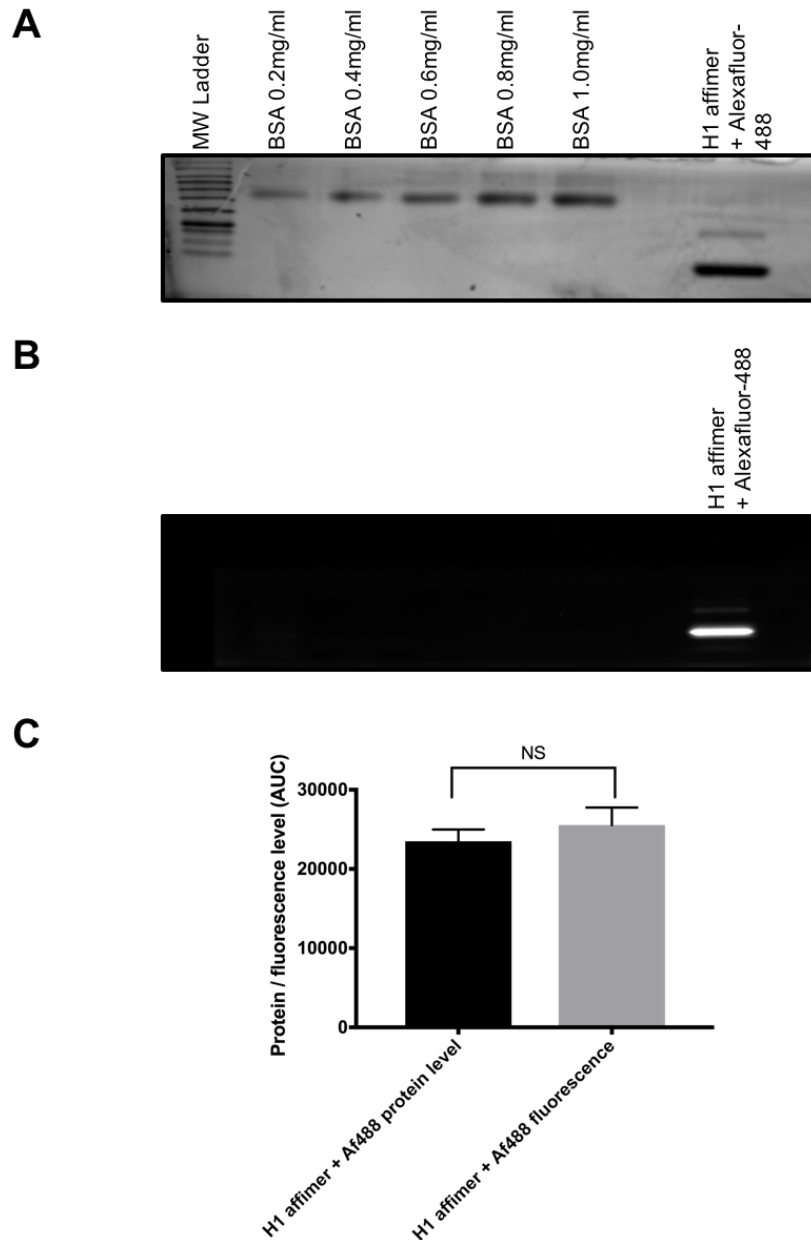


Figure 3.2. Fluorescent labelling of LOX-1-specific H1 Affimer. (A) Gel electrophoresis of Alexafluor-488-labelled LOX-1 H1 Affimer prepared as described in Materials and Methods. (B) Determination of efficiency of Alexafluor-488 conjugation to H1 Affimer using excitation at 488 nm and emission at 520 nm followed by digital imaging. (C) By comparing protein level and measured fluorescence, the binding efficiency is likely to be close to 1:1. Error bars denote \pm SEM (n=3). NS; not significant. AUC; area under curve. Statistical test: unpaired t-test.

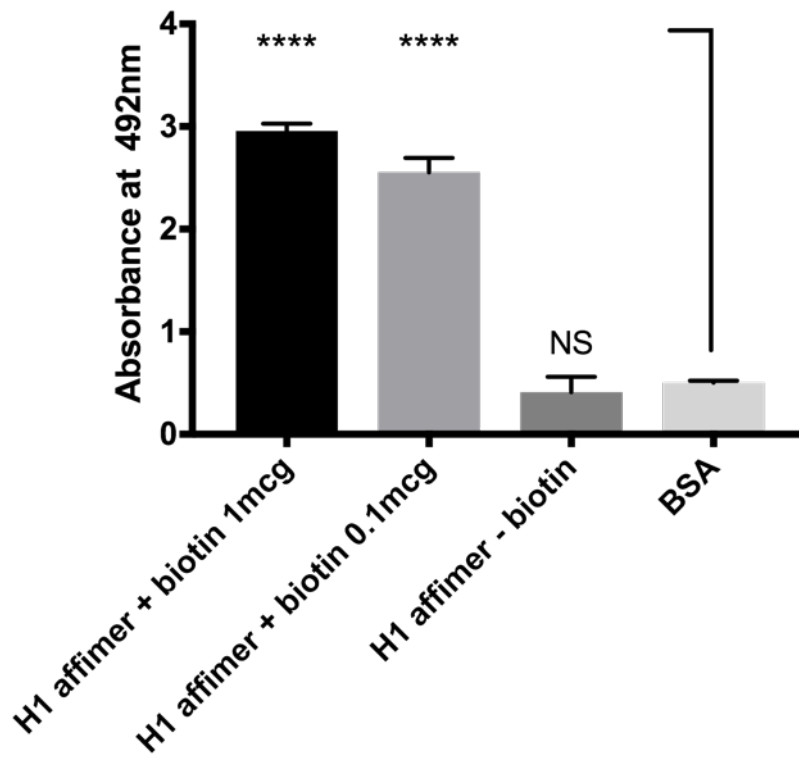


Figure 3.3. Biotinylation of LOX-1-specific H1 Affimer. Biotinylated Affimer bound to an ELISA plate was probed with streptavidin-HRP and absorbance at 492 nm was measured, to check for biotinylation. Error bars denote \pm SEM (n=3). NS; not significant. $p < 0.0001$ (****). Statistical test: One-way ANOVA.

3.2.3 Affinity and cross reactivity studies using biotinylated LOX-1 Affimers

Prior to embarking on cell-based studies, the affinity of LOX-1 Affimers to the LOX-1 protein was measured using an ELISA technique. All 5 species of LOX-1 Affimers were biotinylated and biotinylation confirmed by biotinylation assay. The affinity of LOX-1 Affimers to both human and murine LOX-1 is important for planned future *in vitro* and *in vivo* murine studies. The opportunity was taken to measure affinity to both human and murine extracellular domain LOX-1 in a cross-reactivity study with the added aim of identifying a single isoform to take forward in to such studies.

Two separate ELISA plates were coated overnight with increasing concentrations of either human or mouse soluble LOX-1 protein. BSA was added to each row as a negative control and a yeast-small ubiquitin-like modifier protein (yeast SUMO) specific Affimer was used as a further negative control in a separate row on each ELISA plate. All 5 species of LOX-1-specific Affimer exhibited affinity for human LOX-1 protein. A1, B1 and H1 Affimers tended to perform better compared with A3 and G1 however the difference was not statistically significant (Figure 3.4A). On the mouse soluble LOX-1-coated plate, both B1 and H1 exhibited a significant affinity compared to the control (yeast SUMO Affimer) (Figure 3.4B). By comparing the affinity of each Affimer species to human and mouse LOX-1, we found the only species which has an equal affinity for human and mouse LOX-1 was Affimer H1 (Figure 3.5). Given this result, the H1 Affimer was taken forward for further *in vitro* and *in vivo* studies.

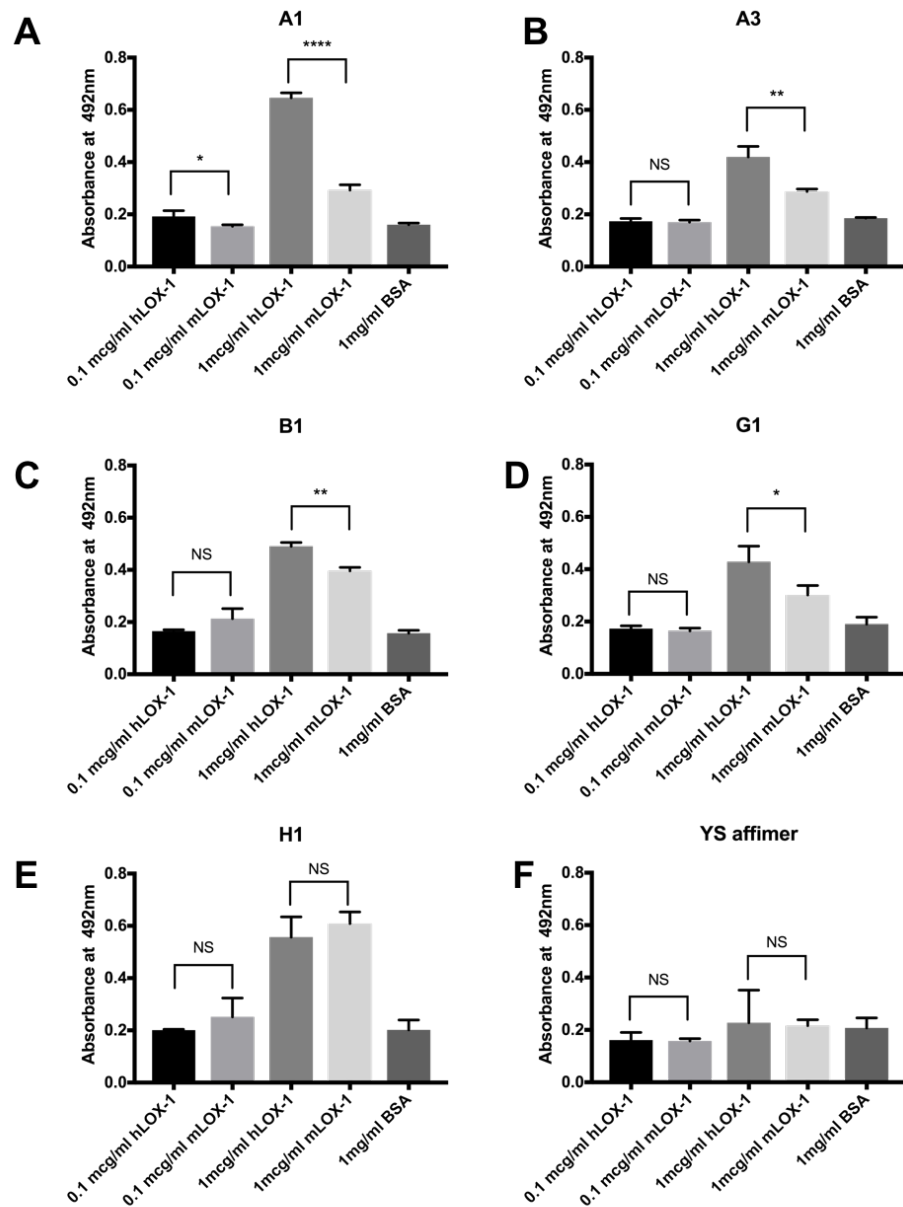


Figure 3.4. Cross-reactivity of LOX-1-specific Affimers for human and mouse soluble LOX-1 proteins. Human and mouse soluble LOX-1 were probed with different biotinylated Affimers such as (A) A1, (B) A3, (C) B1, (D) G1, (E) H1, or (F) negative control Affimer for yeast SUMO (YS) and bound Affimer was detected using streptavidin-HRP. At higher concentrations (1 mg/ml) of LOX-1, there was no significant difference of LOX-1 H1 Affimer to discern between human and mouse LOX-1. Error bars denote \pm SEM (n=3). NS; not significant. $p < 0.05$ (*), $p < 0.01$ (**), $p < 0.0001$ (****). YS; biotinylated yeast sumo specific affimer. hLOX-1; human soluble LOX-1. mLOX-1; mouse soluble LOX-1. Statistical test: One-way ANOVA.

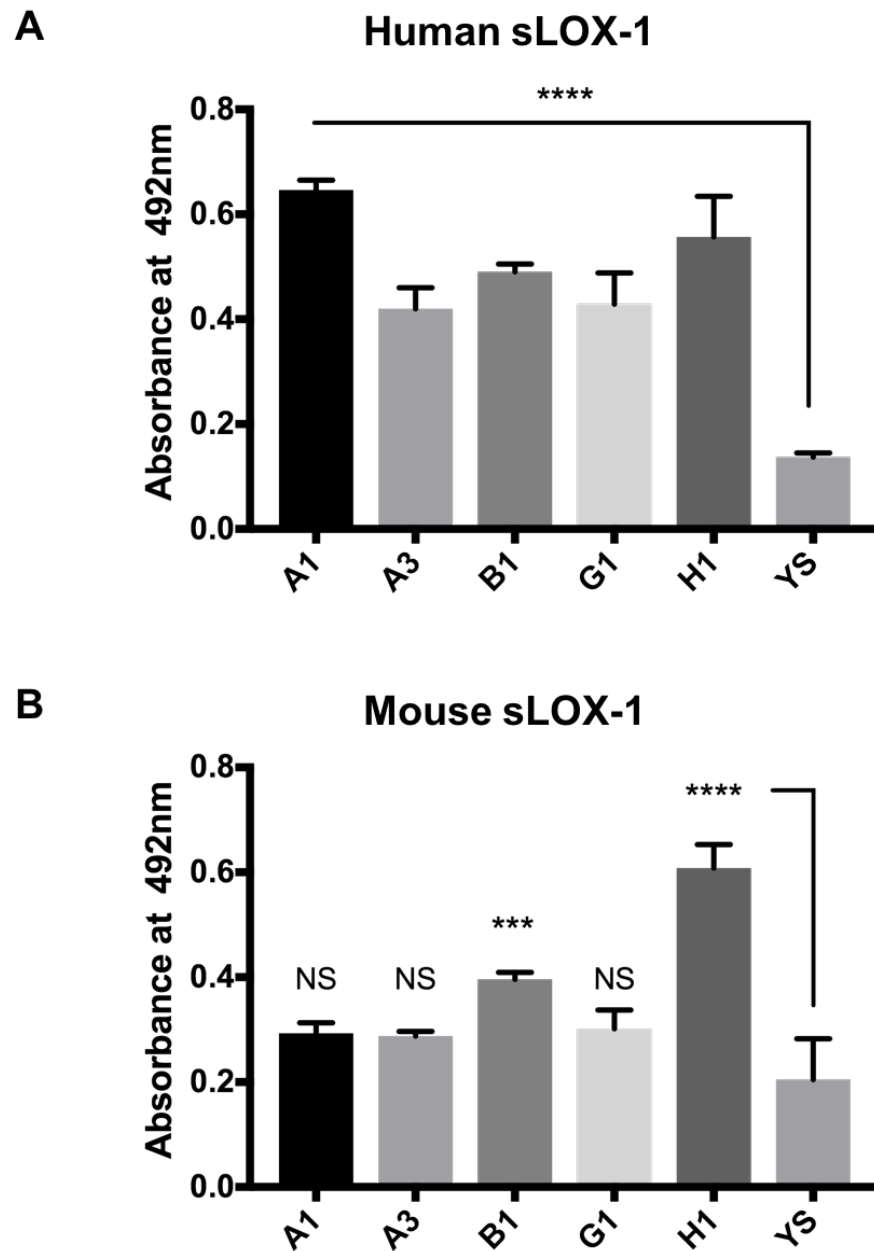


Figure 3.5. Relative affinity of LOX-1-specific Affimers for human and mouse soluble LOX-1. Relative affinities of LOX-1-specific Affimers are compared for (A) human soluble LOX-1, or (B) mouse soluble LOX-1. Error bars denote \pm SEM (n=3). NS; not significant. $p < 0.001$ (***), $p < 0.0001$ (****). YS; biotinylated yeast sumo specific affimer. Statistical test: One-way ANOVA.

3.2.4 LOX-1 Affimers bind to LOX-1 *in vitro*

3.2.4.1 Validation of tetracycline-inducible LOX-1 expression in HEK-293T cells

LOX-1 expression itself is associated with increased programmed cell death (apoptosis), making the study of its function challenging (Li and Mehta, 2009). A tetracycline-inducible expression system in human embryonic kidney cells (HEK293T) has been created to facilitate experiments studying the functional role of LOX-1 (Abdul-Zani (2017) PhD thesis). The Flp-In™ T-Rex™ system uses the flippase recognition target site for integration of the LOX-1 cDNA by flippase recombinase. LOX-1 transgene expression is tightly controlled by the tetracycline repressor which blocks gene transcription by binding to two tetracycline operator sequences upstream of the gene of interest. Utilizing this system enables control of the timing of gene expression by eliminating variability in transgene expression levels caused by genome specific variability (Thomas *et al.*, 2004). Previous work has demonstrated that LOX-1 expression peaks at 16 hours' incubation with 1 µg/ml tetracycline in standard Dulbecco's Modified Eagle Medium (DMEM) (Abdul-Zani (2017) PhD thesis). For negative control purposes, a colony of HEK293T cells were transfected with an empty plasmid, known as "empty vector".

Tetracycline-induced expression of LOX-1-FLAG in HEK-293T cells was validated before embarking on LOX-1-Affimer studies. Permeabilised HEK293T cells were fixed and stained with sheep anti-LOX-1 (Figure 3.6A, 3.6B). A proportion of induced cells were lysed for Western blot analysis. Cell lysates from induced LOX-1 and empty vector HEK-293T cells were probed using sheep anti-LOX-1 using immunoblotting: the data confirmed tetracycline-inducible expression of the engineered LOX-1-FLAG protein (Figure 3.6C, 3.6D).

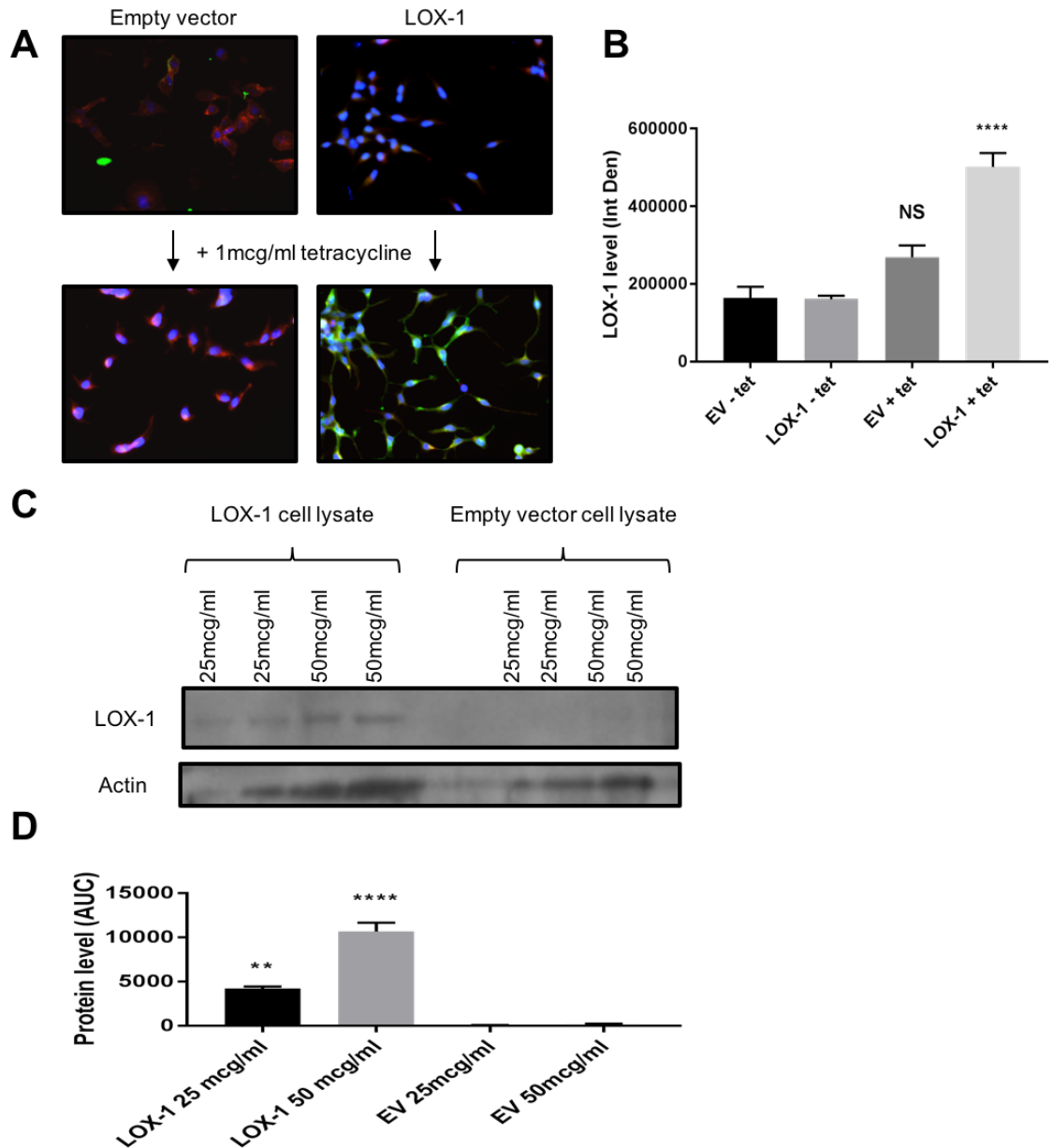


Figure 3.6. LOX-1-FLAG expression in tetracycline-inducible HEK293T cell line. (A) Tetracycline-induced LOX-1-FLAG expressing and empty vector (control) HEK293T cells are probed with sheep anti-LOX-1 antibody (green) by immunocytochemistry. (B) Quantification of relative LOX-1 levels by estimation of fluorescence pixel intensity. (C) HEK-293T cell lysates probed with sheep anti-LOX-1 antibody by immunoblotting. (D) Quantification of immunoblot data and relative LOX-1 expression levels. Error bars denote \pm SEM (n=3). NS; not significant. $p < 0.01$ (**), $p < 0.0001$ (****). EV; empty vector. Tet; tetracycline. AUC; area under curve. Statistical test: One-way ANOVA.

3.2.4.2 Immunofluorescence studies using alexafluor-488 tagged LOX-1 Affimers

To demonstrate the ability of LOX-1 Affimers to bind LOX-1 *in vitro*, Alexafluor-488-labelled Affimers were created and validated as described above. On coverslips, induced HEK-293T cells were incubated with excess Alexafluor-488-labelled LOX-1-specific Affimer in low serum medium on ice for 2 h. Cells were fixed and processed for immunofluorescence microscopy (Figure 3.7). The data demonstrates Affimer-LOX-1 binding in LOX-1 expressing cells while no signal is seen in empty vector cells (Figure 3.7A). To rule out non-specific binding in the LOX-1 expressing cells, an excess of recombinant soluble LOX-1 was added alongside the Affimer. The soluble LOX-1 competitively binds the LOX-1 Affimers. Quantification of microscopy data shows a degree of non-specific effects in the empty vector and soluble LOX-1 co-incubated controls compared with cells without Affimer incubation ($p < 0.05$), however a much greater effect is demonstrated in LOX-1-expressing cells incubated with fluorescent LOX-1-specific Affimer ($p < 0.001$).

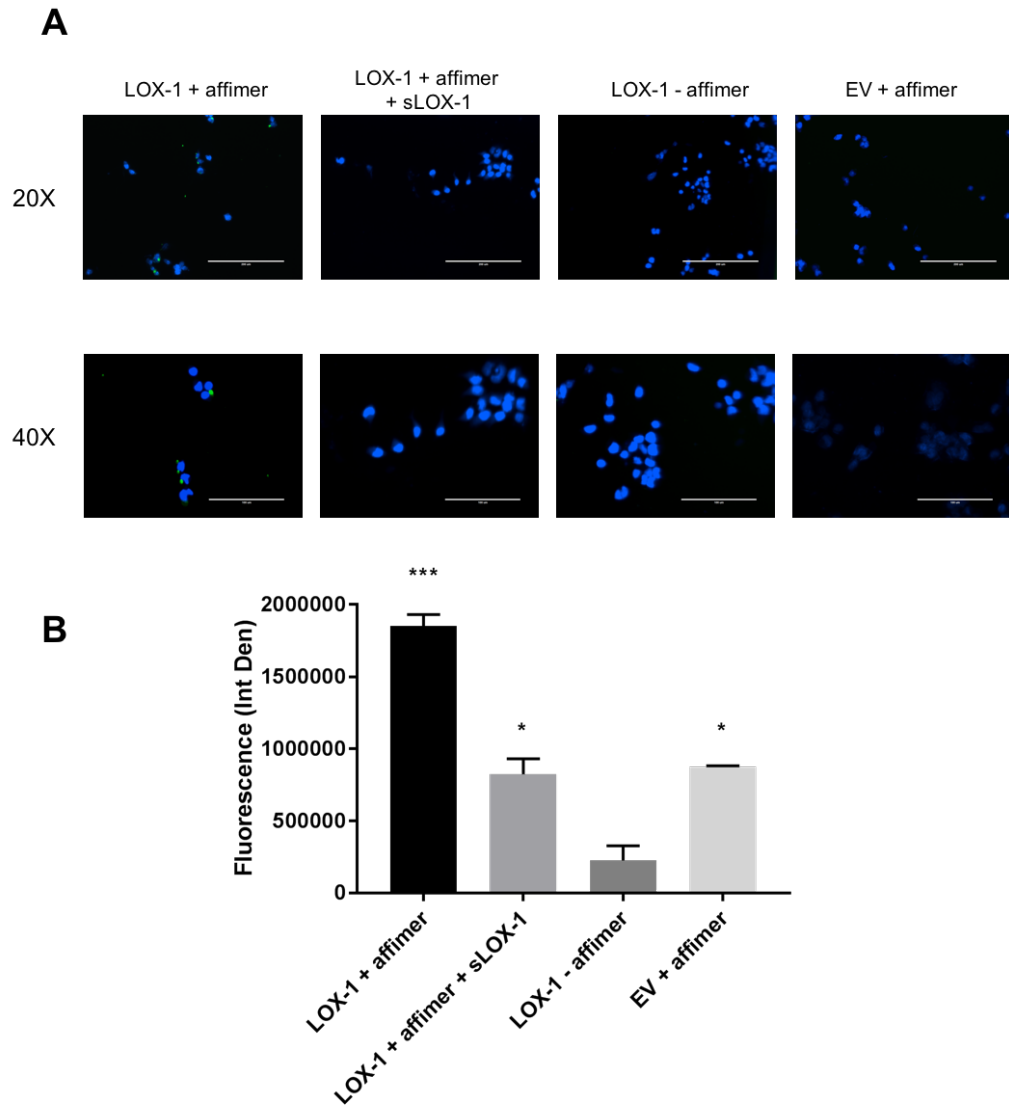


Figure 3.7. Fluorescent labelled LOX-1-specific Affimer binding to LOX-1-expressing cells. (A) Fluorescent LOX-1-specific Affimer tagged with Alexafluor-488 incubated at 100 mg/ml with tetracycline-induced HEK293T cells (EV control). Soluble LOX-1 is added in >10-fold excess to competitively bind Affimer and block binding to cellular LOX-1. (B) Quantification of labelled anti-LOX-1 Affimer binding by counting arbitrary fluorescence pixel intensity. Error bars denote \pm SEM (n=3). $p < 0.05$ (*), $p < 0.001$ (***). sLOX; soluble LOX-1. EV; empty vector. Int Den; integrated density. Bar, 100 μ m. Statistical test: One-way ANOVA.

3.2.5 LOX-1 Affimers inhibit oxLDL uptake *in vitro*

3.2.5.1 Extraction and oxidation of low-density lipoprotein

To facilitate the study of LOX-1 – oxLDL interaction, LDL was isolated from blood samples taken from healthy human volunteers. LDL particles were purified from plasma by ultracentrifugation using self-generating gradients of iodixanol (Graham *et al.*, 1996). This method has several advantages compared with sodium or potassium bromide gradients; the centrifugation times are shorter and it negates the need for salt removal (high salt concentrations can modify lipoprotein structure and therefore require removal) (Chapman *et al.*, 1981; Kelley and Kruski, 1986). There are multiple documented methods for LDL oxidation, such as transition metals or incubation with cultured cells. Incubation with copper sulphate is one of the most reliable and widely used methods for LDL oxidation (Levitan, Volkov and Subbaiah, 2010) and is the preferred method in the Ponnambalam lab. The oxidation is halted with the addition of anti-oxidants ethylene-diaminetetra acetic acid (EDTA) and butylated hydroxytoluene (BHT). Native and oxidized LDL particles treated with the anti-oxidants EDTA and BHT were run on 0.5% weight / volume (w/v) agarose gels followed by Sudan black staining. OxLDL has an increased electrophoretic mobility in comparison to native LDL as shown in figure 3.8. The increased mobility of oxLDL owes itself to an increased negative charge due to reactive aldehyde conjugation to lysine residues during the oxidation process. Oxidation of the LDL particle results in fragmentation of APO-B100 and aggregation of particles, leading to a relative heterogeneity of oxLDL particles in the sample, which can be appreciated in figure 3.8. This method therefore confirms that the LDL particles have undergone oxidation by the copper ions.

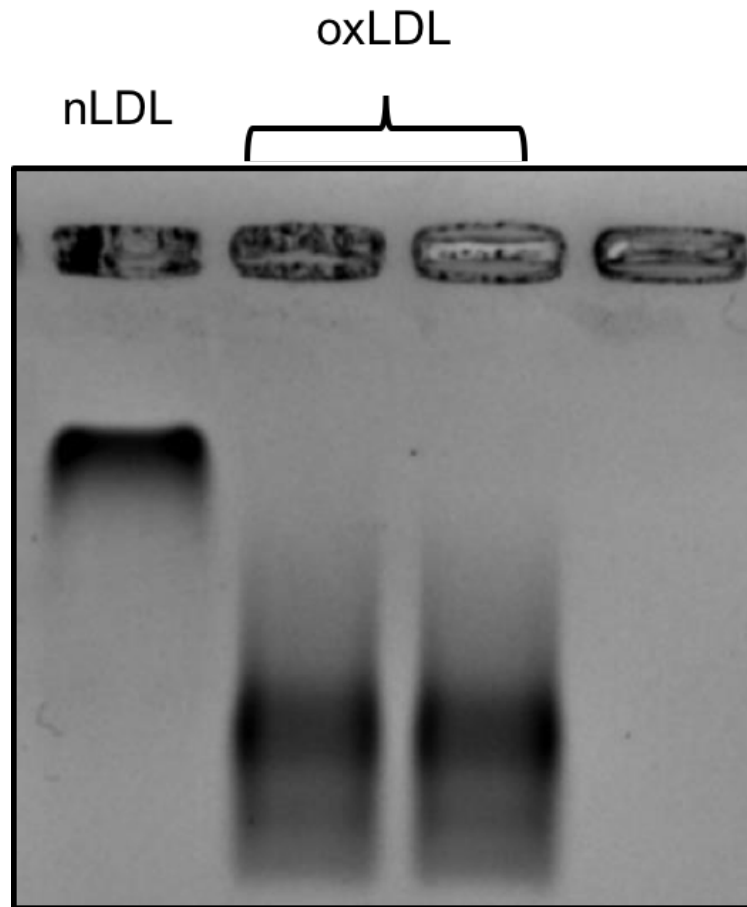


Figure 3.8. Purification and oxidation of low-density lipoprotein particles. Using iodaxonal gradient centrifugation, low-density lipoprotein (LDL) particles were extracted from human plasma. LDL was incubated with 5 μM copper sulphate (CuSO_4) for 24 h at 37°C, leading to oxidation (Oxidised LDL; lanes 2 and 3). A control sample of LDL was incubated with 100 μM EDTA and 20 μM BHT at room temperature (nLDL; lane 1). Samples were analysed on 0.5% (w/v) agarose gel and stained with the lipid stain Sudan black.

3.2.5.2 Inhibition of oxLDL uptake in LOX-1 expressing HEK-293T cells

LOX-1 Affimers have the potential to competitively bind membrane bound LOX-1 receptor and inhibit the uptake and internalization of oxLDL. Inhibition of oxLDL internalization could be of use in the future as a way of attenuating atherosclerosis by reducing foam cell formation and endothelial dysfunction. To study the effect of LOX-1 Affimers on oxLDL binding *in vitro*, oxLDL was labelled with the fluorescent compound 1,1 dioctadecyl-3,3,3',3'-tetramethylindocarbocyanine perchlorate (Dil). An increasing concentration of LOX-1 Affimer was incubated with induced HEK-293T cells on ice for 2 h. After washing, the control (EV) or LOX-FLAG-expressing HEK293T cells were then incubated with 10 μ g/ml Dil labelled oxLDL for 15 min on ice. Cells were then fixed and microscopy analysis (Figure 3.9). As expected, empty vector cells exhibited minimal oxLDL binding and that in LOX-1 expressing cells, there was a dose-dependent relationship on oxLDL binding and inhibition by Affimer (Figure 3.9). A significant reduction in oxLDL binding is observed at 0.1 μ g/ml Affimer and a further reduction is seen at 1 μ g/ml Affimer. Inhibitory effects tended to plateau at concentrations greater than 1 μ g/ml, at which point LOX-1 occupancy by oxLDL must be maximal (Figure 3.10).

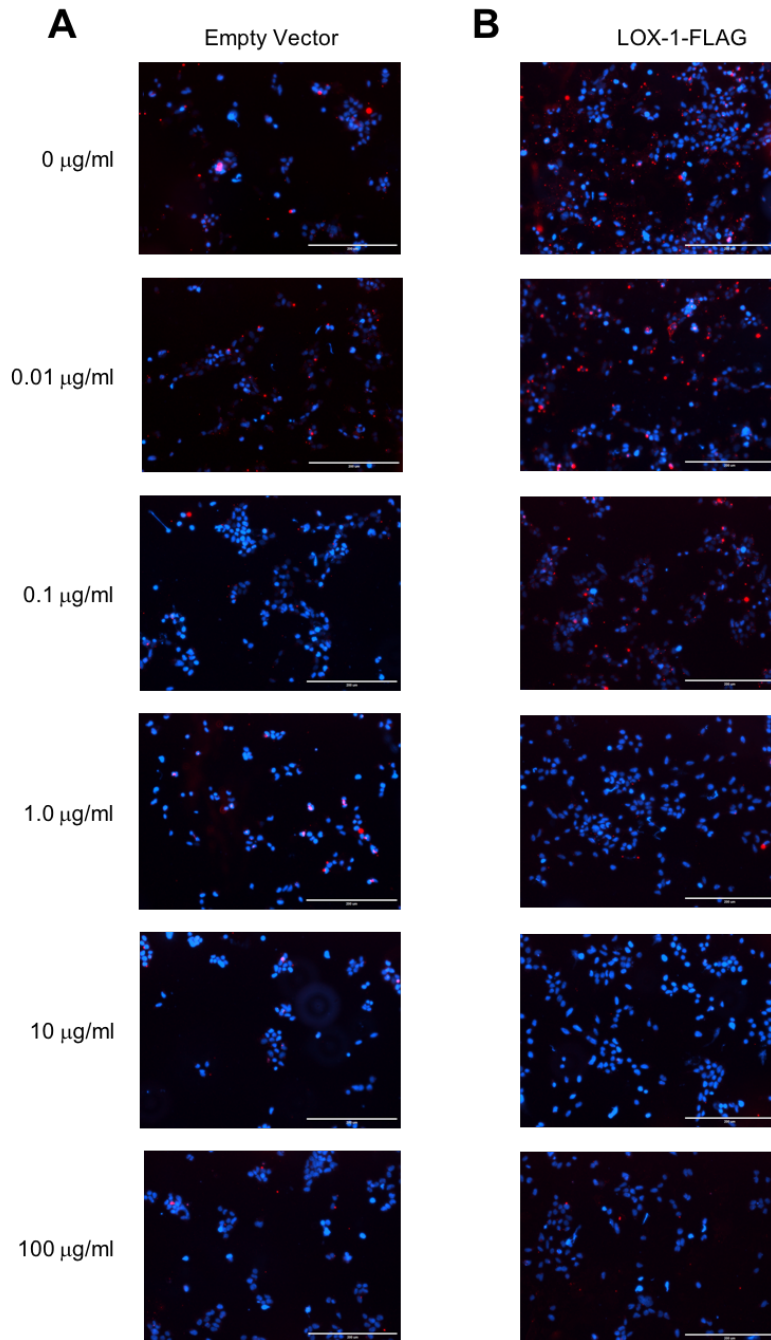


Figure 3.9. LOX-1-specific H1 Affimer inhibits oxLDL uptake in LOX-1-expressing HEK293T cells. Induced cells are pre-incubated with increasing concentrations of H1 Affimer, followed by incubation with DiI-labelled oxLDL (red) for 30 min for either (A) HEK293T-Empty vector, or (B) HEK-293T-LOX-1-FLAG. Cells were washed, chemically fixed and processed for fluorescence microscopy. Bar, 200 µm.

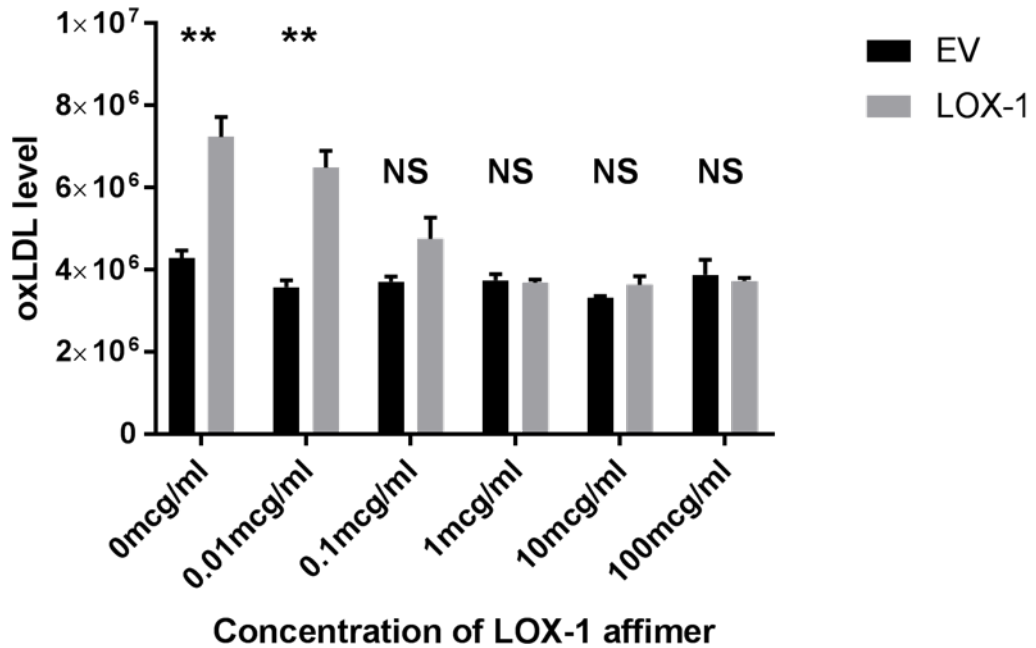


Figure 3.10. Quantification of LOX-1-specific H1 Affimer inhibition of cellular oxLDL uptake. Quantification of data from Figure 3.9.. There is significantly decreased oxLDL uptake in LOX-1-expressing HEK293T cells compared with control empty vector (EV) cells. Error bars denote \pm SEM (n=3). NS; not significant. $p < 0.01$ (**). EV; empty vector. Statistical test: unpaired t-test.

3.3 Discussion

In this chapter I have described the expression and purification of synthetic proteins called Affimers and demonstrated their ability to bind the LOX-1 protein and inhibit oxLDL uptake *in vitro*. Using Affimers in studies which rely on fluorescence to quantify an effect e.g. ELISA and cell immunofluorescence, has clear advantages and drawbacks. Whilst the Affimer scaffold includes a single cysteine residue to allow binding of either biotin or fluorophore, knowing the binding efficiency stability are critical for the interpretation of results to draw confident conclusions. To confirm and quantify Affimer conjugation, the internal

pixel intensity of the fluorescent band was compared with that of the same band after staining with coomassie blue. The assumption made is that for 1:1 binding efficiency one would expect the internal pixel intensity of the two bands to be equal. A similar method is described by authors measuring protein biotinylation *in vitro* and *in vivo* (Sorenson, Askin and Schaeffer, 2015; Li and Sousa, 2012). While this method has clear advantages (quick, accessible), it requires validation.

The LOX-1 SR is encoded by the *ORL-1* gene found on chromosome 12p12-p13 in humans (AOYAMA *et al.*, 1999). Human LOX-1 is a 273 amino acid protein with 4 domains; a short N-terminal cytoplasmic, a transmembrane, a connecting neck, and a lectin-like domain at the C terminus which binds oxLDL (Zani *et al.*, 2015). The conservation of the amino acid sequence of the lectin-like domain is essential for oxLDL binding, where 6 cys repeats are thought to be most critical. This has been demonstrated by Chen *et al.* where truncation and point mutations in the lectin-like domain led to abrogation of oxLDL binding (CHEN *et al.*, 2001; Chen *et al.*, 2001a). OxLDL binding in scavenger receptors SR-A and CD36 are thought to be largely dependent on the expression of electrostatic residues (Andersson and Freeman, 1998; Pearce *et al.*, 1998). Chen *et al.* hypothesize a similar dependence on electrostatic interaction between positively charged residues in LOX-1 lectin-like domain and negatively charged oxLDL, in particular involving the large loop between the 3rd and 4th cys of the lectin-like domain, where mutations in this region led to the abolition of oxLDL binding (Chen *et al.*, 2001a). The Affimer proteins were isolated by phage display against the C-type lectin-like domain region of LOX-1 and should have the ability to bind this region, however the binding properties should not be assumed to be identical to that of oxLDL. The variable regions of the 5 LOX-1 Affimer isoforms may bind the lectin-like domain at different points and with varying affinities. Variations in the amino acid sequence of the Affimer binding region are likely to affect affinity, as shown similarly in the optimization of monoclonal antibodies (Kaneko and Niwa, 2011). Affinity assays against human LOX-1 demonstrate some variation, however these were not statistically significant. Comparative affinity assays against the mouse LOX-1 protein found a significant variation between isoforms. The mouse LOX-1 protein is similar to the human protein in that it contains the same 4 regions, but in contrast contains triple repeats of the extracellular neck

region, increasing its size to 363 amino acids (Hoshikawa *et al.*, 1998) (figure 1.5). Mouse LOX-1 has been shown to bind oxLDL with high affinity similar to the human receptor, however the sequence % identity of the lectin-like domain in mouse LOX-1 compared with human LOX-1 is 59% with % similarity of the protein being relatively conserved at 86%. Variations in the amino acid sequence at the lectin-like domain are likely to influence Affimer binding affinities between isoforms as shown by the affinity assays against mouse LOX-1.

Affimers had the ability to bind membrane-bound LOX-1 and inhibit oxLDL binding *in vitro*. The concentrations required to show binding were higher than those required to begin inhibiting oxLDL binding. One potential explanation for this is that cys-fluorophore disulphide bonds are gradually reduced in storage. Unbound Affimers would have the potential to polymerize with other Affimers via the cys residues or with fluorophores already bound to other Affimer molecules. This would have a negative effect on signal strength as the percentage of conjugated Affimer in solution would be reduced. Alternatively, Affimer binding may be leading to downregulation of LOX-1 expression as observed in similar studies using anti-LOX-1 antibodies (Abdul-Zani (2017) PhD thesis). Downregulation of LOX-1 expression at lower concentrations of LOX-1 Affimer would lead to an enhanced effect on oxLDL binding and internalization compared with competitive inhibition alone. An important limitation to highlight is the use of a non-vascular cell type in the cell-based experiments. The advantage of using the tetracycline-inducible HEK293T cell line is that in the absence of tetracycline, they do not express detectable levels of LOX-1 protein. The same tetracycline-inducible expression system was introduced in primary endothelial cell lines such as porcine aortic endothelial cells by previous researchers in the Ponnambalam group. The endogenous expression of LOX-1 in these cell lines in the absence of tetracycline was significant and therefore the lack of a reliable negative control for the study of LOX-1-oxLDL binding led to the development of the LOX-1 expressing HEK293T cell line. This system is preferable for the study of LOX-1 binding for the above reasons, however it is not physiological and any future studies on the downstream effects of LOX-1-oxLDL binding should take this in to consideration and employ the use of a vascular cell line.

In summary, LOX-1 Affimers can be reliably expressed in *E. coli* and purified using immobilised metal affinity chromatography. LOX-1 Affimers exhibit affinity for human and mouse LOX-1. There is variation in affinity for mouse LOX-1 among Affimer isoforms, which is likely attributable to sequence variations in the lectin-like domain in human and mouse LOX-1, and at each Affimer variable regions. The H1 Affimer binds both human and mouse LOX-1 with high affinity and has the ability to inhibit oxLDL binding *in vitro*.

CHAPTER 4

LOX-1 GENOTYPE INFLUENCE ON DISEASE STATES

4.1 Introduction

Atherosclerosis is a complex systemic disease process resulting from multiple environmental and genetic factors. The complexity of atherosclerosis research has given rise to the use of different animal models which aim to mimic human disease, of which the mouse model is the most frequently used (Mukhopadhyay, 2013). Mouse models come with several advantages, the most important of which is the similarity between the mouse and human genome (95% concordance in protein-coding regions). A recent systematic review of genome-wide association studies (GWASs) in coronary artery disease found a striking concordance in risk factors for atherosclerosis and a significant overlap in the 827 genes identified by GWASs (von Scheidt *et al.*, 2017). Mouse models offer many practical advantages over larger animals:

- The costs of breeding, feeding and maintenance are significantly lower and their growth rate and generation time is rapid.
- Given their small size, the use of pharmaceuticals as part of an experiment becomes more affordable as lower volumes are required.
- There is a wide availability of inbred transgenic strains and genetic knockout techniques are easily employed to study the effects of specific genetic loci (Lee *et al.*, 2017).

One disadvantage of mouse models in the study of atherosclerosis is their relative resistance to the development of atherosclerosis compared with humans (Breslow, 1996). To induce atherosclerosis in wild-type mice, non-physiological levels of cholesterol must be added to their diet; specifically 10-20 times that of a typical Western diet (WD) (Breslow, 1996). In response to this problem, transgenic *APO-E* (apolipoprotein-E) null mice were created using gene knockout technology in the early 1990's (Plump *et al.*, 1992). *APO-E* is surface constituent

of lipoprotein particles and a ligand for lipoprotein recognition and clearance by lipoprotein receptors. Deficiency of APO-E hence leads to the spontaneous development of atherosclerosis, which can be further enhanced by the introduction of a high cholesterol WD (Davignon, 2005). Genetic engineering of APO-E deficient mice to produce double-knockout strains is frequently used to study the role of different proteins in atherogenesis, particularly in the search for potential therapeutic target proteins.

Investigators have studied the relationship between scavenger receptor (SR) expression and atherogenesis using such double knockout mouse models with some success (Babaev *et al.*, 2000; Manning-Tobin *et al.*, 2009; Mehta Jawahar *et al.*, 2007; Aslanian and Charo, 2006; Soro-Paavonen *et al.*, 2008). Much of the literature reports an anti-atherogenic in SR deletion, however there are a small number of conflicting articles, particularly those studying the deletion of multiple SR subtypes in a single subject (Mäkinen *et al.*, 2010; Manning-Tobin *et al.*, 2009; Kuchibhotla *et al.*, 2008). The reciprocal upregulation of one SR when another is downregulated is of particular concern, as reported by Manning-Tobin *et al.* (Manning-Tobin *et al.*, 2009). Such effects represent potential negative implications for the application of SR targeting in the treatment of atherosclerotic disease.

Synthetic binding proteins (Affimers) specific to human LOX-1 inhibit oxLDL uptake in-vitro, as described in Chapter 3. Whilst this result is promising, it does not go as far as proving an anti-atherogenic capability of LOX-1 Affimers as the LOX-1 mediated uptake of oxLDL by immune cells represents only a single step in atherogenesis. Furthermore, these results must be interpreted in the context of highly controlled in-vitro experimental conditions.

To study the effects of LOX-1 Affimers in atherogenesis, a mouse model of atherosclerosis offers a more comprehensive assessment. ELISA was used to identify cross-reactive LOX-1 Affimers between human and mouse LOX-1. The H1 LOX-1 Affimer exhibited equal affinity to both human and mouse LOX-1 extracellular domains, allowing us to move forward with an in-vivo study using LOX-1 Affimer as a potential therapeutic agent in atherosclerosis. One study has reported the attenuation of atherosclerosis with LOX-1 deletion in LDLR deficient

mice and several others have found similar effects using anti-LOX-1 antibody administration (Mehta Jawahar *et al.*, 2007; Dominguez *et al.*, 2008; Li *et al.*, 2002b).

Invasive interventions for atherosclerotic cardiovascular disease e.g. angioplasty / stenting and arterial surgery are key components of current best medical practice. Despite the development of more advanced techniques and improved outcomes in some areas, the problem of neointimal hyperplasia (NIH) persists to negatively impact on durability. NIH is an inflammatory process defined by thickening of the intimal layer due to the proliferation of VSMCs) and the production of extra-cellular matrix (Kijani *et al.*, 2017). Intimal thickening leads to luminal narrowing, restenosis and potentially arterial / graft occlusion. Whilst there is a degree of overlap between NIH and atherosclerosis, the two processes are pathologically separate entities (Subbotin, 2007). The role of SR expression in NIH have been investigated, with reports of potential involvement of LOX-1 and CD36 (Hinagata *et al.*, 2006; Yue *et al.*, 2019). The work in this chapter is to evaluate the effects of LOX-1 Affimer inhibition and *LOX-1* deletion on lipid and glucose metabolism, atherogenesis and NIH in *APO-E* null mice.

4.2 Study design and mouse genotyping

The study was designed to study the effects of both LOX-1 Affimer administration and *LOX-1* deletion on a variety of processes linked to lipid metabolism and atherosclerosis. A proportion of the study was intended to reproduce and add to work completed by the Ponnambalam laboratory on the LOX-1 project.

Three transgenic lines were used for this study:

- *APO-E* null
- *APO-E/LOX-1* null
- *LOX-1* null

The central aim was to compare outcomes between 3 groups (Figure 4.1): *APO-E* null (control) (n=4) vs. *APO-E*-null treated with LOX-1 Affimer (n=4) vs. *APO-*

E/LOX-1 null mice (n=5). The number of mice in each group were decided based on available resources, particularly the availability of osmotic pumps. For this reason, a power calculation was not performed and therefore we accept that this pilot study is underpowered. Due to the small numbers in each group and the limited number of researchers involved in the project, the analysis of specimens was not blinded or randomized as recommended by the “ARRIVE guidelines 2.0” (Percie du Sert *et al.*, 2020).

Both *LOX-1* null and wild type mice were used for additional comparison, particularly to demonstrate specimens free of disease. Maintaining accurate genotyping of transgenic lines is vital to ensure reliability of results and conclusions. Preserving a homozygous *APO-E* null genotype is essential, as heterozygous *APO-E* null mice will not spontaneously exhibit a typical *APO-E* null lipid phenotype. Only small amounts of circulating *APO-E* is necessary to dampen the expected phenotype, leading to protection from diet-induced atherosclerosis (Davignon, 2005).

The genotype of breeding pairs (1 female, 2 males) were regularly assessed by subjecting ear notch tissues to PCR and DNA analysis. The *APO-E* null C57Bl/6 mouse line showed the presence of a 245 bp DNA fragment, consistent with loss of a functional *APO-E* allele. C57Bl/6 wild type DNA was used as a control and showed the presence of a 155 bp DNA fragment, indicating the presence of a functional *APO-E* allele or locus (Figure 4.2A). *LOX-1* null mice displayed loss of 405 bp sequence within exon 7 of the mouse *LOX-1* (*OLR1*) gene compared with the presence of a band at 405 bp in control wild-type mice (Figure 4.2B)

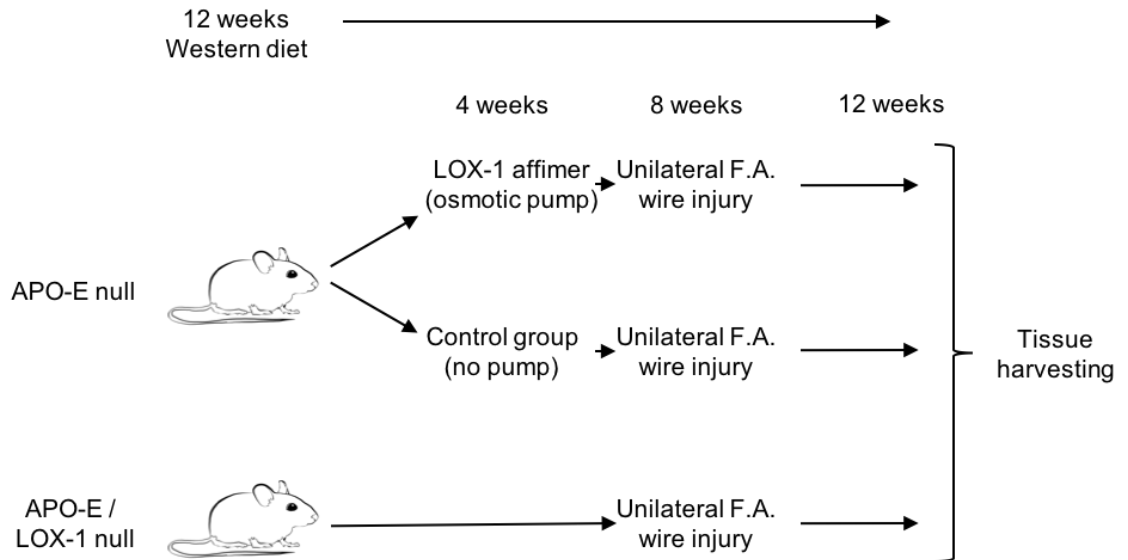


Figure 4.1. Schematic of mouse studies. 3 mouse groups for comparison were *APO-E* null, *APO-E* null treated with 8 weeks of LOX-1-specific Affimer via subcutaneous osmotic pump, and *APO-E/LOX-1* null. Separate experiments in some instances included *LOX-1* null and wild type mice. F.A.; femoral artery.

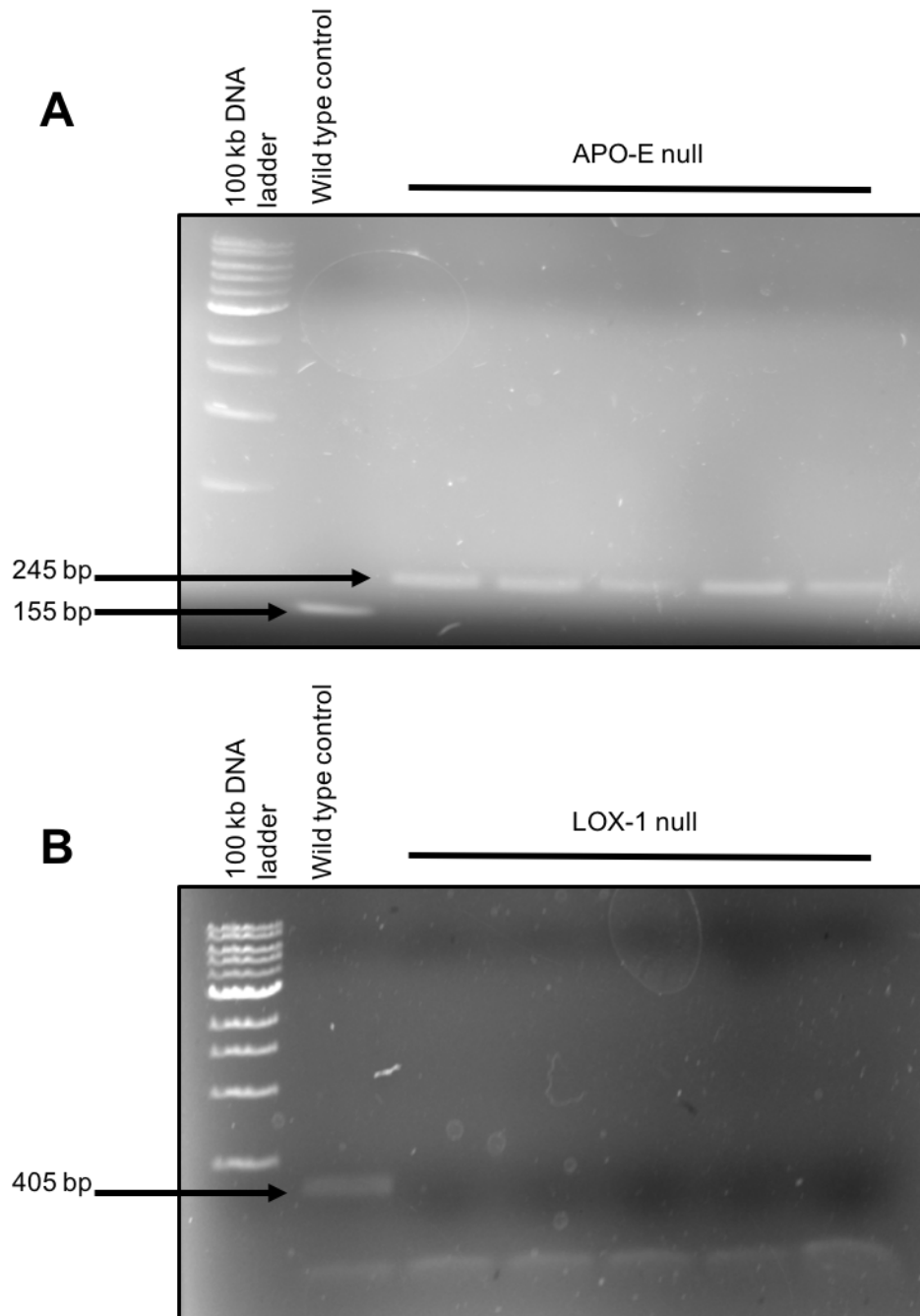


Figure 4.2. Genotyping transgenic mouse lines. *APO-E*-null, *LOX-1*-null, and wild-type mice were genotyped for *LOX-1* and *APO-E* alleles using polymerase chain reaction (PCR). (A) With DNA primers specific for *APO-E* locus, a smaller DNA band (155 bp) indicates presence of the gene whilst a larger DNA band (245 bp) indicates absence of a functional *APO-E* allele. (B) The presence of a DNA band (405 bp) with *LOX-1* primers indicates a functional *LOX-1* (*OLR1*) allele whilst its loss signifies a homozygous knockout strain.

4.3 Results

4.3.1 Influence of LOX-1 on body mass

The association between LOX-1 function and obesity is only partly understood. Animal and human studies have found increased levels of soluble urinary and serum LOX-1 in obese subjects (Kelly *et al.*, 2008; Brinkley *et al.*, 2008). An in-vitro study of oxLDL uptake in adipocytes found that LOX-1 expression in adipocytes was associated with significant increase in fatty acid uptake (Chui *et al.*, 2005). The results from these studies suggest a link between increased LOX-1 expression and obesity, however results from transgenic mouse models of LOX-1 knockout have reported no significant differences in diet-induced weight gain or mesenteric fat deposition in association with LOX-1 knockout (Takanabe-Mori *et al.*, 2010; Mehta Jawahar *et al.*, 2007).

To investigate the effects of LOX-1 modulation in APO-E null mice, transgenic mice were inspected and weighed on a weekly basis from the beginning of their 12 week WD regimen (8 weeks old) until completion at 12 weeks of WD (20 weeks old). In addition, mice undergoing procedures were weighed before starting.

A line graph of the mean weight of mice at 0, 6 and 12 weeks of WD (Figure 4.3A) shows a steeper increase in weight in the APO-E null mice within the first 6 weeks compared with APO-E/LOX-1 null and Affimer-treated APO-E null mice. The mean total weight gain was compared (Figure 4.3B) and showed that both APO-E/LOX-1 null ($p=0.0121$) and Affimer-treated APO-E null mice ($p=0.0210$) gained significantly less weight compared to APO-E null mice.

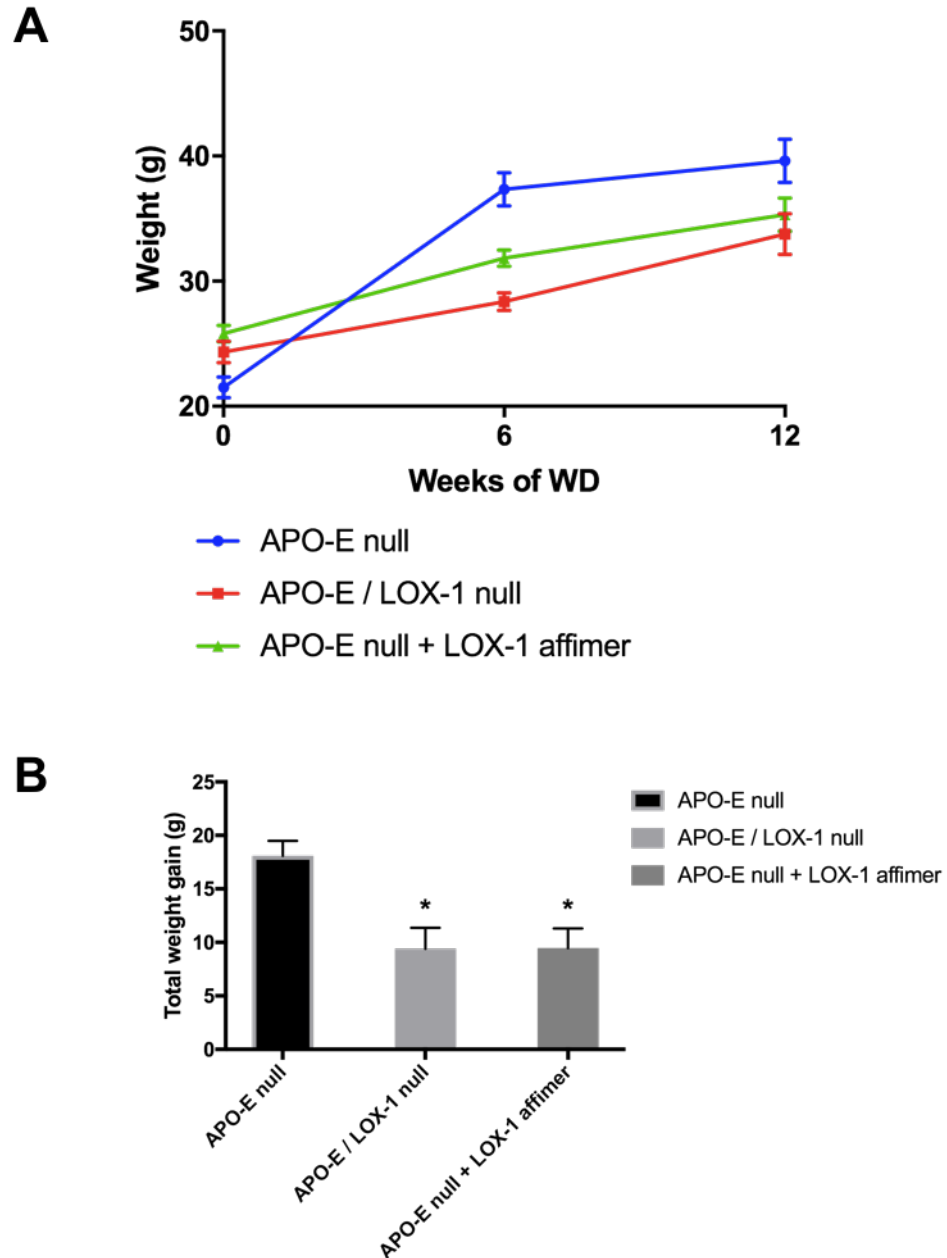


Figure 4.3 Weight of transgenic mice upon Western diet treatment and LOX-1-specific Affimer treatment. (A) Graph showing mouse weight gain over 12 weeks of Western diet. (B) Comparison of total weight gain. At 12 weeks, *APO-E/LOX-1* null and *APO-E* null Affimer treated mice had gained significantly less weight compared with *APO-E* null mice alone. Error bars denote \pm SEM (n=4). $p < 0.05$ (*). Statistical test: One-way ANOVA.

4.3.2 Effects of LOX-1 on insulin resistance

There are multiple reports of an association between glucose homeostasis and LOX-1 expression. Investigators have shown that LOX-1 expression and monocyte adhesion increases when endothelial cells are exposed to increasing concentrations of glucose in-vitro (Li, Sawamura and Renier, 2003). In diabetic rats, vascular LOX-1 expression is increased compared with non-diabetic controls (Chen *et al.*, 2001c). Studies investigating SR expression and insulin resistance in adipocytes have shown that LOX-1 expression leads to increased insulin resistance in adipocytes, suggesting a possible mechanistic association with diabetes mellitus and atherosclerosis (Rasouli *et al.*, 2009; Chui *et al.*, 2005). To investigate the possible association between LOX-1 expression and insulin resistance in mice, subjects within the 3 study arms underwent a glucose tolerance test (GTT) and insulin tolerance test (ITT) at 0 and 12 weeks of WD. There was no significant difference in fasting blood glucose levels between the 3 groups at 0 and 12 weeks after WD (Figure 4.4). The fasting blood glucose levels did not change significantly between 0 to 12 weeks in any group under all conditions examined.

GTT and ITT results were similar for all 3 groups at 0 weeks WD (Figure 4.5A, 4.6A). After 12 weeks of WD treatment, the GTT and ITT curves in the *APO-E* null mice showed differences, whilst curves plotted for *APO-E/LOX-1* null and Affimer-treated *APO-E* null mice remained unchanged (Figure 4.5B, C; Figure 4.6B, C). Area-under-curve (AUC) analysis demonstrated that *APO-E* null mice were significantly more insulin resistant at ITT compared with *APO-E/LOX-1* null ($p=0.0001$) and Affimer-treated *APO-E* null mice ($p=0.0273$) after 12 weeks of WD. *APO-E* null mice were significantly more glucose intolerant compared with Affimer-treated *APO-E* null mice ($p=0.0029$) after 12 weeks of WD. The *APO-E* null mice suggested an increase in glucose intolerance compared to the *APO-E/LOX-1* null mice, but this was not statistically significant. In *APO-E* null mice, blood glucose levels increased in response to glucose administration (GTT) and decreased less in response to insulin administration (ITT), indicating increased insulin resistance associated with WD treatment. Interestingly, this change was not observed in the *APO-E/LOX-1* null or Affimer-treated *APO-E* null mice,

suggesting the possibility of a protective effect associated with *LOX-1* deletion or functional inhibition.

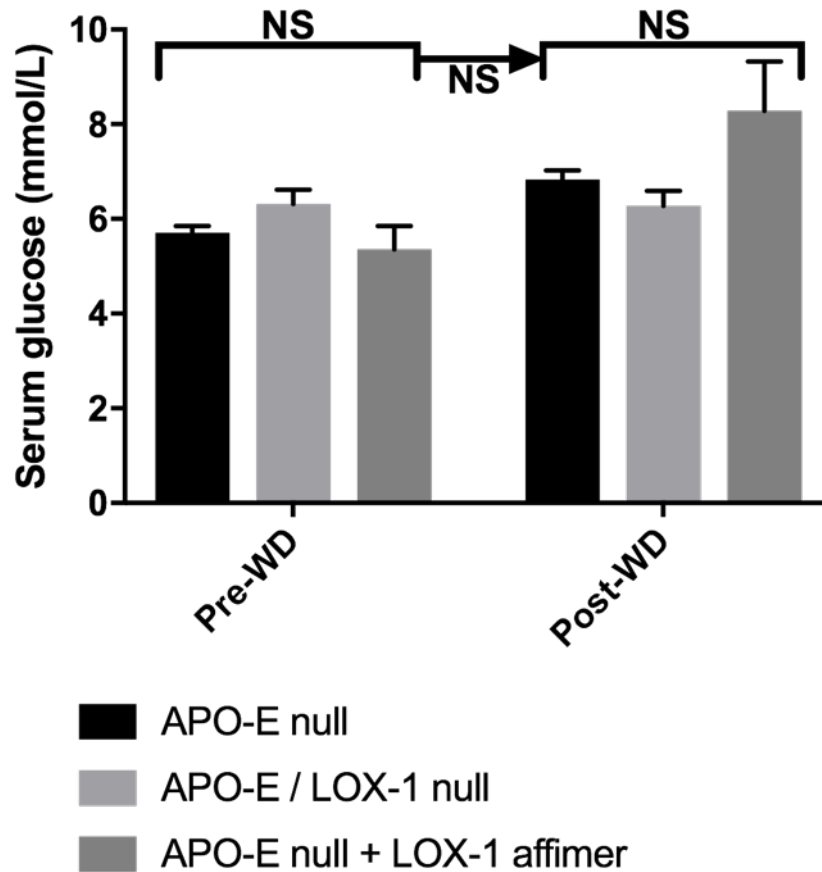


Figure 4.4. Fasting glucose effects in transgenic mice after Western diet. Mice were fasted for 6 h prior to serum glucose measurement. There were no significant differences between lines pre- and post-Western diet. Fasting serum glucose in each transgenic line was compared pre- and post-Western diet and there were no significant differences. Error bars denote \pm SEM (n=4). NS; not significant. Statistical test: One-way ANOVA.

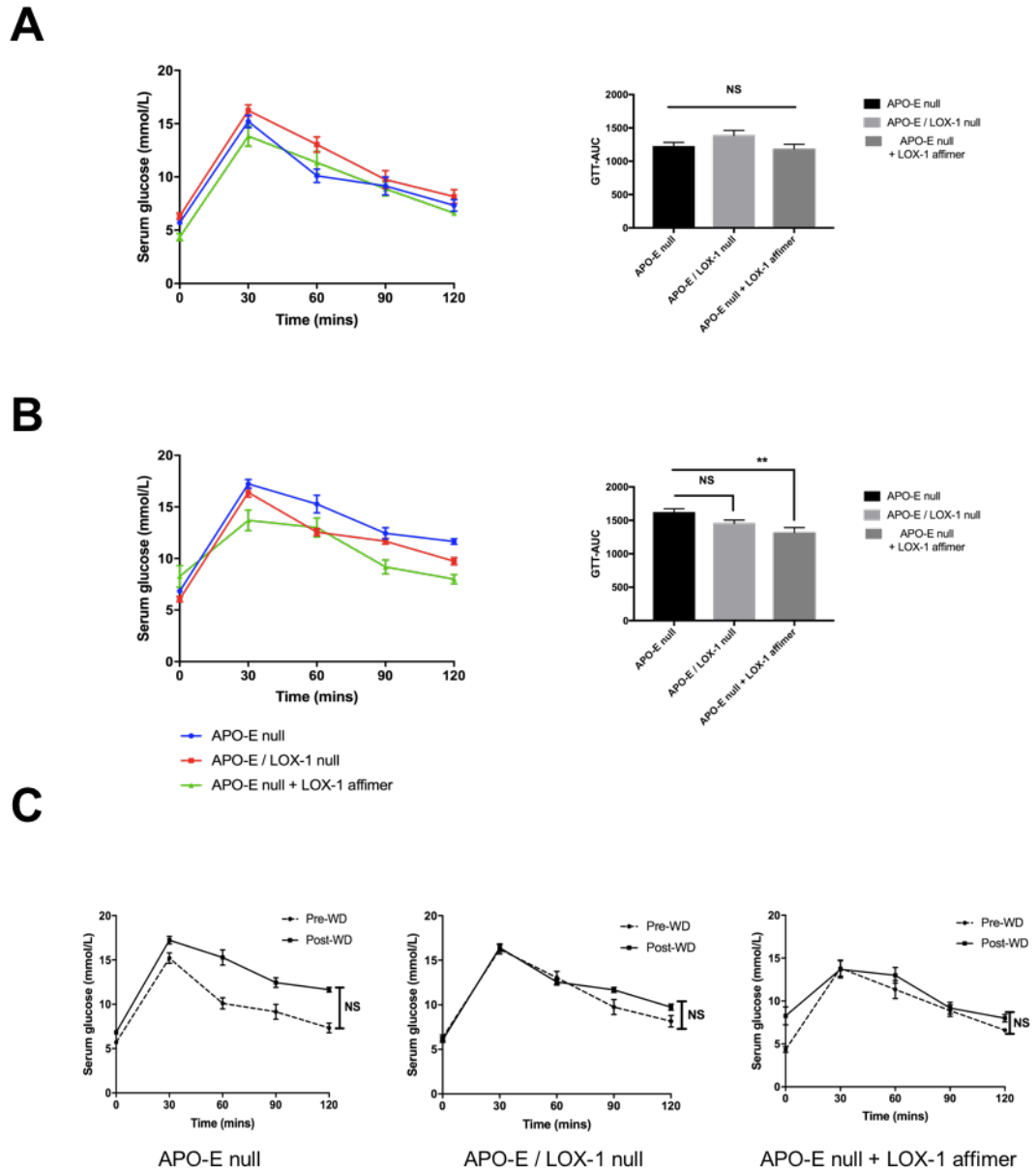


Figure 4.5. Glucose tolerance test (GTT) of transgenic mice after Western diet. (A) pre-Western diet, showing little or no difference. (B) GTT post-Western diet shows that the *APO-E* null subjected to LOX-1-specific Affimer treatment group had a significantly improved glucose tolerance compared with untreated *APO-E* mice. (C) GTT data analysis for each separate group. Error bars denote \pm SEM (n=4). NS; not significant. $p < 0.01$ (**). GTT; glucose tolerance test. AUC; area under the curve. WD; Western diet. Statistical test: (A), (B) One-way ANOVA, (C) Paired t-test.

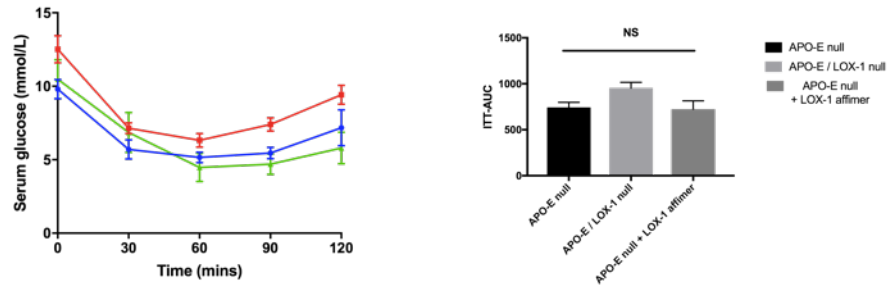
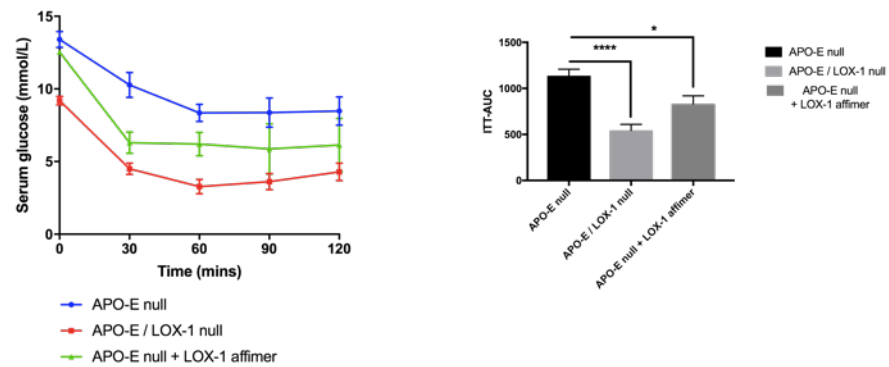
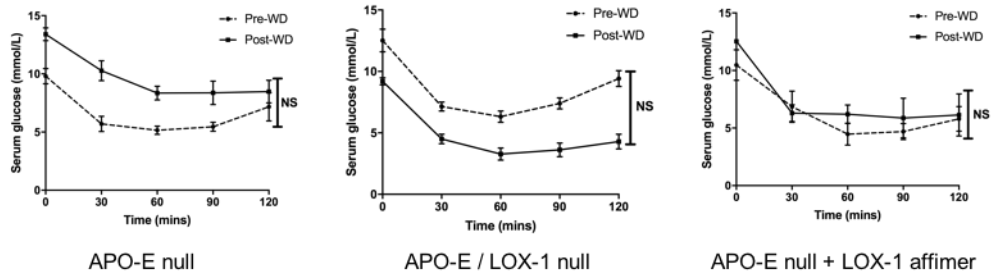
A**B****C**

Figure 4.6. Insulin tolerance test (ITT) of transgenic mice after Western diet.

(A) ITT analysis pre-Western diet, showing there is no significant difference between groups. (B) ITT analysis post-Western diet, The APO-E/LOX-1 null and APO-E + affimer groups exhibit increased insulin sensitivity compared with APO-E null mice. (C) ITT comparison in each of group pre- and post-Western diet. Error bars denote \pm SEM (n=4). NS; not significant. $p < 0.05$ (*). $p < 0.0001$ (****). ITT; insulin tolerance test. AUC; area under the curve. WD; western diet. Statistical test: (A), (B) One-way ANOVA, (C) Paired t-test.

4.3.3 Effects of LOX-1 on hepatic steatosis

Non-alcoholic steatohepatitis (NASH) is the most common cause of chronic liver disease worldwide and its prevalence worldwide is increasing (Rafiq and Younossi, 2009). NASH is widely accepted to be a hepatic manifestation of metabolic syndrome. It has been linked to mechanisms involving lipid-mediated macrophage activation, a feature it holds in common with atherogenesis and the development of cardiovascular disease (Ho *et al.*, 2019). The potential role of LOX-1 in NASH has been investigated in both experimental animal models and in patients. A mouse model of NASH found that LOX-1 expression was required for hepatic fibrogenesis while cohort studies of patients with known NASH demonstrate that hepatic LOX-1 expression and soluble serum LOX-1 levels are increased in the presence of NASH (Ho *et al.*, 2019; Musso *et al.*, 2011; Ozturk *et al.*, 2015). The opportunity was taken as part of our study to investigate the role of LOX-1 in the development of hepatic steatosis.

After 12 weeks of WD, all major abdominal organs in mouse groups subjected to different experimental regimes were harvested along with the aorta, carotid and femoral arteries as described in Materials and Methods. During each tissue harvest, the most anterior segment of the liver was taken for processing followed by paraffin embedding. 5 µm thick liver sections were processed for histological analysis and stained with haematoxylin and eosin (Figure 4.7). The total surface area of steatosis was measured and used to calculate the % hepatic steatosis using previously published methods (Matsuzawa *et al.*, 2007; Ho *et al.*, 2019).

All 5 groups exhibited varying degrees of hepatic steatosis (Figure 4.7A). The degree of fat infiltration was quite marked in all groups except for wild-type genotype (Figure 4.7A). Increased % of coverage of tissue exhibiting the hepatic steatosis phenotype was observed in *APO-E* null, *APO-E/LOX-1* null and Affimer-treated *APO-E* null mice compared to wild-type mice (Figure 4.7A), however these were not statistically significant (Figure 4.7B). Unexpectedly, *LOX-1* null mice exhibited large areas of fat infiltration and we found the % fat infiltration was significantly increased compared with wild type mice ($p=0.0027$) (Figure 4.7B). These findings suggest that the *LOX-1* null genotype influences hepatic fat accumulation.

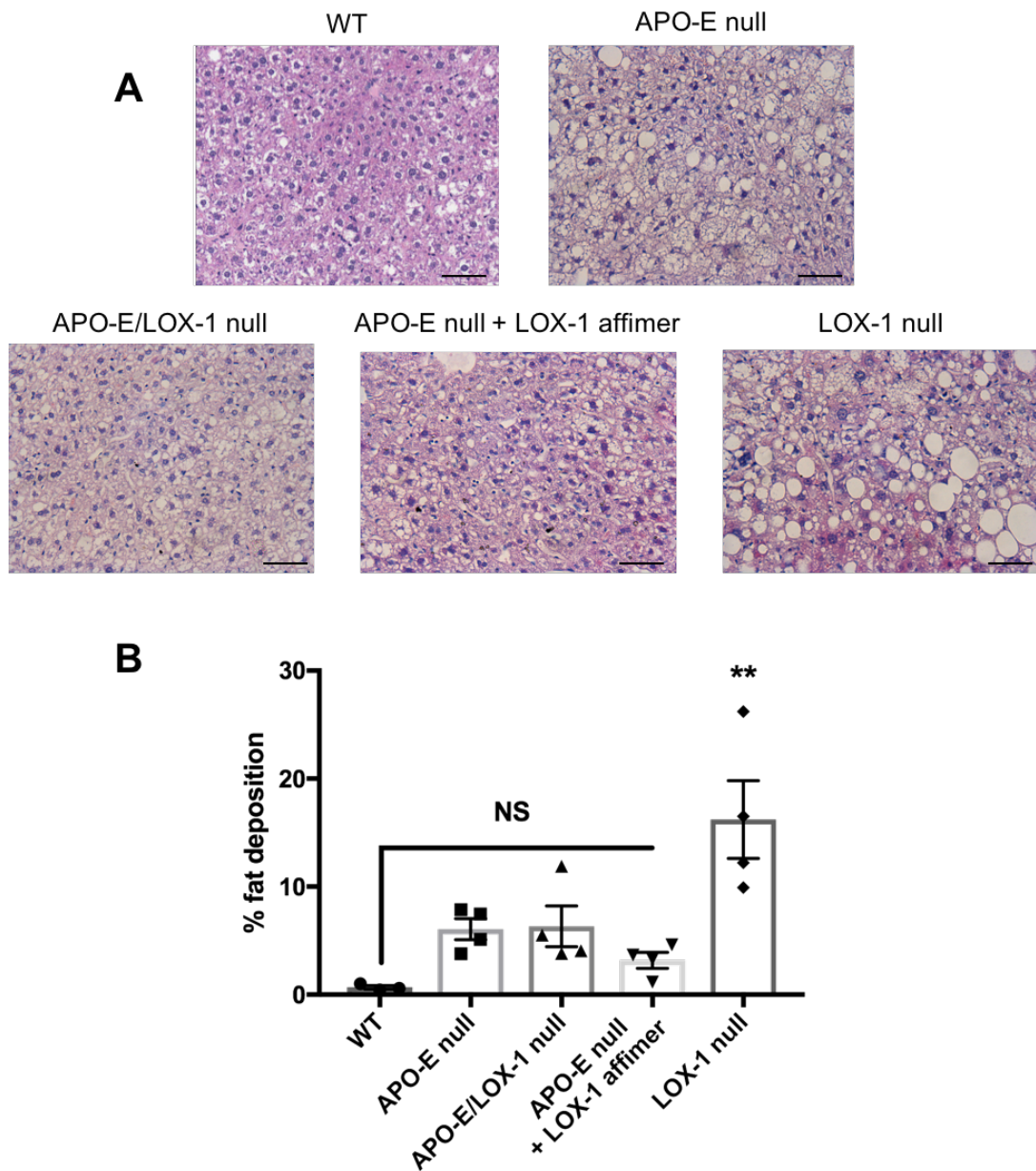


Figure 4.7. Effect of LOX-1 on hepatic fat deposition. (A) Sections of liver from mice subjected to Western diet, processed for histology and stained with haematoxylin and eosin. The fat cells are discrete rounded areas containing no stain. (B) Compared with wild-type mice, *LOX-1* null mice showed a significant increase in fat deposition after Western diet. Magnification 20X, scale bar = 100 μ m. Error bars denote \pm SEM. All groups n=4. NS; not significant. $p < 0.01$ (**). WT; wild type. Statistical test: One-way ANOVA.

4.3.4 LOX-1 influence on atherogenesis

To achieve a comprehensive assessment of atherogenesis, regions most prone to large vessel disease were harvested for analysis. The analyzed regions included whole aorta, femoral artery and the common carotid bifurcation. Measurement of % plaque area in whole aortic specimens is an established method for assessing atherosclerotic burden in mouse models of atherosclerosis (Lee *et al.*, 2017; Emini Veseli *et al.*, 2017). Probably the most clinically relevant sites of large vessel atherosclerosis in humans are at the femoral and carotid bifurcations. Disease at these locations can lead to peripheral arterial and cerebrovascular disease, respectively. Upregulation of LOX-1 in a mouse model of atherosclerosis is associated with greater carotid plaque burden (White, Sala-Newby and Newby, 2011). Sites of arterial branching or bifurcation are most susceptible to atherosclerosis. Haemodynamic shear stress in these areas has been shown to modulate endothelial expression of a variety of molecules involved in atherogenesis, including LOX-1 (Murase *et al.*, 1998).

Whole aortic mouse specimens were fixed and stained with oil red O as described in Materials and Methods. There was a reduction in % plaque area in all groups compared to the *APO-E* null group (Figure 4.8A, 8B). The >60% reduction in plaque area was statistically significant in the *APO-E/LOX-1* null mice ($p=0.0075$) (Figure 4.8B). The reduction in plaque area in the Affimer-treated group was not statistically significant (Figure 4.8B). For comparison, whole aortic specimens from LOX-1 null mice fed 12 weeks of WD are included in the analysis (Figure 4.8A).

Carotid bifurcation atherosclerosis is important clinically as disease at this location can give rise to cerebrovascular accidents in humans. Bilateral carotid arteries were harvested and stained with Miller / Van Gieson stain and analysed for % plaque area at or immediately distal to the common carotid bifurcation (Figure 4.9). All groups exhibited a degree of bifurcation disease except for the *LOX-1* null genotype, which was generally low in plaque staining (Figure 4.9A). Carotid bifurcation atherosclerotic plaque incidence was reduced non-significantly in *APO-E/LOX-1* null and statistically significantly in Affimer-treated *APO-E* null mice ($p=0.0328$) compared with *APO-E* controls (Figure 4.9B). *LOX-*

1 null mice exhibited significantly less carotid atherosclerosis compared with *APO-E* null controls ($p= 0.009$) (Figure 4.9B).

Atherosclerotic disease at the level of the femoral artery is also important clinically as disease at this level is a common cause of peripheral artery disease, which can lead to limb and life threatening complications in humans. Bilateral femoral arteries were harvested and specimens were stained and analysed (Figure 4.10). Mice which had undergone unilateral femoral artery wire injury at week 8 of Western diet had the contralateral femoral artery analysed for plaque incidence and distribution (Figure 4.10). All groups exhibited a degree of femoral artery disease except for the *LOX-1* genotype, which was generally disease free (Figure 4.10A). There were significant reductions in atherosclerosis at this level in *APO-E/LOX-1* null ($p=0.0296$) and *LOX-1* null mice ($p=0.0153$) (Figure 4.10B). There was a reduction in atherosclerosis in the Affimer-treated *APO-E* null mice, but this was not statistically significant (Figure 4.10B).

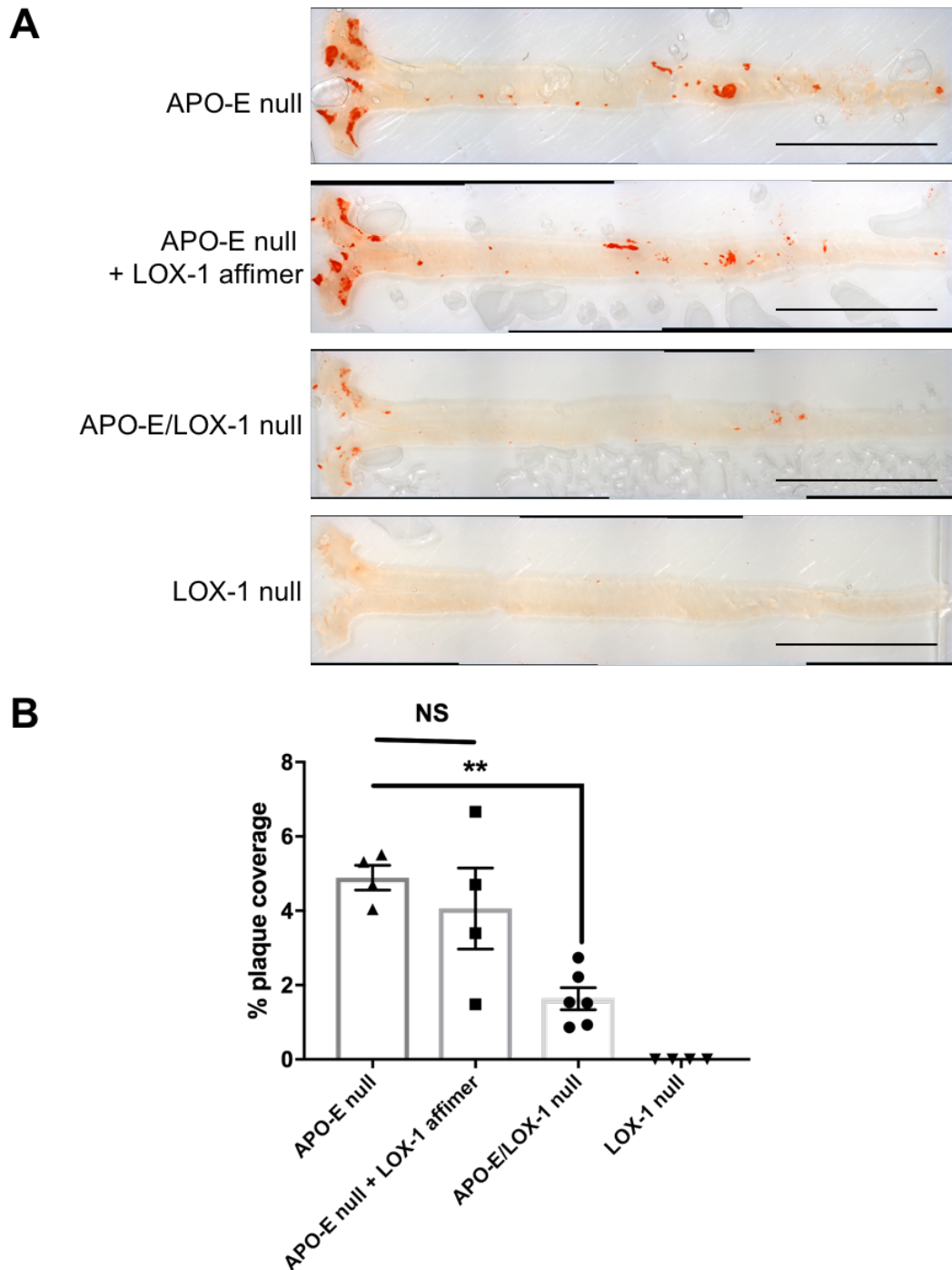


Figure 4.8. LOX-1 allele influences atherosclerotic plaque incidence in APO-E null mice. The total atherosclerotic load in harvested aortae stained with oil red O (A). Whilst the *LOX-1* null genotype significantly modulated atherosclerotic load, reductions observed in the LOX-1 Affimer treated group was non-significant (B). Scale bar = 10mm. Error bars denote \pm SEM. *APO-E* null n=4, *APO-E* null + affimer n=4, *APO-E/LOX-1* null n=6, *LOX-1* null n=4. NS; not significant. $p < 0.01$ (**). Statistical test: One-way ANOVA.

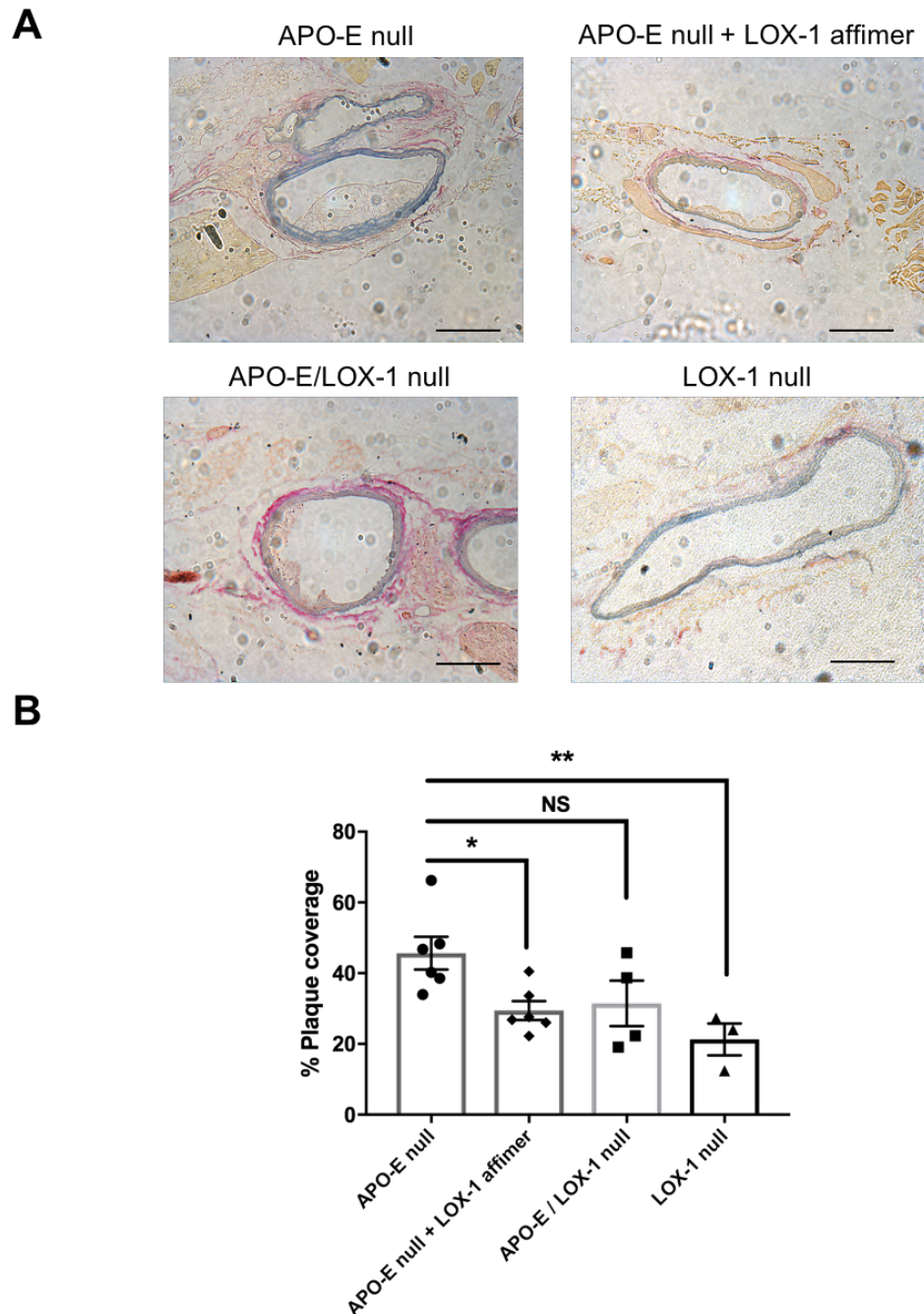


Figure 4.9. LOX-1-specific Affimer effect on carotid atherosclerosis. (A) The carotid arteries of Western diet fed transgenic mice were processed for histology and Miller elastin staining and analysed immediately distal to the common carotid bifurcation. (B) Quantification of % plaque in carotid areas under the different treatment conditions. Magnification 10X, scale bar = 100 μ m. Error bars denote \pm SEM. *APO-E* null n=6, *APO-E* null + affimer n=6, *APO-E/LOX-1* null n=4, *LOX-1* null n=3. (n=4). NS; not significant. $p < 0.05$ (*), $p < 0.01$ (**). Statistical test: One-way ANOVA.

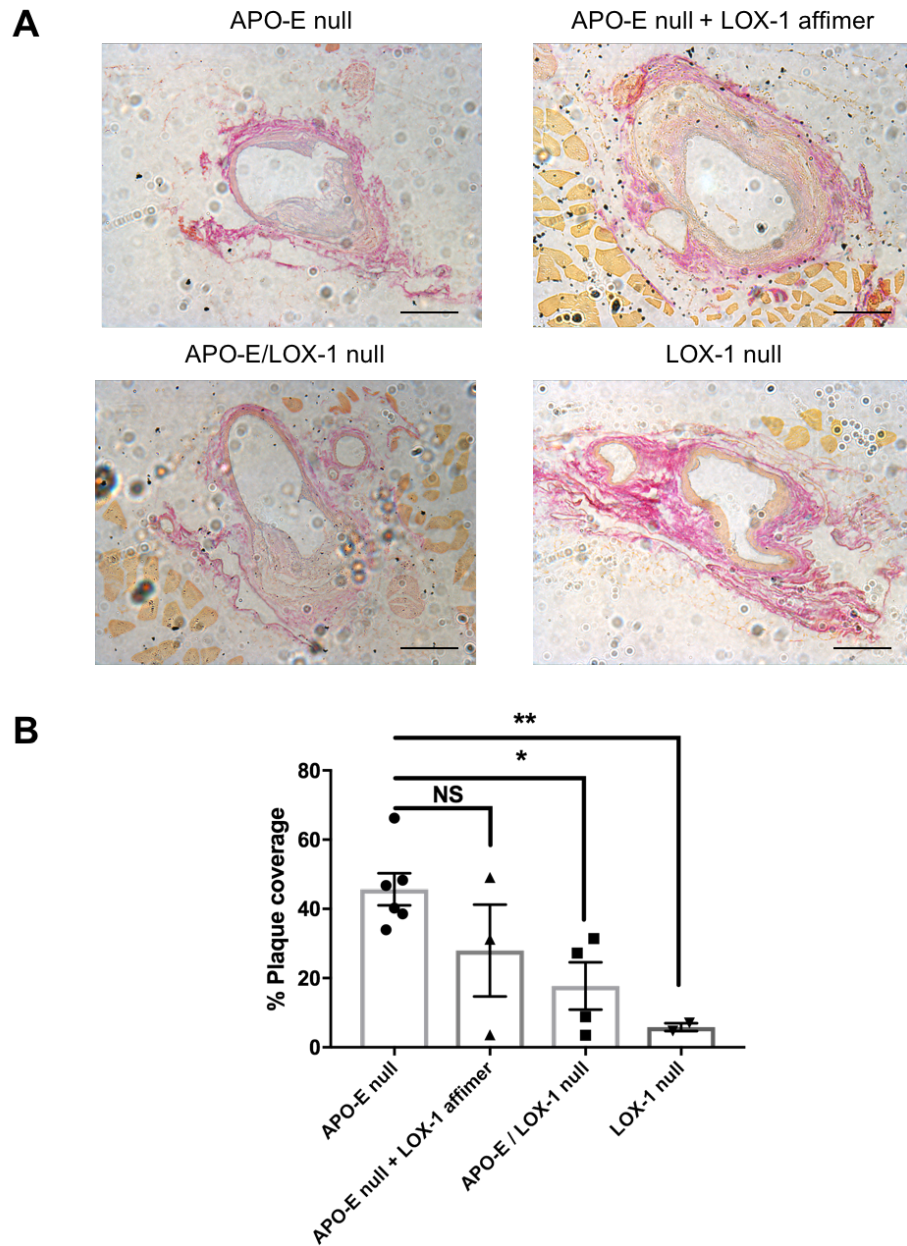


Figure 4.10 LOX-1-specific Affimer effects on femoral atherosclerosis. (A) The femoral arteries of Western diet fed transgenic mice were processed for histology and Miller elastin staining and analysed at and immediately proximal to the femoral bifurcation. B) Quantification of % plaque in carotid areas under the different treatment conditions. Magnification 10X, scale bar = 100 μ m. Error bars denote \pm SEM. APO-E null n=6, APO-E null + affimer n=3, APO-E/LOX-1 null n=4, LOX-1 null n=3. NS; not significant. p<0.05 (*), p<0.01 (**). Statistical test: One-way ANOVA.

4.3.5 The influence of LOX-1 on neointimal hyperplasia in the femoral artery

NIH is a phenomenon which primarily affects arteries and vein grafts which have been subject to either open surgery in the form of bypass grafting and / or radiological intervention in the form of angioplasty and/or stenting. Post-procedural NIH can give rise to graft failure, arterial restenosis, and/or occlusion, leading to potential limb or life threatening consequences for patients. Animal studies investigating the role of LOX-1 in NIH have found that LOX-1 expression in VSMC is upregulated post-vascular injury; the proliferation of VSMCs increased when exposed to oxLDL, suggesting that LOX-1 may mediate an oxLDL-induced VSMC proliferation in NIH post-vascular injury (Eto *et al.*, 2006). Hingata *et al.* demonstrated that LOX-1 inhibition using an anti-LOX-1 antibody reduced NIH, oxidative stress and leucocyte infiltration in a rat model of carotid artery injury (Hinagata *et al.*, 2006).

Two mouse models for NIH are well described in the literature: carotid artery ligation with cessation of blood flow and mechanically-induced denudation of endothelium in the carotid or the femoral arteries (Hui, 2008). To denude the endothelium, normally either an angioplasty guide-wire or an angioplasty balloon is used to injure the vessel. We have experience of using wire-guided damage to the femoral artery to assess effects of genotype and experimental conditions (Kahn *et al.*, 2011; Cubbon *et al.*, 2014). WD-fed mice in the *APO-E* null, *APO-E/LOX-1* null and Affimer-treated *APO-E* null mice underwent unilateral femoral artery wire injury after 8 weeks of WD. This allowed 4 weeks for NIH lesions to form by the date of harvest. Femoral artery specimens were stained with Miller / Van Gieson technique and analysed for % plaque coverage of the arterial bed. Identification of the outer and inner elastic lamina of the medial layer proved difficult in most specimens due to hyperplasia and distortion in the medial layer. This was likely a result of injury to the medial layer in addition to the intimal layer during wire injury.

At microtomy, multiple sections of femoral artery from distal to proximal were mounted and viewed (Figure 4.11). For each mouse, the specimen showing the highest degree of NIH was analysed. All 3 groups formed femoral artery NIH lesions after wire injury (Figure 4.11A). There was a significant reduction in NIH in the femoral arteries of *APO-E/LOX-1* null mice compared with *APO-E* null mice

($p=0.0368$) (Figure 4.11B). Affimer-treated *APO-E* null mice exhibited a non-significant reduction in NIH compared with *APO-E* null mice (Figure 4.11B).

4.3.6 LOX-1 affimer biodistribution studies

To evaluate the delivery of Affimer protein using continuous subcutaneous infiltration via osmotic pumps, pumps containing 1 mg/ml biotinylated LOX-1 Affimer were implanted in to 4 *LOX-1* null mice. At 1, 2, 3 and 4 weeks' post-implantation, a mouse was culled and serum, urine and major organs were harvested for analysis. Serum and urine samples were serially diluted and analysed by SDS-PAGE electrophoresis, followed by western blotting using a streptavidin-HRP detection system. Major organs were snap frozen in liquid nitrogen immediately after harvesting. Frozen organ samples were ground using a pestle and mortar and lysed using 1 X Radio-immunoprecipitation assay (RIPA) buffer. The lysate was extracted after centrifugation and analysed in the manner described above.

In serum, urine and organ lysates, biotinylated LOX-1 Affimer was not detectable in the western blots. Bands at 11-14 kDa on electrophoresis were obscured by high density bands at this level.

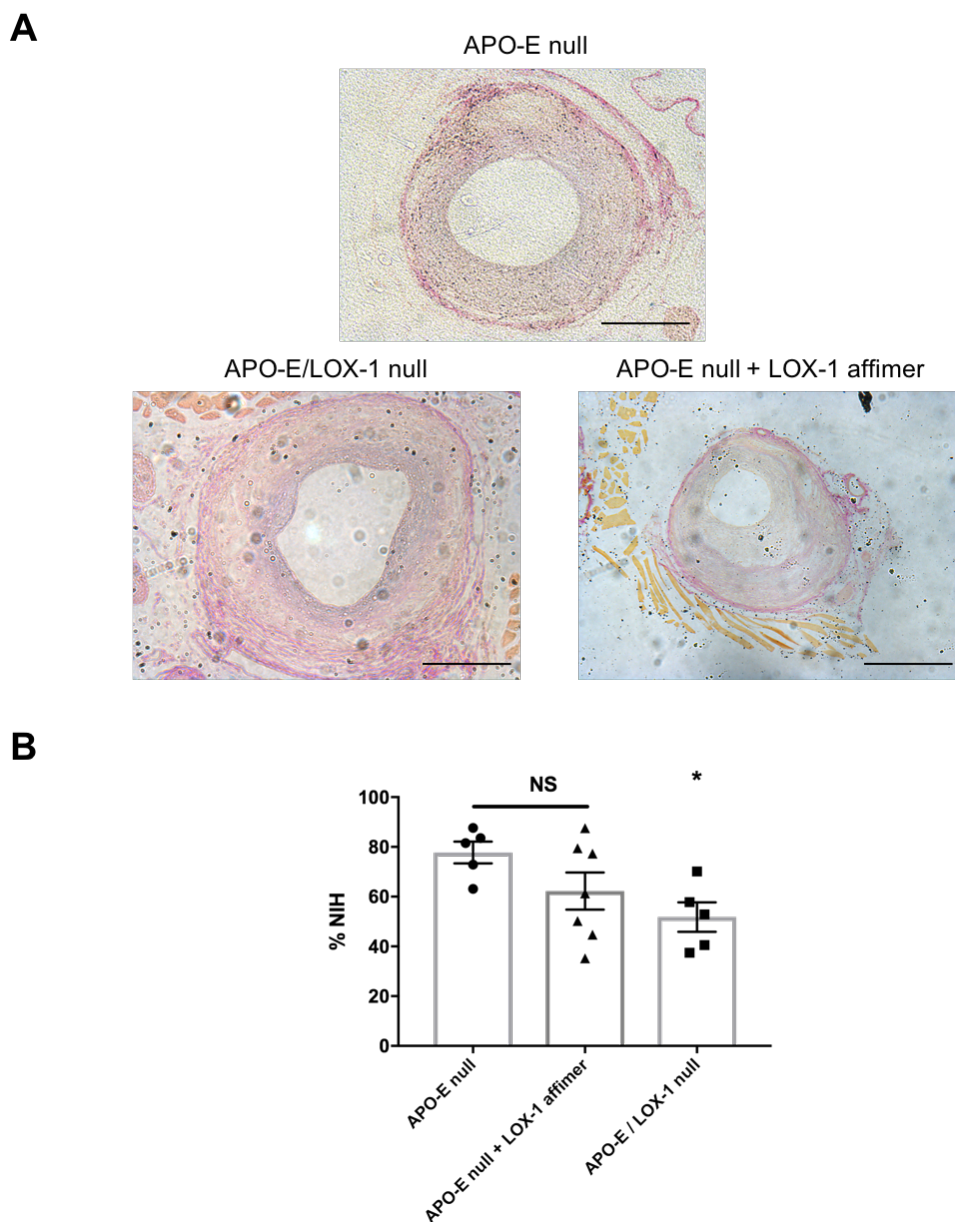


Figure 4.11 LOX-1 knockout reduces neointimal hyperplasia in APO-E null mice. (A) Unilateral femoral artery wire injury was carried out after 8 weeks of Western diet and the degree of neointimal hyperplasia (NIH) after a further 4 weeks was assessed using histology as previously described. (B) Quantification of morphological effects staining in femoral artery areas under the different treatment conditions. Magnification 10X, scale bar = 100 μ m. Error bars denote \pm SEM. APO-E null n=5, APO-E null + affimer n=7, APO-E/LOX-1 null n=5. NS; not significant. $p < 0.05$ (*). NIH; neointimal hyperplasia. Statistical test: One-way ANOVA.

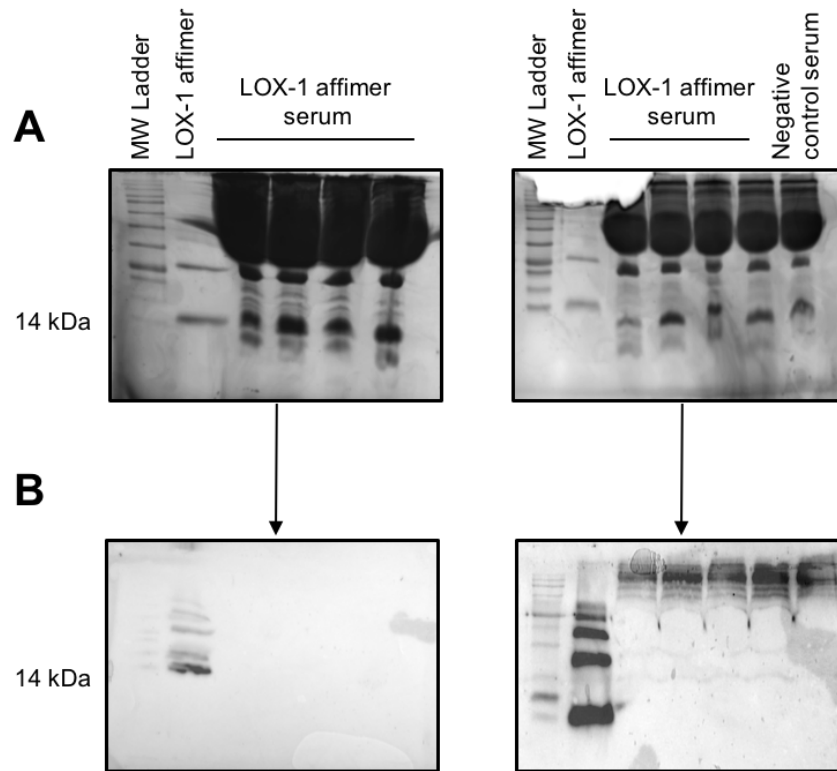


Figure 4.12. Detection of biotinylated LOX-1 affimers in mouse serum. (A) Coomassie stained protein gel electrophoresis of harvested serum from mice treated with biotinylated LOX-1 affimer, compared with positive control (LOX-1 affimer in solution) and negative control (serum from an untreated mouse). (B) Western blotting with streptavidin-HRP detection system failed to detect the presence of a band at 11-14 kDa.

4.4 Discussion

The main aim of these studies using animal models was to evaluate the effects of the LOX-1 inhibition using Affimers in the development of atherosclerosis and NIH. Furthermore, the contribution of *LOX-1* to other disease states including insulin resistance and hepatic steatosis was explored in this context. In summary, we found that *LOX-1* ablation was associated with reduced insulin resistance, reduced atherosclerotic burden and protection against NIH. It was unexpected that the *LOX-1* null mice would have a significantly increased accumulation of lipid within the liver, given the apparent association between increased LOX-1 expression and NASH in humans, and the observed resistance to atherogenesis seen in the *LOX-1* null mice.

The first transgenic study of *LOX-1* knockout was published by Mehta, Sawamura and colleagues in 2007 (Mehta Jawahar *et al.*, 2007). *LDLR* null and *LDLR/LOX-1* null mice were fed a high cholesterol diet for 18 weeks and aortic plaque coverage was compared between colonies. The authors reported amelioration of atherogenesis with LOX-1 ablation in the *LDLR* null mice. From our study of LOX-1 ablation in *APO-E* null mice, findings from the analysis of aortic atherosclerosis reproduce previous work, adding strength to the argument that LOX-1 plays an important role in oxLDL mediated atherogenesis and that it is an attractive potential therapeutic target. Aortic atherosclerosis is useful as a surrogate measure of global atherosclerotic burden in experimental animal models, however this method is limited by the lack of information on plaque thickness and cellular composition.

Aortic atherosclerosis in human subjects is relevant for its association with clinical outcomes. Multiple studies of the relationship between aortic plaque and the incidence of embolic stroke have reported an association between plaque severity or thickness and the risk of embolic stroke (Kronzon and Tunick Paul, 2006). These studies also found that plaque severity was associated with increased atherosclerosis at the carotid bifurcation and the prevalence of other risk factors such as advanced age, hypertension, hypercholesterolaemia and smoking status, suggesting that aortic plaque is a marker for global atherosclerotic burden and cardiovascular risk, rather than playing a direct role

in pathogenesis. Our study was designed to include an analysis of carotid and femoral artery bifurcation atherosclerosis, as disease at these anatomical locations do give rise to clinical manifestations in humans. *LOX-1* knockout in *APO-E* null mice did result in a reduction in atherosclerosis in the carotid and femoral arteries, however only significantly in the femoral arteries. Endothelial *LOX-1* expression is modulated by alterations in shear stress, implicating it as a likely contributor in the development of lesions at arterial bifurcations and branch ostia (Murase *et al.*, 1998). Our findings support this theory, suggesting that *LOX-1* targeting has a potential role in reducing atherogenesis at clinically important regions of altered shear stress and turbulent flow. The differences in the topography and causation of atherosclerosis between mice and humans puts limitations on the interpretation of our results. In a mouse model, experimental conditions are tightly controlled and while variables and their relationship to *LOX-1* can be investigated individually, any drawn conclusion is limited when applied to the average co-morbid arteriopathic patient. The anatomical distribution of atherosclerosis in atherosclerosis-prone transgenic mice (*APO-E* null / *LDLR* null) differs from humans: they are particularly prone to disease at the aortic sinus, the lesser curvature of the aortic arch and branch points of the brachiocephalic, subclavian and left carotid arteries (Emini Veseli *et al.*, 2017). In contrast, the distribution of disease in humans is highly variable and strongly depends on a wide variety of risk factors including smoking status, diabetes mellitus, hypertension and lipid profile to name only a few (VanderLaan Paul, Reardon Catherine and Getz Godfrey, 2004; Yasaka, Yamaguchi and Shichiri, 1993).

Mice are well understood to be resistant to atherosclerosis, hence the need for gene knockout models to accelerate diet-induced atherogenesis for research purposes (VanderLaan Paul, Reardon Catherine and Getz Godfrey, 2004). The pro-atherogenic genetic knockout component of the model (in this case, *APO-E* knockout) must also be taken in to account when considering the transferability of results to human patients. *APO-E* is a 34 kDa glycoprotein synthesized mainly in the liver and brain (Curtiss and Boisvert, 2000). It is a structural component of all lipoprotein particles except low-density lipoprotein particles and serves as a ligand for cell surface lipoprotein receptors whose function is to clear

chylomicrons and VLDL particle remnants (Curtiss and Boisvert, 2000). When fed a high cholesterol diet, *APO-E* null mice exhibit a lipid phenotype which is atypical of the human profile, with disproportionately raised VLDL levels and a total plasma cholesterol level 4 times that of chow-fed wild type mice (Plump *et al.*, 1992; Nakashima *et al.*, 1994; Emini Veseli *et al.*, 2017). LDL levels are raised in *APO-E* null mice albeit to a lesser extent than VLDL, therefore the role of LOX-1/oxLDL mediated atherosclerosis may be less so in the *APO-E* null mice compared with humans, in whom the most abundant lipoprotein particle is LDL. The *APO-E* protein is multi-functional, with roles in inflammation, oxidation, reverse cholesterol transport by macrophages, and smooth muscle proliferation and migration (Emini Veseli *et al.*, 2017; von Scheidt *et al.*, 2017). It is conceivable that these additional functions might affect atherosclerotic plaque development in the *APO-E* null mice, independent of plasma lipid levels. A further limitation of the *APO-E* null, diet-induced atherosclerosis model is the enhanced stability of atherosclerotic plaque. Plaque rupture and thrombosis is relatively infrequent in this model when compared with humans (Smith and Breslow, 1997; Emini Veseli *et al.*, 2017). Animal models of mechanically induced atherosclerosis tend to induce the formation of plaque which more closely resembles human plaque in terms of morphology and stability (Emini Veseli *et al.*, 2017). Future work may include a comparison of LOX-1 expression in plaque derived by these different methods.

NIH is an inflammatory process which is unique from atherosclerosis. It remains an important aspect of atherosclerosis research, as it manifests as a complicating secondary event following vascular injury sustained from invasive treatments such as angioplasty or open surgery. Atherosclerosis and NIH do share some common features. Both are accelerated by oxidative stress; involve the chemotaxis of immune cells and release of cytokines; and lead to the migration and proliferation of VSMCs in from the media to the sub-intimal space (Hinagata *et al.*, 2006). Evidence of a role for LOX-1 in NIH originates from experimental animal models of vascular injury. A rat model of carotid artery balloon injury found that mice treated with anti-LOX-1 antibody formed significantly less NIH 14 days post injury (Hinagata *et al.*, 2006). The authors also examined the expression of LOX-1 in VSMCs following injury and found that LOX-1 expression increased

significantly at 24 hours and peaked at 7 days' post injury. A similar study of balloon arterial injury found that in rats pre-treated with a synthetic selective superoxide scavenger, M40401 (a manganese(II) complex with a bis(cyclohexylpyridine-substituted) macrocyclic ligand), LOX-1 expression, lipid oxidation and NIH were significantly reduced at 14 days post injury (Muscoli *et al.*, 2004). Our model of NIH differs in many ways in comparison to these studies. We combined the NIH model with a dyslipidaemic model of atherosclerosis. The advantage from our model is that it may reflect more accurately on human pathology: most patients undergoing procedures which lead to NIH are chronically dyslipidaemic. The major drawback from combining the two models is the possibility that knockout of the APO-E gene may have had some effect on NIH formation. We allowed NIH to develop over 4 weeks which is double that of previously published studies. Hinagata *et al.* found that LOX-1 expression in VSMCs peaked at 7 days' post-injury. If we apply this timeframe to our results, it may be that the contribution of LOX-1 knockout or inhibition in our model had begun to plateau or decline between 7 and 28 days. Ongoing changes within this period may have been driven by the expression of other known mediators such as the SR CD36, vascular endothelial growth factor, or platelet-derived growth factor, naming only a few (Yue *et al.*, 2019; Kwon *et al.*, 2015; Pakh *et al.*, 2019). We found that LOX-1 knockout did lead to a significant reduction in femoral artery NIH, however treatment with LOX-1 Affimers did not. It is conceivable that the many other factors contributing to NIH drown out any small effect that partial LOX-1 inhibition with Affimers may produce. Complete ablation in LOX-1 knockout however has a more profound effect. The contribution of LOX-1 in NIH may be less than in atherosclerosis. Furthermore, the development of NIH is focal, whereas atherosclerosis is a systemic problem. The administration of LOX-1 Affimer in our model was systemic. It may be necessary to administer LOX-1 inhibitors locally to more effectively reduce NIH.

The metabolic effects of LOX-1 ablation are important to consider as metabolic syndrome is highly prevalent in patients presenting with cardiovascular disease (Alshehri, 2010). Metabolic syndrome is characterized by dyslipidaemia, central obesity, hypertension and insulin resistance (Grundy *et al.*, 2004). In addition to cardiovascular risk, metabolic syndrome is associated with NASH, the leading

cause of liver impairment in the developed world (Marchesini and Marzocchi, 2007). The role of LOX-1 in insulin resistance and NASH remains under investigation. A cohort study of obese patients with NASH found that particular LOX-1 polymorphisms were associated with more severe liver disease and insulin resistance (Musso *et al.*, 2011). The findings from a transgenic mouse model of obesity comparing *LOX-1* null and wild type colonies suggest that the expression of LOX-1 in adipocytes is required for pro-inflammatory cytokine secretion and lipid-induced insulin resistance. An ex-vivo model of NASH using harvested and cultured hepatic stellate cells and Kupffer cells from wild type rats also suggests an association between LOX-1 expression, dyslipidaemia and the triggering of hepatic fibrogenesis (Lu *et al.*, 1999). We found that *LOX-1* ablation was protective against obesity and diet induced insulin resistance. Prior to feeding with WD, *APO-E* null and *APO-E/LOX-1* null mice were a similar weight and produced similar results in both glucose and insulin tolerance tests. After 12 weeks of WD, the *APO-E* mice gained significantly more weight and became more insulin resistant. *APO-E/LOX-1* null and Affimer-treated *APO-E* null mice maintained similar glycaemic homeostatic profiles. These findings support the understanding that LOX-1 expression plays an important role in adipocyte insulin resistance and deposition. When we assessed the effects of LOX-1 ablation on hepatic steatosis, the results were surprising. Considering the data published linking LOX-1 to NASH, we postulated that *LOX-1* ablation would ameliorate the deposition of adipocytes. In fact, *LOX-1* ablation led to an increase in steatosis. We took further steps to examine diet-induced steatosis in *LOX-1* null mice (without the *APO-E* null background) and found that this dramatically increased steatosis. We know from our measurements of atherosclerosis and NIH that *LOX-1* null mice are relatively protected against diet-induced atherosclerosis, indicating that the processes linking LOX-1 to hepatic steatosis must be independent of those in atherogenesis. The results also suggest that there may be some interplay between APO-E and LOX-1, given the rise in hepatic steatosis when APO-E expression is restored. Previous work by members of the Ponnambalam laboratory (Abdul-Zani, 2017) has demonstrated that blood concentration of oxLDL increases when the *LOX-1* gene is knocked out (supplementary Figure B1). Analysis of liver tissue from *LOX-1* null mice found that after 12 weeks of WD, pro-inflammatory signaling was significantly increased

compared to wild type mice. The suggested underlying mechanism was increased inflammatory signaling in response to raised serum levels of oxLDL. The observed increase in hepatic steatosis in *LOX-1* null mice in our study is in keeping with this theory and warrants further investigation.

Taken together, the results from LOX-1 Affimer administration were promising. The administration of LOX-1 Affimers did exert significant protective effects against diet induced obesity and insulin resistance. These benefits are one advantage of systemic administration, although the biodistribution of affimers remains to be established. The obvious argument against systemic therapy with LOX-1 Affimers from our research is the potential for increased hepatic steatosis. The effect of LOX-1 Affimers on hepatic steatosis is less dramatic compared with the other groups which is unsurprising, given that one would assume more pronounced effects would arise in a model of *LOX-1* knockout compared with a model of LOX-1 systemic inhibition. Further work is needed to establish whether these effects are innocuous or result in more serious side effects.

Our study demonstrated that LOX-1 Affimers did reduce atherosclerosis and NIH in general, however the reductions were lower compared with *APO-E/LOX-1* null mice and were not significantly significant in most experiments. We expected any reduction in atherosclerosis and NIH in the LOX-1 Affimer treated group to be less compared with the *APO-E/LOX-1* null group. The trend towards an overall reduction does provide grounds for further studies, given that our study was underpowered, and aspects of the experimental protocol could be further optimized, particularly the establishment of a proven delivery method and the study of LOX-1 Affimer biodistribution. An adequately powered study would require far larger groups to detect marginal benefits and this should be strongly considered in any future projects using LOX-1 affimers.

LOX-1 Affimers were administered subcutaneously by continuous infusion over 8 weeks, however the Affimers were not detectable in any harvested mouse tissues (figure 4.12). There are multiple explanations for the failure of this method to detect the Affimers, including non-specific Affimer - tissue binding, the presence of free biotin in tissues and the possibility that the serum concentration of Affimers was too low to allow detection. The short half-life of the Affimer

protein, owing to its low molecular weight, has been discussed previously as a potentially problematic in any future role in therapeutics (Tiede *et al.*, 2017). A short half-life would indeed keep serum concentrations low and may have contributed to non-detection. Non-specific tissue-binding or multimerization of the proteins either in solution or in the serum may have led the loss of a band at 11-14 kDa. The failure to validate the delivery system and to generate information about the biodistribution of the LOX-1 Affimers is the most important drawback of this experimental model. To understand the ability of LOX-1 Affimers in any future animal model, the importance of evaluating and comparing delivery systems must not be underestimated. Studies investigating the effects of anti-LOX-1 antibodies in atherosclerosis have chosen intra-peritoneal injection rather than osmotic infusion pumps. In mouse models, intra-peritoneal injection is a widely-accepted method of drug delivery and perhaps should be more strongly considered in future work. The addition of larger proteins to Affimers, e.g. PEG-ylation to improve serum half-life is also an avenue for further studies.

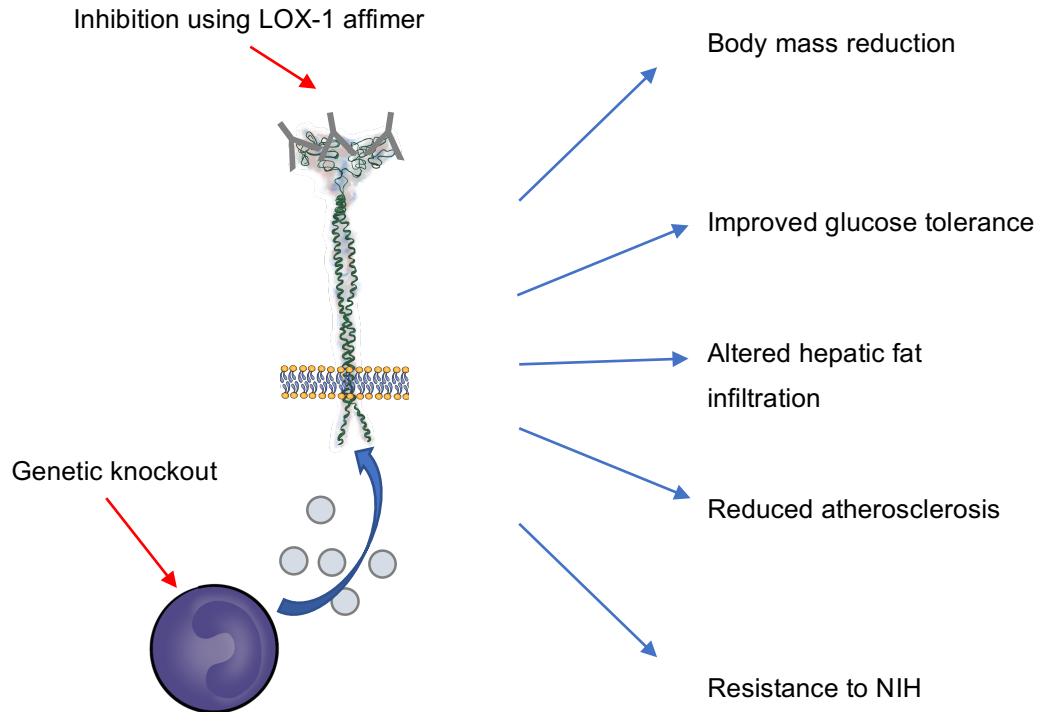


Figure 4.13 Schematic of in vivo role for LOX-1 in lipid metabolism and atherosclerosis. *LOX-1* knockout and to a lesser extent *LOX-1* targeting using Affimers leads to a vascular protective effect. Metabolic effects including glucose metabolism and fat deposition were also observed. While *LOX-1* knockout reduces body mass and improves glucose tolerance, there may be an increase in hepatic fat deposition.

CHAPTER 5

OVERVIEW AND CONCLUDING REMARKS

5.1 Discussion

LOX-1 is part of a “super-family” of SRs, many of which play key roles in atherosclerosis. There is a large body of evidence and consensus in the field that the LOX-1 protein acts by scavenging oxLDL from the circulation and promotes the development of atherosclerotic plaques. Human cohort studies have linked LOX-1 polymorphisms to cardiovascular risk, and shown that circulating sLOX-1 in the blood can be a biomarker for disease states (Kume *et al.*, 2010; Kobayashi *et al.*, 2011; Fukui *et al.*, 2013). Other studies which examine pro-atherogenic SRs such as SR-A and CD36 have suggested that signaling crosstalk between these membrane receptors exists and that ablation of one SR can lead to the upregulation of another. There are conflicting findings and conclusions, which may serve as an important warning when considering SRs in general as therapeutic targets. SRs are expressed by a wide range of cell-types and have been implicated in other disease processes such as neurodegenerative disease, malignancy and infection. There exists a strong potential for off-target effects, particularly if considering systemic SR inhibition.

5.1.1 LOX-1 and disease states

The work presented in this thesis investigating the utility of LOX-1 as a therapeutic target in atherosclerosis using cell and animal models suggests that functional LOX-1 inhibition can ameliorate atherosclerosis. The results from our studies of *LOX-1* ablation demonstrate advantages and potential drawbacks and limitations. *LOX-1* knockout significantly reduced atherosclerosis in the aorta and femoral artery and protected against the development of insulin resistance. *LOX-1* ablation had beneficial effects on the development of NIH, however these results must be interpreted in the context of a small sample size and potential for variance in the degree of vascular intimal damage incurred at the time of wire injury.

LOX-1 ablation has significant effects on liver physiology and metabolism. We demonstrated that the hepatic steatosis phenotype increased in *LOX-1* knockout when mice were fed a WD: we hypothesize based on this information and results from previous researchers (Walenbergh *et al.*, 2013; Ho *et al.*, 2019) that this results from increased levels of circulating oxLDL leading to increased hepatic cell inflammatory signaling and adipocyte deposition. SR crosstalk leading to the upregulation of SRs in the liver is another possibility; however, we currently have no data to support this theory. Further studies investigating the effects of SR knockout on hepatic steatosis and inflammation are warranted. Optimization of the design of any future animal model of hepatic steatosis could involve the use of *LDLR* null mice, as opposed to *APO-E* null line, given the higher levels of circulating LDL rather than VLDL. This could offer a more accurate representation of the effects of oxLDL-SR interaction. Researchers may wish to consider cryo-sectioning and immunostaining of fresh frozen liver, as this would allow the staining of adipocytes with Oil Red O and improve the ease and accuracy of analysis. Immunostaining for markers of hepatic fibrosis should also be considered.

5.1.2 Affimer-based LOX-1 targeting

Affimer proteins are synthetic proteins and versatile renewable affinity reagents which have far reaching potential applications as research tools and pharmaceuticals. Anti-*LOX-1* antibody administration ameliorates aortic atherosclerosis in rats, and in principle, *LOX-1* Affimers have the potential to cause similar effects. Unfortunately, our results from the use of *LOX-1* Affimers were inconsistent. Cellular studies demonstrated that *LOX-1* Affimers convincingly inhibited oxLDL–*LOX-1* binding at concentrations of 0.1-1 µg/ml. The analysis of *LOX-1* Affimer binding to *LOX-1* expressing live cells was less convincing. Immunofluorescence techniques using a variety of fluorescent labels more frequently yielded either negative or very low signal results, making interpretation challenging. Systemic administration of *LOX-1* Affimer in a mouse model protected against obesity and insulin resistance, however such treatment exerted only a moderate benefit in atherogenesis and NIH and most of the results did not reach statistical significance. One likelihood is that methods of drug

delivery and the biodistribution of LOX-1 Affimers should be assessed and improved before further work along these lines is carried out.

5.2 General limitations

The most important limitations of this project are the strict physiological conditions under which the effects have been measured. The tetracycline inducible cell line is not a vascular cell line and the downstream signaling effects of Affimer-LOX-1 binding have not been assessed.

The pattern and morphology of atherosclerotic disease in patients presenting to our clinic varies greatly from patient-to-patient due to a multitude of factors such as their lifestyle and risk factor profile, their genetic pre-disposition and their pre-existing co-morbidities. As discussed in chapter 4, our transgenic mouse model of atherosclerosis is diet-induced and does not account for some of the other major factors which promote atherosclerosis in humans, such as tobacco smoking and diabetes mellitus. The role of LOX-1 in atherosclerosis has been established using *in-vitro* and *in-vivo* models similar to those presented in this thesis and share the same limitation in this regard. Our understanding of plaque morphology and the nature of its relationship with clinical outcomes in patients is an important evolving field. We have not assessed the effects of LOX-1 ablation on plaque morphology, which is important to consider when considering the potential translation of LOX-1 affimers to clinical use.

5.3 Future Perspectives

Human studies have demonstrated the increased expression of LOX-1 in atherosclerotic tissues *ex-vivo* and the increased release of sLOX-1 in the circulation of patients presenting with acute atherosclerotic events, however targeted therapy with a LOX-1 inhibitor has not yet reached human trials. LOX-1 Affimers remain in the fledgling stages of development and much work is yet to be done. Our results are encouraging as they do inhibit oxLDL-LOX-1 binding and they are safe for use in animal models of disease. Systemic administration exerted greater influence on weight gain and insulin resistance compared with atherogenesis and NIH, and perhaps novel methods of local drug delivery could

improve efficacy while minimizing unwanted side-effects. Biodistribution and the improvement of serum half-life using conjugation techniques is an important area for future development. Future studies should focus on the effects of LOX-1 ablation on the development of hepatic steatosis and the potential for steatohepatitis. The role of LOX-1 in organ systems implicated in the development of insulin resistance is an interesting avenue for future research and its importance cannot be overstated, given the rising prevalence of diabetes mellitus in the global population.

References

- Adachi, H. and Tsujimoto, M. (1999) '[Structure and function of a novel scavenger receptor expressed in human endothelial cells]', *Tanpakushitsu Kakusan Koso*, 44(8 Suppl), pp. 1282-6.
- Adachi, H. and Tsujimoto, M. (2002) 'FEEL-1, a novel scavenger receptor with in vitro bacteria-binding and angiogenesis-modulating activities', *J Biol Chem*, 277(37), pp. 34264-70.
- Akaishi, T. and Nakashima, I. (2017) 'Efficiency of antibody therapy in demyelinating diseases', *International Immunology*, 29(7), pp. 327-335.
- Alshehri, A. M. (2010) 'Metabolic syndrome and cardiovascular risk', *Journal of family & community medicine*, 17(2), pp. 73-78.
- Andersson, L. and Freeman, M. W. (1998) 'Functional Changes in Scavenger Receptor Binding Conformation Are Induced by Charge Mutants Spanning the Entire Collagen Domain', *Journal of Biological Chemistry*, 273(31), pp. 19592-19601.
- Anguera, I., Miranda-Guardiola, F., Bosch, X., Filella, X., Sitges, M., Marin, J. L., Betriu, A. and Sanz, G. (2002) 'Elevation of serum levels of the anti-inflammatory cytokine interleukin-10 and decreased risk of coronary events in patients with unstable angina', *Am Heart J*, 144(5), pp. 811-7.
- Anitschkow, N. 1913. Ueber experimentelle Cholesterinsteatose und ihre Bedeutung fur die Entstehung einiger pathologischer Prozesse. Zentralbl Allg Pathol.
- Antoniades, C., Shirodaria, C., Crabtree, M., Rinze, R., Alp, N., Cunnington, C., Diesch, J., Tousoulis, D., Stefanadis, C., Leeson, P., Ratnatunga, C., Pillai, R. and Channon, K. M. (2007) 'Altered plasma versus vascular biopterins in human atherosclerosis reveal relationships between endothelial nitric oxide synthase coupling, endothelial function, and inflammation', *Circulation*, 116(24), pp. 2851-9.

AOYAMA, T., SAWAMURA, T., FURUTANI, Y., MATSUOKA, R., YOSHIDA, M. C., FUJIWARA, H. and MASAKI, T. (1999) 'Structure and chromosomal assignment of the human lectin-like oxidized low-density-lipoprotein receptor-1 (LOX-1) gene', *Biochemical Journal*, 339(1), pp. 177-184.

Arai, T., Wang, N., Bezouevski, M., Welch, C. and Tall, A. R. (1999) 'Decreased Atherosclerosis in Heterozygous Low Density Lipoprotein Receptor-deficient Mice Expressing the Scavenger Receptor BI Transgene', *Journal of Biological Chemistry*, 274(4), pp. 2366-2371.

Arjuman, A. and Chandra, N. C. (2017) 'LOX-1: A potential target for therapy in atherosclerosis; an in vitro study', *The International Journal of Biochemistry & Cell Biology*, 91, pp. 65-80.

Aslanian, A. M. and Charo, I. F. (2006) 'Targeted Disruption of the Scavenger Receptor and Chemokine CXCL16 Accelerates Atherosclerosis', *Circulation*, 114(6), pp. 583-590.

Aslanian Ara, M. and Charo Israel, F. (2006) 'Targeted Disruption of the Scavenger Receptor and Chemokine CXCL16 Accelerates Atherosclerosis', *Circulation*, 114(6), pp. 583-590.

Babaev, V. R., Gleaves, L. A., Carter, K. J., Suzuki, H., Kodama, T., Fazio, S. and Linton, M. F. (2000) 'Reduced Atherosclerotic Lesions in Mice Deficient for Total or Macrophage-Specific Expression of Scavenger Receptor-A', *Arteriosclerosis, Thrombosis, and Vascular Biology*, 20(12), pp. 2593-2599.

Bachli, E. B., Schaer, D. J., Walter, R. B., Fehr, J. and Schoedon, G. (2006) 'Functional expression of the CD163 scavenger receptor on acute myeloid leukemia cells of monocytic lineage', *J Leukoc Biol*, 79(2), pp. 312-8.

Baldus, S., Eiserich, J. P., Mani, A., Castro, L., Figueroa, M., Chumley, P., Ma, W., Tousson, A., White, C. R., Bullard, D. C., Brennan, M. L., Lusis, A. J., Moore, K. P. and Freeman, B. A. (2001) 'Endothelial transcytosis of myeloperoxidase confers specificity to vascular ECM proteins as targets of tyrosine nitration', *J Clin Invest*, 108(12), pp. 1759-70.

Ballinger, S. W., Patterson, C., Knight-Lozano, C. A., Burow, D. L., Conklin, C. A., Hu, Z., Reuf, J., Horaist, C., Lebovitz, R., Hunter, G. C., McIntyre, K. and Runge, M. S. (2002) 'Mitochondrial integrity and function in atherogenesis', *Circulation*, 106(5), pp. 544-9.

Balzan, S. and Lubrano, V. (2018) 'LOX-1 receptor: A potential link in atherosclerosis and cancer', *Life Sciences*, 198, pp. 79-86.

Basta, G., Del Turco, S., Navarra, T., Mazzarisi, A., Cocci, F., Coceani, M., Bianchi, M., Schlueter, M. and Marraccini, P. (2012) 'Inverse Association between Circulating Levels of Soluble Receptor for Advanced Glycation End-Products and Coronary Plaque Burden', *Journal of Atherosclerosis and Thrombosis*, 19(10), pp. 941-948.

Bedard, K. and Krause, K.-H. (2007a) 'The NOX Family of ROS-Generating NADPH Oxidases: Physiology and Pathophysiology', *Physiological Reviews*, 87(1), pp. 245-313.

Bedard, K. and Krause, K. H. (2007b) 'The NOX family of ROS-generating NADPH oxidases: physiology and pathophysiology', *Physiol Rev*, 87(1), pp. 245-313.

Besli, F., Gullulu, S., Sag, S., Kecebas, M., Acikgoz, E., Sarandol, E. and Aydinlar, A. (2016) 'The relationship between serum lectin-like oxidized LDL receptor-1 levels and systolic heart failure', *Acta Cardiologica*, 71(2), pp. 185-190.

Bhatnagar, P., Wickramasinghe, K., Williams, J., Rayner, M. and Townsend, N. (2015) 'The epidemiology of cardiovascular disease in the UK 2014', *Heart (British Cardiac Society)*, 101(15), pp. 1182-1189.

Bhatt, D. L., Steg, P. G., Ohman, E. M., Hirsch, A. T., Ikeda, Y., Mas, J.-L., Goto, S., Liao, C.-S., Richard, A. J., Röther, J., Wilson, P. W. F. and REACH Registry Investigators, f. t. (2006) 'International Prevalence, Recognition, and Treatment of Cardiovascular Risk Factors in Outpatients With Atherothrombosis', *JAMA*, 295(2), pp. 180-189.

- Bierhaus, A., Hofmann, M. A., Ziegler, R. and Nawroth, P. P. (1998) 'AGEs and their interaction with AGE-receptors in vascular disease and diabetes mellitus. I. The AGE concept', *Cardiovascular Research*, 37(3), pp. 586-600.
- Binz, H. K., Stumpp, M. T., Forrer, P., Amstutz, P. and Pluckthun, A. (2003) 'Designing repeat proteins: well-expressed, soluble and stable proteins from combinatorial libraries of consensus ankyrin repeat proteins', *J Mol Biol*, 332(2), pp. 489-503.
- Biocca, S., Iacovelli, F., Matarazzo, S., Vindigni, G., Oteri, F., Desideri, A. and Falconi, M. (2015) 'Molecular mechanism of statin-mediated LOX-1 inhibition', *Cell cycle (Georgetown, Tex.)*, 14(10), pp. 1583-1595.
- Bornhorst, J. A. and Falke, J. J. (2000) 'Purification of proteins using polyhistidine affinity tags', *Methods in enzymology*, 326, pp. 245-254.
- Borst, O., Schaub, M., Walker, B., Sauter, M., Muenzer, P., Gramlich, M., Mueller, K., Geisler, T., Lang, F., Klingel, K., Kandolf, R., Bigalke, B., Gawaz, M. and Zuern, C. S. (2014) 'CXCL16 is a novel diagnostic marker and predictor of mortality in inflammatory cardiomyopathy and heart failure', *Int J Cardiol*, 176(3), pp. 896-903.
- Borén, J., Olin, K., Lee, I., Chait, A., Wight, T. N. and Innerarity, T. L. (1998) 'Identification of the principal proteoglycan-binding site in LDL. A single-point mutation in apo-B100 severely affects proteoglycan interaction without affecting LDL receptor binding', *The Journal of clinical investigation*, 101(12), pp. 2658-2664.
- Brennan, M. L., Anderson, M. M., Shih, D. M., Qu, X. D., Wang, X., Mehta, A. C., Lim, L. L., Shi, W., Hazen, S. L., Jacob, J. S., Crowley, J. R., Heinecke, J. W. and Lusis, A. J. (2001) 'Increased atherosclerosis in myeloperoxidase-deficient mice', *J Clin Invest*, 107(4), pp. 419-30.
- Breslow, J. L. (1996) 'Mouse Models of Atherosclerosis', *Science*, 272(5262), pp. 685.

Brinkley, T. E., Kume, N., Mitsuoka, H., Phares, D. A. and Hagberg, J. M. (2008) 'Elevated soluble lectin-like oxidized LDL receptor-1 (sLOX-1) levels in obese postmenopausal women', *Obesity (Silver Spring, Md.)*, 16(6), pp. 1454-1456.

Brown, M. S., Basu, S. K., Falck, J. R., Ho, Y. K. and Goldstein, J. L. (1980) 'The scavenger cell pathway for lipoprotein degradation: specificity of the binding site that mediates the uptake of negatively-charged LDL by macrophages', *J Supramol Struct*, 13(1), pp. 67-81.

Bujold, K., Mellal, K., Zoccal, K. F., Rhainds, D., Brissette, L., Febbraio, M., Marleau, S. and Ong, H. (2013) 'EP 80317, a CD36 selective ligand, promotes reverse cholesterol transport in apolipoprotein E-deficient mice', *Atherosclerosis*, 229(2), pp. 408-414.

Burrage, P. S., Mix, K. S. and Brinckerhoff, C. E. (2006) 'Matrix metalloproteinases: role in arthritis', *Front Biosci*, 11, pp. 529-43.

Cai, Y., Xu, M.-J., Teng, X., Zhou, Y. B., Chen, L., Zhu, Y., Wang, X., Tang, C. S. and Qi, Y. F. (2009) 'Intermedin inhibits vascular calcification by increasing the level of matrix γ -carboxyglutamic acid protein', *Cardiovascular Research*, 85(4), pp. 864-873.

Castelli, W. P., Garrison, R. J., Wilson, P. W., Abbott, R. D., Kalousdian, S. and Kannel, W. B. (1986) 'Incidence of coronary heart disease and lipoprotein cholesterol levels. The Framingham Study', *Jama*, 256(20), pp. 2835-8.

Chames, P., Van Regenmortel, M., Weiss, E. and Baty, D. (2009) 'Therapeutic antibodies: successes, limitations and hopes for the future', *British Journal of Pharmacology*, 157(2), pp. 220-233.

Chapman, M. J., Goldstein, S., Lagrange, D. and Laplaud, P. M. (1981) 'A density gradient ultracentrifugal procedure for the isolation of the major lipoprotein classes from human serum', *Journal of Lipid Research*, 22(2), pp. 339-358.

Che, J. J., Shao, Y. X. and Li, G. P. (2014) 'Association between rs1049673 polymorphism in CD36 and premature coronary heart disease', *Genet Mol Res*, 13(3), pp. 7708-17.

Chen, J., Li, D., Schaefer, R. and Mehta, J. L. (2006) 'Cross-talk between dyslipidemia and renin-angiotensin system and the role of LOX-1 and MAPK in atherogenesis studies with the combined use of rosuvastatin and candesartan', *Atherosclerosis*, 184(2), pp. 295-301.

Chen, J. and Mehta, J. L. (2006) 'Interaction of oxidized low-density lipoprotein and the renin-angiotensin system in coronary artery disease', *Curr Hypertens Rep*, 8(2), pp. 139-43.

Chen, L. Y., Mehta, P. and Mehta, J. L. (1996) 'Oxidized LDL decreases L-arginine uptake and nitric oxide synthase protein expression in human platelets: relevance of the effect of oxidized LDL on platelet function', *Circulation*, 93(9), pp. 1740-6.

Chen, M., Inoue, K., Narumiya, S., Masaki, T. and Sawamura, T. (2001a) 'Requirements of basic amino acid residues within the lectin-like domain of LOX-1 for the binding of oxidized low-density lipoprotein', *FEBS Letters*, 499(3), pp. 215-219.

Chen, M., Kakutani, M., Naruko, T., Ueda, M., Narumiya, S., Masaki, T. and Sawamura, T. (2001b) 'Activation-Dependent Surface Expression of LOX-1 in Human Platelets', *Biochemical and Biophysical Research Communications*, 282(1), pp. 153-158.

Chen, M., Nagase, M., Fujita, T., Narumiya, S., Masaki, T. and Sawamura, T. (2001c) 'Diabetes enhances lectin-like oxidized LDL receptor-1 (LOX-1) expression in the vascular endothelium: possible role of LOX-1 ligand and AGE', *Biochem Biophys Res Commun*, 287(4), pp. 962-8.

CHEN, M., NARUMIYA, S., MASAKI, T. and SAWAMURA, T. (2001) 'Conserved C-terminal residues within the lectin-like domain of LOX-1 are essential for oxidized low-density-lipoprotein binding', *Biochemical Journal*, 355(2), pp. 289-296.

Chistiakov, D. A., Orekhov, A. N. and Bobryshev, Y. V. (2016) 'LOX-1-Mediated Effects on Vascular Cells in Atherosclerosis', *Cellular Physiology and Biochemistry*, 38(5), pp. 1851-1859.

Chnari, E., Nikitczuk, J. S., Wang, J., Uhrich, K. E. and Moghe, P. V. (2006) 'Engineered Polymeric Nanoparticles for Receptor-Targeted Blockage of Oxidized Low Density Lipoprotein Uptake and Atherogenesis in Macrophages', *Biomacromolecules*, 7(6), pp. 1796-1805.

Cho, S. (2012) 'CD36 as a therapeutic target for endothelial dysfunction in stroke', *Curr Pharm Des*, 18(25), pp. 3721-30.

Cho, S. and Kim, E. (2009) 'CD36: a multi-modal target for acute stroke therapy', *J Neurochem*, 109 Suppl 1(Suppl 1), pp. 126-32.

Cho, S., Szeto, H. H., Kim, E., Kim, H., Tolhurst, A. T. and Pinto, J. T. (2007) 'A Novel Cell-permeable Antioxidant Peptide, SS31, Attenuates Ischemic Brain Injury by Down-regulating CD36', *Journal of Biological Chemistry*, 282(7), pp. 4634-4642.

Christie, R. H., Freeman, M. and Hyman, B. T. (1996) 'Expression of the macrophage scavenger receptor, a multifunctional lipoprotein receptor, in microglia associated with senile plaques in Alzheimer's disease', *The American journal of pathology*, 148(2), pp. 399-403.

Chui, P. C., Guan, H. P., Lehrke, M. and Lazar, M. A. (2005) 'PPARgamma regulates adipocyte cholesterol metabolism via oxidized LDL receptor 1', *J Clin Invest*, 115(8), pp. 2244-56.

Colhoun, H. M., Betteridge, D. J., Durrington, P., Hitman, G., Neil, A., Livingstone, S., Charlton-Menys, V., Bao, W., DeMicco, D. A., Preston, G. M., Deshmukh, H., Tan, K. and Fuller, J. H. (2011) 'Total Soluble and Endogenous Secretory Receptor for Advanced Glycation End Products as Predictive Biomarkers of Coronary Heart Disease Risk in Patients With Type 2 Diabetes', *An Analysis From the CARDS Trial*, 60(9), pp. 2379-2385.

Cominacini, L., Pasini, A. F., Garbin, U., Davoli, A., Tosetti, M. L., Campagnola, M., Rigoni, A., Pastorino, A. M., Lo Cascio, V. and Sawamura, T. (2000) 'Oxidized low density lipoprotein (ox-LDL) binding to ox-LDL receptor-1 in endothelial cells induces the activation of NF-kappaB through an increased production of intracellular reactive oxygen species', *J Biol Chem*, 275(17), pp. 12633-8.

Corral-Debrinski, M., Shoffner, J. M., Lott, M. T. and Wallace, D. C. (1992) 'Association of mitochondrial DNA damage with aging and coronary atherosclerotic heart disease', *Mutat Res*, 275(3-6), pp. 169-80.

Cubbon, R. M., Yuldasheva, N. Y., Viswambharan, H., Mercer, B. N., Baliga, V., Stephen, S. L., Askham, J., Sukumar, P., Skromna, A., Mughal, R. S., Walker, A. M., Bruns, A., Bailey, M. A., Galloway, S., Imrie, H., Gage, M. C., Rakobowchuk, M., Li, J., Porter, K. E., Ponnambalam, S., Wheatcroft, S. B., Beech, D. J. and Kearney, M. T. (2014) 'Restoring Akt1 activity in outgrowth endothelial cells from South Asian men rescues vascular reparative potential', *Stem Cells*, 32(10), pp. 2714-23.

Cuccurullo, C., Iezzi, A., Fazia Maria, L., De Cesare, D., Di Francesco, A., Muraro, R., Bei, R., Uchino, S., Spigonardo, F., Chiarelli, F., Schmidt Ann, M., Cuccurullo, F., Mezzetti, A. and Cipollone, F. (2006) 'Suppression of RAGE as a Basis of Simvastatin-Dependent Plaque Stabilization in Type 2 Diabetes', *Arteriosclerosis, Thrombosis, and Vascular Biology*, 26(12), pp. 2716-2723.

Curtiss, L. K. and Boisvert, W. A. (2000) 'Apolipoprotein E and atherosclerosis', *Current Opinion in Lipidology*, 11(3), pp. 243-251.

Dai, X.-Y., Cai, Y., Mao, D.-D., Qi, Y.-F., Tang, C., Xu, Q., Zhu, Y., Xu, M.-J. and Wang, X. (2012) 'Increased stability of phosphatase and tensin homolog by intermedin leading to scavenger receptor A inhibition of macrophages reduces atherosclerosis in apolipoprotein E-deficient mice', *Journal of Molecular and Cellular Cardiology*, 53(4), pp. 509-520.

Dai, Y., Wu, X., Dai, D., Li, J. and Mehta, J. L. (2018) 'MicroRNA-98 regulates foam cell formation and lipid accumulation through repression of LOX-1', *Redox biology*, 16, pp. 255-262.

Davignon, J. (2005) 'Apolipoprotein E and Atherosclerosis', *Arteriosclerosis, Thrombosis, and Vascular Biology*, 25(2), pp. 267-269.

de Beer, M. C., Zhao, Z., Webb, N. R., van der Westhuyzen, D. R. and de Villiers, W. J. (2003) 'Lack of a direct role for macrosialin in oxidized LDL metabolism', *J Lipid Res*, 44(4), pp. 674-85.

De Siqueira, J., Abdul Zani, I., Russell, D. A., Wheatcroft, S. B., Ponnambalam, S. and Homer-Vanniasinkam, S. (2015) 'Clinical and Preclinical Use of LOX-1-Specific Antibodies in Diagnostics and Therapeutics', *Journal of Cardiovascular Translational Research*, 8(8), pp. 458-465.

Ding, Z., Liu, S., Wang, X., Deng, X., Fan, Y., Shahanawaz, J., Shmookler Reis, R. J., Varughese, K. I., Sawamura, T. and Mehta, J. L. (2015) 'Cross-talk between LOX-1 and PCSK9 in vascular tissues', *Cardiovascular Research*, 107(4), pp. 556-567.

Dobrian, A. D., Lieb, D. C., Cole, B. K., Taylor-Fishwick, D. A., Chakrabarti, S. K. and Nadler, J. L. (2011) 'Functional and pathological roles of the 12- and 15-lipoxygenases', *Progress in lipid research*, 50(1), pp. 115-131.

Dominguez, J. H., Mehta, J. L., Li, D., Wu, P., Kelly, K. J., Packer, C. S., Temm, C., Goss, E., Cheng, L., Zhang, S., Patterson, C. E., Hawes, J. W. and Peterson, R. (2008) 'Anti-LOX-1 therapy in rats with diabetes and dyslipidemia: ablation of renal vascular and epithelial manifestations', *American Journal of Physiology-Renal Physiology*, 294(1), pp. F110-F119.

Draude, G., Hrboticky, N. and Lorenz, R. L. (1999) 'The expression of the lectin-like oxidized low-density lipoprotein receptor (LOX-1) on human vascular smooth muscle cells and monocytes and its down-regulation by lovastatin', *Biochemical Pharmacology*, 57(4), pp. 383-386.

El Khoury, J., Hickman, S. E., Thomas, C. A., Cao, L., Silverstein, S. C. and Loike, J. D. (1996) 'Scavenger receptor-mediated adhesion of microglia to beta-amyloid fibrils', *Nature*, 382(6593), pp. 716-9.

Emini Veseli, B., Perrotta, P., De Meyer, G. R. A., Roth, L., Van der Donckt, C., Martinet, W. and De Meyer, G. R. Y. (2017) 'Animal models of atherosclerosis', *European Journal of Pharmacology*, 816, pp. 3-13.

Emura, I., Usuda, H., Fujita, T., Ebe, K. and Nagai, T. (2007) 'Increase of scavenger receptor A-positive monocytes in patients with acute coronary syndromes', *Pathol Int*, 57(8), pp. 502-8.

Emura, I., Usuda, H., Fujita, T., Ebe, K. and Nagai, T. (2011) 'Scavenger receptor A index and coronary thrombus in patients with acute ST elevation myocardial infarction', *Pathology International*, 61(6), pp. 351-355.

Eto, H., Miyata, M., Kume, N., Minami, M., Itabe, H., Orihara, K., Hamasaki, S., Biro, S., Otsuji, Y., Kita, T. and Tei, C. (2006) 'Expression of lectin-like oxidized LDL receptor-1 in smooth muscle cells after vascular injury', *Biochem Biophys Res Commun*, 341(2), pp. 591-8.

Etzerodt, A., Maniecki, M. B., Graversen, J. H., Møller, H. J., Torchilin, V. P. and Moestrup, S. K. (2012) 'Efficient intracellular drug-targeting of macrophages using stealth liposomes directed to the hemoglobin scavenger receptor CD163', *J Control Release*, 160(1), pp. 72-80.

Falcone, C., Emanuele, E., D'Angelo, A., Buzzi Maria, P., Belvito, C., Cuccia, M. and Geroldi, D. (2005) 'Plasma Levels of Soluble Receptor for Advanced Glycation End Products and Coronary Artery Disease in Nondiabetic Men', *Arteriosclerosis, Thrombosis, and Vascular Biology*, 25(5), pp. 1032-1037.

Falk, E. (2006) 'Pathogenesis of Atherosclerosis', *Journal of the American College of Cardiology*, 47(8, Supplement), pp. C7-C12.

Fan, Q., Cai, H., Yang, H., Li, L., Yuan, C., Lu, X. and Wan, L. (2014) 'Biological evaluation of ¹³¹I- and CF750-labeled Dmab(scFv)-Fc antibodies for xenograft imaging of CD25-positive tumors', *BioMed research international*, 2014, pp. 459676-459676.

Febbraio, M., Hajjar, D. P. and Silverstein, R. L. (2001) 'CD36: a class B scavenger receptor involved in angiogenesis, atherosclerosis, inflammation, and lipid metabolism', *The Journal of clinical investigation*, 108(6), pp. 785-791.

Feingold, K. and Grunfeld, C. (2018) *Introduction to lipid and lipoproteins. Endotext*. South Dartmouth (MA). MDtext.

Fichtlscherer, S., Breuer, S., Heeschen, C., Dimmeler, S. and Zeiher, A. M. (2004) 'Interleukin-10 serum levels and systemic endothelial vasoreactivity in patients with coronary artery disease', *J Am Coll Cardiol*, 44(1), pp. 44-9.

Forstermann, U., Xia, N. and Li, H. (2017) 'Roles of Vascular Oxidative Stress and Nitric Oxide in the Pathogenesis of Atherosclerosis', *Circ Res*, 120(4), pp. 713-735.

Fujisawa, K., Katakami, N., Kaneto, H., Naka, T., Takahara, M., Sakamoto, F., Irie, Y., Miyashita, K., Kubo, F., Yasuda, T., Matsuoka, T.-a. and Shimomura, I. (2013) 'Circulating soluble RAGE as a predictive biomarker of cardiovascular event risk in patients with type 2 diabetes', *Atherosclerosis*, 227(2), pp. 425-428.

Fukui, M., Tanaka, M., Senmaru, T., Nakanishi, M., Mukai, J., Ohki, M., Asano, M., Yamazaki, M., Hasegawa, G. and Nakamura, N. (2013) 'LOX-1 is a novel marker for peripheral artery disease in patients with type 2 diabetes', *Metabolism*, 62(7), pp. 935-8.

Fulton, D. J. R. and Barman, S. A. (2016) 'Clarity on the Isoform-Specific Roles of NADPH Oxidases and NADPH Oxidase-4 in Atherosclerosis', *Arteriosclerosis, thrombosis, and vascular biology*, 36(4), pp. 579-581.

Gao, H., Li, H., Li, W., Shen, X. and Di, B. (2017) 'Pioglitazone Attenuates Atherosclerosis in Diabetic Mice by Inhibition of Receptor for Advanced Glycation End-Product (RAGE) Signaling', *Medical science monitor : international medical journal of experimental and clinical research*, 23, pp. 6121-6131.

Gavrilov, K. and Saltzman, W. M. (2012) 'Therapeutic siRNA: principles, challenges, and strategies', *The Yale journal of biology and medicine*, 85(2), pp. 187-200.

Gebauer, M. and Skerra, A. (2009) 'Engineered protein scaffolds as next-generation antibody therapeutics', *Current Opinion in Chemical Biology*, 13(3), pp. 245-255.

Gistera, A. and Hansson, G. K. (2017) 'The immunology of atherosclerosis', *Nat Rev Nephrol*, 13(6), pp. 368-380.

Gistera, A., Robertson, A. K., Andersson, J., Ketelhuth, D. F., Ovchinnikova, O., Nilsson, S. K., Lundberg, A. M., Li, M. O., Flavell, R. A. and Hansson, G. K. (2013) 'Transforming growth factor-beta signaling in T cells promotes stabilization of atherosclerotic plaques through an interleukin-17-dependent pathway', *Sci Transl Med*, 5(196), pp. 196ra100.

Glintborg, D., Højlund, K., Andersen, M., Henriksen, J. E., Beck-Nielsen, H. and Handberg, A. (2008) 'Soluble CD36 and Risk Markers of Insulin Resistance and Atherosclerosis Are Elevated in Polycystic Ovary Syndrome and Significantly Reduced During Pioglitazone Treatment', *Diabetes Care*, 31(2), pp. 328-334.

'Global, regional, and national age-sex specific all-cause and cause-specific mortality for 240 causes of death, 1990-2013: a systematic analysis for the Global Burden of Disease Study 2013', (2015) *Lancet*, 385(9963), pp. 117-71.

Goldstein, J. L., Ho, Y. K., Basu, S. K. and Brown, M. S. (1979) 'Binding site on macrophages that mediates uptake and degradation of acetylated low density lipoprotein, producing massive cholesterol deposition', *Proc Natl Acad Sci U S A*, 76(1), pp. 333-7.

Gonzalez, L. and Trigatti, B. L. (2017) 'Macrophage Apoptosis and Necrotic Core Development in Atherosclerosis: A Rapidly Advancing Field with Clinical Relevance to Imaging and Therapy', *Can J Cardiol*, 33(3), pp. 303-312.

Gough, P. J., Greaves, D. R., Suzuki, H., Hakkinen, T., Hiltunen, M. O., Turunen, M., Herttuala, S. Y., Kodama, T. and Gordon, S. (1999) 'Analysis of macrophage scavenger receptor (SR-A) expression in human aortic atherosclerotic lesions', *Arterioscler Thromb Vasc Biol*, 19(3), pp. 461-71.

Graham, J. M., Higgins, J. A., Gillott, T., Taylor, T., Wilkinson, J., Ford, T. and Billington, D. (1996) 'A novel method for the rapid separation of plasma lipoproteins using self-generating gradients of iodixanol', *Atherosclerosis*, 124(1), pp. 125-35.

Greaves, D. R. and Gordon, S. (2002) 'Macrophage-Specific Gene Expression: Current Paradigms and Future Challenges', *International Journal of Hematology*, 76(1), pp. 6-15.

Grundy, S. M., Brewer, H. B., Jr., Cleeman, J. I., Smith, S. C., Jr. and Lenfant, C. (2004) 'Definition of metabolic syndrome: Report of the National Heart, Lung, and Blood Institute/American Heart Association conference on scientific issues related to definition', *Circulation*, 109(3), pp. 433-8.

Han, J., Parsons, M., Zhou, X., Nicholson Andrew, C., Gotto Antonio, M. and Hajjar David, P. (2004) 'Functional Interplay Between the Macrophage Scavenger Receptor Class B Type I and Pitavastatin (NK-104)', *Circulation*, 110(22), pp. 3472-3479.

Hawkes, N. (2017) 'NICE guidelines could put 12 million UK adults on statins', *BMJ*, 358, pp. j3674.

Hehir, S., Plourde, N. M., Gu, L., Poree, D. E., Welsh, W. J., Moghe, P. V. and Urich, K. E. (2012) 'Carbohydrate composition of amphiphilic macromolecules influences physicochemical properties and binding to atherogenic scavenger receptor A', *Acta Biomater*, 8(11), pp. 3956-62.

Herre, J., Willment, J. A., Gordon, S. and Brown, G. D. (2004) 'The role of Dectin-1 in antifungal immunity', *Crit Rev Immunol*, 24(3), pp. 193-203.

Hinagata, J., Kakutani, M., Fujii, T., Naruko, T., Inoue, N., Fujita, Y., Mehta, J. L., Ueda, M. and Sawamura, T. (2006) 'Oxidized LDL receptor LOX-1 is involved in neointimal hyperplasia after balloon arterial injury in a rat model', *Cardiovasc Res*, 69(1), pp. 263-71.

Hirsch, H. A., Iliopoulos, D., Joshi, A., Zhang, Y., Jaeger, S. A., Bulyk, M., Tschlis, P. N., Shirley Liu, X. and Struhl, K. (2010) 'A transcriptional signature

and common gene networks link cancer with lipid metabolism and diverse human diseases', *Cancer Cell*, 17(4), pp. 348-61.

Ho, C.-M., Ho, S.-L., Jeng, Y.-M., Lai, Y.-S., Chen, Y.-H., Lu, S.-C., Chen, H.-L., Chang, P.-Y., Hu, R.-H. and Lee, P.-H. (2019) 'Accumulation of free cholesterol and oxidized low-density lipoprotein is associated with portal inflammation and fibrosis in nonalcoholic fatty liver disease', *Journal of Inflammation*, 16(1), pp. 7.

Hofnagel, O., Engel, T., Severs, N. J., Robenek, H. and Buers, I. (2011) 'SR-PSOX at sites predisposed to atherosclerotic lesion formation mediates monocyte-endothelial cell adhesion', *Atherosclerosis*, 217(2), pp. 371-8.

Hofnagel, O., Luechtenborg, B., Plenz, G. and Robenek, H. (2002) 'Expression of the novel scavenger receptor SR-PSOX in cultured aortic smooth muscle cells and umbilical endothelial cells', *Arterioscler Thromb Vasc Biol*, 22(4), pp. 710-1.

Holness, C. L. and Simmons, D. L. (1993) 'Molecular cloning of CD68, a human macrophage marker related to lysosomal glycoproteins', *Blood*, 81(6), pp. 1607-13.

Hoshikawa, H., Sawamura, T., Kakutani, M., Aoyama, T., Nakamura, T. and Masaki, T. (1998) 'High affinity binding of oxidized LDL to mouse lectin-like oxidized LDL receptor (LOX-1)', *Biochem Biophys Res Commun*, 245(3), pp. 841-6.

Hu, W., Xie, Q., Liu, L. and Xiang, H. (2018) 'Enhanced Bioactivity of the Anti-LOX-1 scFv Engineered by Multimerization Strategy', *Appl Biochem Biotechnol*, 185(1), pp. 233-247.

Hu, W., Xie, Q. and Xiang, H. (2017) 'Improved scFv Anti-LOX-1 Binding Activity by Fusion with LOX-1-Binding Peptides', *BioMed research international*, 2017, pp. 8946935-8946935.

Hu, Z. B., Chen, Y., Gong, Y. X., Gao, M., Zhang, Y., Wang, G. H., Tang, R. N., Liu, H., Liu, B. C. and Ma, K. L. (2016) 'Activation of the CXCL16/CXCR6 Pathway by Inflammation Contributes to Atherosclerosis in Patients with End-stage Renal Disease', *Int J Med Sci*, 13(11), pp. 858-867.

Hughes, D. A., Fraser, I. P. and Gordon, S. (1995) 'Murine macrophage scavenger receptor: in vivo expression and function as receptor for macrophage adhesion in lymphoid and non-lymphoid organs', *Eur J Immunol*, 25(2), pp. 466-73.

Hui, D. Y. (2008) 'Intimal hyperplasia in murine models', *Current drug targets*, 9(3), pp. 251-260.

Irjala, H., Alanen, K., Grénman, R., Heikkilä, P., Joensuu, H. and Jalkanen, S. (2003a) 'Mannose receptor (MR) and common lymphatic endothelial and vascular endothelial receptor (CLEVER)-1 direct the binding of cancer cells to the lymph vessel endothelium', *Cancer Res*, 63(15), pp. 4671-6.

Irjala, H., Elima, K., Johansson, E. L., Merinen, M., Kontula, K., Alanen, K., Grenman, R., Salmi, M. and Jalkanen, S. (2003b) 'The same endothelial receptor controls lymphocyte traffic both in vascular and lymphatic vessels', *Eur J Immunol*, 33(3), pp. 815-24.

Ishigaki, T., Ohki, I., Utsunomiya-Tate, N. and Tate, S. I. (2007) 'Chimeric structural stabilities in the coiled-coil structure of the NECK domain in human lectin-like oxidized low-density lipoprotein receptor 1 (LOX-1)', *J Biochem*, 141(6), pp. 855-66.

Ishii, J., Adachi, H., Aoki, J., Koizumi, H., Tomita, S., Suzuki, T., Tsujimoto, M., Inoue, K. and Arai, H. (2002) 'SREC-II, a new member of the scavenger receptor type F family, trans-interacts with SREC-I through its extracellular domain', *J Biol Chem*, 277(42), pp. 39696-702.

Ishikawa, M., Ito, H., Akiyoshi, M., Kume, N., Yoshitomi, H., Mitsuoka, H., Tanida, S., Murata, K., Shibuya, H., Kasahara, T., Kakino, A., Fujita, Y., Sawamura, T., Yasuda, T. and Nakamura, T. (2012) 'Lectin-like oxidized low-density lipoprotein receptor 1 signal is a potent biomarker and therapeutic target for human rheumatoid arthritis', *Arthritis Rheum*, 64(4), pp. 1024-34.

Iverson, N. M., Plourde, N. M., Sparks, S. M., Wang, J., Patel, E. N., Shah, P. S., Lewis, D. R., Zablocki, K. R., Nackman, G. B., Uhrich, K. E. and Moghe, P. V.

(2011) 'Dual use of amphiphilic macromolecules as cholesterol efflux triggers and inhibitors of macrophage athero-inflammation', *Biomaterials*, 32(32), pp. 8319-8327.

Iwai-Kanai, E., Hasegawa, K., Sawamura, T., Fujita, M., Yanazume, T., Toyokuni, S., Adachi, S., Kihara, Y. and Sasayama, S. (2001) 'Activation of Lectin-Like Oxidized Low-Density Lipoprotein Receptor-1 Induces Apoptosis in Cultured Neonatal Rat Cardiac Myocytes', *Circulation*, 104(24), pp. 2948-2954.

Jacobs, S. A., Diem, M. D., Luo, J., Teplyakov, A., Obmolova, G., Malia, T., Gilliland, G. L. and O'Neil, K. T. (2012) 'Design of novel FN3 domains with high stability by a consensus sequence approach', *Protein Engineering, Design and Selection*, 25(3), pp. 107-117.

Jain, M., Dhanesha, N., Doddapattar, P., Chorawala, M. R., Nayak, M. K., Cornelissen, A., Guo, L., Finn, A. V., Lentz, S. R. and Chauhan, A. K. (2020) 'Smooth muscle cell-specific fibronectin-EDA mediates phenotypic switching and neointimal hyperplasia', *The Journal of clinical investigation*, 130(1), pp. 295-314.

Jansson, A. M., Aukrust, P., Ueland, T., Smith, C., Omland, T., Hartford, M. and Caidahl, K. (2009) 'Soluble CXCL16 Predicts Long-Term Mortality in Acute Coronary Syndromes', *Circulation*, 119(25), pp. 3181-3188.

Jayewardene, A. F., Gwinn, T., Hancock, D. P., Mavros, Y. and Rooney, K. B. (2014) 'The associations between polymorphisms in the CD36 gene, fat oxidation and cardiovascular disease risk factors in a young adult Australian population: A pilot study', *Obesity Research & Clinical Practice*, 8(6), pp. e618-e621.

Jin, G. (2017) 'The relationship between serum CXCL16 level and carotid vulnerable plaque in patients with ischemic stroke', *Eur Rev Med Pharmacol Sci*, 21(17), pp. 3911-3915.

Kahn, M., Yuldasheva, N., Cubbon, R., Smith, J., Rashid, S., Viswambharan, H., Imrie, H., Abbas, A., Rajwani, A., Aziz, A., Sukumar, P., Gage, M., Kearney, M. and Wheatcroft, S. (2011) 'Insulin Resistance Impairs Circulating Angiogenic

Progenitor Cell Function and Delays Endothelial Regeneration', *Diabetes*, 60, pp. 1295-303.

Kakinuma, T., Yasuda, T., Nakagawa, T., Hiramitsu, T., Akiyoshi, M., Akagi, M., Sawamura, T. and Nakamura, T. (2004) 'Lectin-like oxidized low-density lipoprotein receptor 1 mediates matrix metalloproteinase 3 synthesis enhanced by oxidized low-density lipoprotein in rheumatoid arthritis cartilage', *Arthritis Rheum*, 50(11), pp. 3495-503.

Kakutani, M., Sawamura, T., Chen, M. and Masaki, T. 'Role of LOX-1 in thrombosis'. *Circulation*: LIPPINCOTT WILLIAMS & WILKINS 530 WALNUT ST, PHILADELPHIA, PA 19106-3621 USA, 191-191.

Kaneko, E. and Niwa, R. (2011) 'Optimizing Therapeutic Antibody Function', *BioDrugs*, 25(1), pp. 1-11.

Karunakaran, D., Geoffrion, M., Wei, L., Gan, W., Richards, L., Shangari, P., DeKemp, E. M., Beanlands, R. A., Perisic, L., Maegdefessel, L., Hedin, U., Sad, S., Guo, L., Kolodgie, F. D., Virmani, R., Ruddy, T. and Rayner, K. J. (2016) 'Targeting macrophage necroptosis for therapeutic and diagnostic interventions in atherosclerosis', *Sci Adv*, 2(7), pp. e1600224.

Katakami, N. (2018) 'Mechanism of Development of Atherosclerosis and Cardiovascular Disease in Diabetes Mellitus', *Journal of atherosclerosis and thrombosis*, 25(1), pp. 27-39.

Kataoka, H., Kume, N., Miyamoto, S., Minami, M., Morimoto, M., Hayashida, K., Hashimoto, N. and Kita, T. (2001) 'Oxidized LDL modulates Bax/Bcl-2 through the lectinlike Ox-LDL receptor-1 in vascular smooth muscle cells', *Arterioscler Thromb Vasc Biol*, 21(6), pp. 955-60.

Kataoka, H., Kume, N., Miyamoto, S., Minami, M., Moriwaki, H., Murase, T., Sawamura, T., Masaki, T., Hashimoto, N. and Kita, T. (1999) 'Expression of lectinlike oxidized low-density lipoprotein receptor-1 in human atherosclerotic lesions', *Circulation*, 99(24), pp. 3110-7.

Kataoka, H., Kume, N., Miyamoto, S., Minami, M., Murase, T., Sawamura, T., Masaki, T., Hashimoto, N. and Kita, T. (2000) 'Biosynthesis and post-translational processing of lectin-like oxidized low density lipoprotein receptor-1 (LOX-1). N-linked glycosylation affects cell-surface expression and ligand binding', *J Biol Chem*, 275(9), pp. 6573-9.

Kelley, J. L. and Kruski, A. W. (1986) '[7] Density gradient ultracentrifugation of serum lipoproteins in a swinging bucket rotor', *Methods in Enzymology*: Academic Press, pp. 170-181.

Kelley, J. L., Ozment, T. R., Li, C., Schweitzer, J. B. and Williams, D. L. (2014) 'Scavenger receptor-A (CD204): a two-edged sword in health and disease', *Crit Rev Immunol*, 34(3), pp. 241-61.

Kelly, K. J., Wu, P., Patterson, C. E., Temm, C. and Dominguez, J. H. (2008) 'LOX-1 and inflammation: a new mechanism for renal injury in obesity and diabetes', *Am J Physiol Renal Physiol*, 294(5), pp. F1136-45.

Khan, A. A., Alsaqli, M. A. and Rahmani, A. H. (2018) 'Myeloperoxidase as an Active Disease Biomarker: Recent Biochemical and Pathological Perspectives', *Medical sciences (Basel, Switzerland)*, 6(2), pp. 33.

Kijani, S., Vázquez, A. M., Levin, M., Borén, J. and Fogelstrand, P. (2017) 'Intimal hyperplasia induced by vascular intervention causes lipoprotein retention and accelerated atherosclerosis', *Physiological reports*, 5(14), pp. e13334.

Kobayashi, N., Hata, N., Kume, N., Shinada, T., Tomita, K., Shirakabe, A., Kitamura, M., Nozaki, A., Inami, T., Seino, Y. and Mizuno, K. (2011) 'Soluble lectin-like oxidized LDL receptor-1 and high-sensitivity troponin T as diagnostic biomarkers for acute coronary syndrome. Improved values with combination usage in emergency rooms', *Circ J*, 75(12), pp. 2862-71.

Kobayashi, N., Yoshida, K., Nakano, S., Ohno, T., Honda, T., Tsubokou, Y. and Matsuoka, H. (2006) 'Cardioprotective Mechanisms of Eplerenone on Cardiac Performance and Remodeling in Failing Rat Hearts', *Hypertension*, 47(4), pp. 671-679.

Koide, A., Bailey, C. W., Huang, X. and Koide, S. (1998) 'The fibronectin type III domain as a scaffold for novel binding proteins', *J Mol Biol*, 284(4), pp. 1141-51.

Kojima, Y., Weissman, I. L. and Leeper, N. J. (2017) 'The Role of Efferocytosis in Atherosclerosis', *Circulation*, 135(5), pp. 476-489.

Kristiansen, M., Graversen, J. H., Jacobsen, C., Sonne, O., Hoffman, H. J., Law, S. K. and Moestrup, S. K. (2001) 'Identification of the haemoglobin scavenger receptor', *Nature*, 409(6817), pp. 198-201.

Kronzon, I. and Tunick Paul, A. (2006) 'Aortic Atherosclerotic Disease and Stroke', *Circulation*, 114(1), pp. 63-75.

Kuchibhotla, S., Vanegas, D., Kennedy, D. J., Guy, E., Nimako, G., Morton, R. E. and Febbraio, M. (2008) 'Absence of CD36 protects against atherosclerosis in ApoE knock-out mice with no additional protection provided by absence of scavenger receptor A I/II', *Cardiovasc Res*, 78(1), pp. 185-96.

Kume, N., Mitsuoka, H., Hayashida, K., Tanaka, M., Kominami, G. and Kita, T. (2010) 'Soluble lectin-like oxidized LDL receptor-1 (sLOX-1) as a sensitive and specific biomarker for acute coronary syndrome—Comparison with other biomarkers', *Journal of Cardiology*, 56(2), pp. 159-165.

Kume, N., Murase, T., Moriwaki, H., Aoyama, T., Sawamura, T., Masaki, T. and Kita, T. (1998) 'Inducible Expression of Lectin-like Oxidized LDL Receptor-1 in Vascular Endothelial Cells', *Circulation Research*, 83(3), pp. 322-327.

Kwon, S. H., Li, L., He, Y., Tey, J. C. S., Li, H., Zhuplatov, I., Kim, S. J., Terry, C. M., Blumenthal, D. K., Shiu, Y. T. and Cheung, A. K. (2015) 'Prevention of Venous Neointimal Hyperplasia by a Multitarget Receptor Tyrosine Kinase Inhibitor', *Journal of Vascular Research*, 52(4), pp. 244-256.

Landsberger, M., Zhou, J., Wilk, S., Thaumüller, C., Pavlovic, D., Otto, M., Whynot, S., Hung, O., Murphy, M. F., Cerny, V., Felix, S. B. and Lehmann, C. (2010) 'Inhibition of lectin-like oxidized low-density lipoprotein receptor-1 reduces leukocyte adhesion within the intestinal microcirculation in experimental endotoxemia in rats', *Critical care (London, England)*, 14(6), pp. R223-R223.

Lee, S., Shafe, A. C. and Cowie, M. R. (2011) 'UK stroke incidence, mortality and cardiovascular risk management 1999-2008: time-trend analysis from the General Practice Research Database', *BMJ Open*, 1(2), pp. e000269.

Lee, S.-C., Park, K., Han, J., Lee, J.-j., Kim, H. J., Hong, S., Heu, W., Kim, Y. J., Ha, J.-S., Lee, S.-G., Cheong, H.-K., Jeon, Y. H., Kim, D. and Kim, H.-S. (2012) 'Design of a binding scaffold based on variable lymphocyte receptors of jawless vertebrates by module engineering', *Proceedings of the National Academy of Sciences of the United States of America*, 109(9), pp. 3299-3304.

Lee, Y. T., Lin, H. Y., Chan, Y. W. F., Li, K. H. C., To, O. T. L., Yan, B. P., Liu, T., Li, G., Wong, W. T., Keung, W. and Tse, G. (2017) 'Mouse models of atherosclerosis: a historical perspective and recent advances', *Lipids in health and disease*, 16(1), pp. 12-12.

Leelahavanichkul, A., Bocharov, A. V., Kurlander, R., Baranova, I. N., Vishnyakova, T. G., Souza, A. C., Hu, X., Doi, K., Vaisman, B., Amar, M., Sviridov, D., Chen, Z., Remaley, A. T., Csako, G., Patterson, A. P., Yuen, P. S., Star, R. A. and Eggerman, T. L. (2012) 'Class B scavenger receptor types I and II and CD36 targeting improves sepsis survival and acute outcomes in mice', *J Immunol*, 188(6), pp. 2749-58.

Levitan, I., Volkov, S. and Subbaiah, P. V. (2010) 'Oxidized LDL: diversity, patterns of recognition, and pathophysiology', *Antioxidants & redox signaling*, 13(1), pp. 39-75.

Levy, R. (2000) 'A perspective on monoclonal antibody therapy: where we have been and where we are going', *Semin Hematol*, 37(4 Suppl 7), pp. 43-6.

Li, D., Chen, H., Romeo, F., Sawamura, T., Saldeen, T. and Mehta, J. L. (2002a) 'Statins Modulate Oxidized Low-Density Lipoprotein-Mediated Adhesion Molecule Expression in Human Coronary Artery Endothelial Cells: Role of LOX-1', *Journal of Pharmacology and Experimental Therapeutics*, 302(2), pp. 601.

Li, D. and Mehta, J. L. (2000) 'Antisense to LOX-1 inhibits oxidized LDL-mediated upregulation of monocyte chemoattractant protein-1 and monocyte adhesion to human coronary artery endothelial cells', *Circulation*, 101(25), pp. 2889-95.

Li, D. and Mehta, J. L. (2009) 'Intracellular signaling of LOX-1 in endothelial cell apoptosis', *Circ Res*, 104(5), pp. 566-8.

Li, D., Williams, V., Liu, L., Chen, H., Sawamura, T., Antakli, T. and Mehta, J. L. (2002b) 'LOX-1 inhibition in myocardial ischemia-reperfusion injury: modulation of MMP-1 and inflammation', *American Journal of Physiology-Heart and Circulatory Physiology*, 283(5), pp. H1795-H1801.

Li, D., Williams, V., Liu, L., Chen, H., Sawamura, T., Romeo, F. and Mehta, J. L. (2003) 'Expression of lectin-like oxidized low-density lipoprotein receptors during ischemia-reperfusion and its role in determination of apoptosis and left ventricular dysfunction', *Journal of the American College of Cardiology*, 41(6), pp. 1048-1055.

Li, D.-J., Fu, H., Tong, J., Li, Y.-H., Qu, L.-F., Wang, P. and Shen, F.-M. (2018a) 'Cholinergic anti-inflammatory pathway inhibits neointimal hyperplasia by suppressing inflammation and oxidative stress', *Redox biology*, 15, pp. 22-33.

Li, D. Y., Zhang, Y. C., Philips, M. I., Sawamura, T. and Mehta, J. L. (1999) 'Upregulation of endothelial receptor for oxidized low-density lipoprotein (LOX-1) in cultured human coronary artery endothelial cells by angiotensin II type 1 receptor activation', *Circ Res*, 84(9), pp. 1043-9.

Li, L., Sawamura, T. and Renier, G. (2003) 'Glucose Enhances Endothelial LOX-1 Expression', *Diabetes*, 52(7), pp. 1843.

Li, Q., Zhao, W., Zeng, X. and Hao, Z. (2018b) 'Ursolic Acid Attenuates Atherosclerosis in ApoE(-/-) Mice: Role of LOX-1 Mediated by ROS/NF- κ B Pathway', *Molecules (Basel, Switzerland)*, 23(5), pp. 1101.

Li, Y. and Sousa, R. (2012) 'Expression and purification of E. coli BirA biotin ligase for in vitro biotinylation', *Protein Expression and Purification*, 82(1), pp. 162-167.

Liao, J. K. (2002) 'Beyond lipid lowering: the role of statins in vascular protection', *Int J Cardiol*, 86(1), pp. 5-18.

Libby, P., Ridker, P. M. and Hansson, G. K. (2009) 'Inflammation in atherosclerosis: from pathophysiology to practice', *J Am Coll Cardiol*, 54(23), pp. 2129-38.

Linton, M., Yancey, P. and Davies, S. Jan 2019. The Role of Lipids and Lipoproteins in Atherosclerosis. Endotext.

Liu, M., Tao, G., Liu, Q., Liu, K. and Yang, X. (2017) 'MicroRNA let-7g alleviates atherosclerosis via the targeting of LOX-1 in vitro and in vivo', *International journal of molecular medicine*, 40(1), pp. 57-64.

Liu, Z., Xu, S., Huang, X., Wang, J., Gao, S., Li, H., Zhou, C., Ye, J., Chen, S., Jin, Z.-G. and Liu, P. (2015) 'Cryptotanshinone, an orally bioactive herbal compound from Danshen, attenuates atherosclerosis in apolipoprotein E-deficient mice: role of lectin-like oxidized LDL receptor-1 (LOX-1)', *British journal of pharmacology*, 172(23), pp. 5661-5675.

Lu, J., Mitra, S., Wang, X., Khaidakov, M. and Mehta, J. L. (2011) 'Oxidative stress and lectin-like ox-LDL-receptor LOX-1 in atherogenesis and tumorigenesis', *Antioxid Redox Signal*, 15(8), pp. 2301-33.

Lu, L., Zeng, M., Li, J., Hua, J., Fan, J., Fan, Z., Qiu, D. and Xiao, S. (1999) 'Effects of Kupffer cells stimulated by triglyceride and very low-density lipoprotein on proliferation of rat hepatic stellate cells', *Chin Med J (Engl)*, 112(4), pp. 325-9.

Lusis, A. J. (2000) 'Atherosclerosis', *Nature*, 407(6801), pp. 233-241.

Ma, L., Liu, X., Zhao, Y., Chen, B., Li, X. and Qi, R. (2013) 'Ginkgolide B reduces LOX-1 expression by inhibiting Akt phosphorylation and increasing Sirt1 expression in oxidized LDL-stimulated human umbilical vein endothelial cells', *PloS one*, 8(9), pp. e74769-e74769.

Ma, Z., Jin, X., He, L. and Wang, Y. (2016) 'CXCL16 regulates renal injury and fibrosis in experimental renal artery stenosis', *Am J Physiol Heart Circ Physiol*, 311(3), pp. H815-21.

Mango, R., Clementi, F., Borgiani, P., Forleo, G. B., Federici, M., Contino, G., Giardina, E., Garza, L., Fahdi, I. E., Lauro, R., Mehta, J. L., Novelli, G. and Romeo, F. (2003) 'Association of single nucleotide polymorphisms in the oxidised LDL receptor 1 (OLR1) gene in patients with acute myocardial infarction', *Journal of medical genetics*, 40(12), pp. 933-936.

Mango, R., Predazzi, I. M., Romeo, F. and Novelli, G. (2011) 'LOX-1/LOXIN: the yin/yang of atherosclerosis', *Cardiovasc Drugs Ther*, 25(5), pp. 489-94.

Manning-Tobin, J. J., Moore, K. J., Seimon, T. A., Bell, S. A., Sharuk, M., Alvarez-Leite, J. I., de Winther, M. P., Tabas, I. and Freeman, M. W. (2009) 'Loss of SR-A and CD36 activity reduces atherosclerotic lesion complexity without abrogating foam cell formation in hyperlipidemic mice', *Arterioscler Thromb Vasc Biol*, 29(1), pp. 19-26.

Marchesini, G. and Marzocchi, R. (2007) 'Metabolic syndrome and NASH', *Clin Liver Dis*, 11(1), pp. 105-17, ix.

Marcovecchio, P. M., Thomas, G. D., Mikulski, Z., Ehinger, E., Mueller, K. A. L., Blatchley, A., Wu, R., Miller, Y. I., Nguyen, A. T., Taylor, A. M., McNamara, C. A., Ley, K. and Hedrick, C. C. (2017) 'Scavenger Receptor CD36 Directs Nonclassical Monocyte Patrolling Along the Endothelium During Early Atherogenesis', *Arterioscler Thromb Vasc Biol*, 37(11), pp. 2043-2052.

Marleau, S., Harb, D., Bujold, K., Avallone, R., Iken, K., Wang, Y., Demers, A., Sirois, M. G., Febbraio, M., Silverstein, R. L., Tremblay, A. and Ong, H. (2005) 'EP 80317, a ligand of the CD36 scavenger receptor, protects apolipoprotein E-deficient mice from developing atherosclerotic lesions', *The FASEB Journal*, 19(13), pp. 1869-1871.

Martin, H. L., Bedford, R., Heseltine, S. J., Tang, A. A., Haza, K. Z., Rao, A., McPherson, M. J. and Tomlinson, D. C. (2018) 'Non-immunoglobulin scaffold

proteins: Precision tools for studying protein-protein interactions in cancer', *New Biotechnology*, 45, pp. 28-35.

Mashima, R. and Okuyama, T. (2015) 'The role of lipoxygenases in pathophysiology; new insights and future perspectives', *Redox Biology*, 6, pp. 297-310.

Matloubian, M., David, A., Engel, S., Ryan, J. E. and Cyster, J. G. (2000) 'A transmembrane CXC chemokine is a ligand for HIV-coreceptor Bonzo', *Nat Immunol*, 1(4), pp. 298-304.

Matsumoto, A., Naito, M., Itakura, H., Ikemoto, S., Asaoka, H., Hayakawa, I., Kanamori, H., Aburatani, H., Takaku, F. and Suzuki, H. (1990) 'Human macrophage scavenger receptors: primary structure, expression, and localization in atherosclerotic lesions', *Proceedings of the National Academy of Sciences of the United States of America*, 87(23), pp. 9133-9137.

Matsushita, N., Kashiwagi, M., Wait, R., Nagayoshi, R., Nakamura, M., Matsuda, T., Hogger, P., Guyre, P. M., Nagase, H. and Matsuyama, T. (2002) 'Elevated levels of soluble CD163 in sera and fluids from rheumatoid arthritis patients and inhibition of the shedding of CD163 by TIMP-3', *Clin Exp Immunol*, 130(1), pp. 156-61.

Matsuzawa, N., Takamura, T., Kurita, S., Misu, H., Ota, T., Ando, H., Yokoyama, M., Honda, M., Zen, Y., Nakanuma, Y., Miyamoto, K.-i. and Kaneko, S. (2007) 'Lipid-induced oxidative stress causes steatohepatitis in mice fed an atherogenic diet', *Hepatology*, 46(5), pp. 1392-1403.

McDonald, R. A., Hata, A., MacLean, M. R., Morrell, N. W. and Baker, A. H. (2012) 'MicroRNA and vascular remodelling in acute vascular injury and pulmonary vascular remodelling', *Cardiovascular research*, 93(4), pp. 594-604.

McMonagle, M. P. (2020) 'The quest for effective pharmacological suppression of neointimal hyperplasia', *Curr Probl Surg*, 57(8), pp. 100807.

McNally, J. S., Davis, M. E., Giddens, D. P., Saha, A., Hwang, J., Dikalov, S., Jo, H. and Harrison, D. G. (2003) 'Role of xanthine oxidoreductase and NAD(P)H

oxidase in endothelial superoxide production in response to oscillatory shear stress', *Am J Physiol Heart Circ Physiol*, 285(6), pp. H2290-7.

Mehta Jawahar, L., Sanada, N., Hu Chang, P., Chen, J., Dandapat, A., Sugawara, F., Satoh, H., Inoue, K., Kawase, Y., Jishage, K.-i., Suzuki, H., Takeya, M., Schnackenberg, L., Beger, R., Hermonat Paul, L., Thomas, M. and Sawamura, T. (2007) 'Deletion of LOX-1 Reduces Atherogenesis in LDLR Knockout Mice Fed High Cholesterol Diet', *Circulation Research*, 100(11), pp. 1634-1642.

Mehta, J. L., Li, D. Y., Chen, H. J., Joseph, J. and Romeo, F. (2001) 'Inhibition of LOX-1 by Statins May Relate to Upregulation of eNOS', *Biochemical and Biophysical Research Communications*, 289(4), pp. 857-861.

Michowitz, Y., Kisil, S., Guzner-Gur, H., Rubinstein, A., Wexler, D., Sheps, D., Keren, G. and George, J. (2008) 'Usefulness of serum myeloperoxidase in prediction of mortality in patients with severe heart failure', *Isr Med Assoc J*, 10(12), pp. 884-8.

Minami, M., Kume, N., Shimaoka, T., Kataoka, H., Hayashida, K., Akiyama, Y., Nagata, I., Ando, K., Nobuyoshi, M., Hanyuu, M., Komeda, M., Yonehara, S. and Kita, T. (2001) 'Expression of SR-PSOX, a Novel Cell-Surface Scavenger Receptor for Phosphatidylserine and Oxidized LDL in Human Atherosclerotic Lesions', *Arteriosclerosis, Thrombosis, and Vascular Biology*, 21(11), pp. 1796-1800.

Misaka, T., Suzuki, S., Sakamoto, N., Yamaki, T., Sugimoto, K., Kunii, H., Nakazato, K., Saitoh, S.-i., Sawamura, T., Ishibashi, T. and Takeishi, Y. (2014) 'Significance of soluble lectin-like oxidized LDL receptor-1 levels in systemic and coronary circulation in acute coronary syndrome', *BioMed research international*, 2014, pp. 649185-649185.

Mitsuoka, H., Toyohara, M., Kume, N., Hayashida, K., Jinnai, T., Tanaka, M. and Kita, T. (2009) 'Circulating Soluble SR-PSOX/CXCL16 as a Biomarker for Acute Coronary Syndrome -Comparison with High-Sensitivity C-Reactive Protein', *Journal of Atherosclerosis and Thrombosis*, 16(5), pp. 586-593.

Morawietz, H., Rueckschloss, U., Niemann, B., Duerrschmidt, N., Galle, J., Hakim, K., Zerkowski, H. R., Sawamura, T. and Holtz, J. (1999) 'Angiotensin II induces LOX-1, the human endothelial receptor for oxidized low-density lipoprotein', *Circulation*, 100(9), pp. 899-902.

Morini, E., Rizzacasa, B., Pucci, S., Polidoro, C., Ferrè, F., Caporossi, D., Helmer Citterich, M., Novelli, G. and Amati, F. (2016) 'The human rs1050286 polymorphism alters LOX-1 expression through modifying miR-24 binding', *Journal of cellular and molecular medicine*, 20(1), pp. 181-187.

Mukhopadhyay, R. (2013) 'Mouse models of atherosclerosis: explaining critical roles of lipid metabolism and inflammation', *J Appl Genet*, 54(2), pp. 185-92.

Murase, T., Kume, N., Korenaga, R., Ando, J., Sawamura, T., Masaki, T. and Kita, T. (1998) 'Fluid Shear Stress Transcriptionally Induces Lectin-like Oxidized LDL Receptor-1 in Vascular Endothelial Cells', *Circulation Research*, 83(3), pp. 328-333.

Murdocca, M., Mango, R., Pucci, S., Biocca, S., Testa, B., Capuano, R., Paolesse, R., Sanchez, M., Orlandi, A., di Natale, C., Novelli, G. and Sangiuolo, F. (2016) 'The lectin-like oxidized LDL receptor-1: a new potential molecular target in colorectal cancer', *Oncotarget*, 7(12), pp. 14765-14780.

Muscoli, C., Sacco, I., Alecce, W., Palma, E., Nisticò, R., Costa, N., Clementi, F., Rotiroti, D., Romeo, F., Salvemini, D., Mehta, J. L. and Mollace, V. (2004) 'The Protective Effect of Superoxide Dismutase Mimetic M40401 on Balloon Injury-Related Neointima Formation: Role of the Lectin-Like Oxidized Low-Density Lipoprotein Receptor-1', *Journal of Pharmacology and Experimental Therapeutics*, 311(1), pp. 44-50.

Musso, G., Cassader, M., De Michieli, F., Saba, F., Bo, S. and Gambino, R. (2011) 'Effect of lectin-like oxidized LDL receptor-1 polymorphism on liver disease, glucose homeostasis, and postprandial lipoprotein metabolism in nonalcoholic steatohepatitis', *The American Journal of Clinical Nutrition*, 94(4), pp. 1033-1042.

Mwaikambo, B. R., Yang, C., Ong, H., Chemtob, S. and Hardy, P. (2008) 'Emerging roles for the CD36 scavenger receptor as a potential therapeutic target for corneal neovascularization', *Endocr Metab Immune Disord Drug Targets*, 8(4), pp. 255-72.

Mäkinen, P. I., Lappalainen, J. P., Heinonen, S. E., Leppänen, P., Lähteenvuo, M. T., Aarnio, J. V., Heikkilä, J., Turunen, M. P. and Ylä-Herttuala, S. (2010) 'Silencing of either SR-A or CD36 reduces atherosclerosis in hyperlipidaemic mice and reveals reciprocal upregulation of these receptors', *Cardiovascular Research*, 88(3), pp. 530-538.

Nagai, M., Hirayama, K., Ebihara, I., Higuchi, T., Shimohata, H. and Kobayashi, M. (2016) 'Serum levels of the soluble haemoglobin scavenger receptor CD163 in MPO-ANCA-associated renal vasculitis', *Scand J Rheumatol*, 45(5), pp. 397-403.

Nagase, M., Abe, J., Takahashi, K., Ando, J., Hirose, S. and Fujita, T. (1998) 'Genomic Organization and Regulation of Expression of the Lectin-like Oxidized Low-density Lipoprotein Receptor (LOX-1) Gene', *Journal of Biological Chemistry*, 273(50), pp. 33702-33707.

Nagase, M., Hirose, S., Sawamura, T., Masaki, T. and Fujita, T. (1997) 'Enhanced expression of endothelial oxidized low-density lipoprotein receptor (LOX-1) in hypertensive rats', *Biochemical and biophysical research communications*, 237(3), pp. 496-498.

Nakagami, H. (2017) 'Design of therapeutic vaccines as a novel antibody therapy for cardiovascular diseases', *J Cardiol*, 70(3), pp. 201-205.

Nakamura, K., Yamagishi, S.-i., Adachi, H., Kurita-Nakamura, Y., Matsui, T., Yoshida, T., Sato, A. and Imaizumi, T. (2007) 'Elevation of soluble form of receptor for advanced glycation end products (sRAGE) in diabetic subjects with coronary artery disease', *Diabetes/Metabolism Research and Reviews*, 23(5), pp. 368-371.

Nakano, A., Inoue, N., Sato, Y., Nishimichi, N., Takikawa, K., Fujita, Y., Kakino, A., Otsui, K., Yamaguchi, S., Matsuda, H. and Sawamura, T. (2010) 'LOX-1 mediates vascular lipid retention under hypertensive state', *J Hypertens*, 28(6), pp. 1273-80.

Nakashima, Y., Plump, A. S., Raines, E. W., Breslow, J. L. and Ross, R. (1994) 'ApoE-deficient mice develop lesions of all phases of atherosclerosis throughout the arterial tree', *Arterioscler Thromb*, 14(1), pp. 133-40.

Nakayama, M., Kudoh, T., Kaikita, K., Yoshimura, M., Oshima, S., Miyamoto, Y., Takeya, M. and Ogawa, H. (2008) 'Class A macrophage scavenger receptor gene expression levels in peripheral blood mononuclear cells specifically increase in patients with acute coronary syndrome', *Atherosclerosis*, 198(2), pp. 426-433.

Nathan, C. and Ding, A. (2010) 'Nonresolving inflammation', *Cell*, 140(6), pp. 871-82.

Nicholson, A. C., Han, J., Febbraio, M., Silverstein, R. L. and Hajjar, D. P. (2001) 'Role of CD36, the macrophage class B scavenger receptor, in atherosclerosis', *Ann N Y Acad Sci*, 947, pp. 224-8.

Nie, S., Zhang, J., Martinez-Zaguilan, R., Sennoune, S., Hossen, M. N., Lichtenstein, A. H., Cao, J., Meyerrose, G. E., Paone, R., Soontrapa, S., Fan, Z. and Wang, S. (2015) 'Detection of atherosclerotic lesions and intimal macrophages using CD36-targeted nanovesicles', *J Control Release*, 220(Pt A), pp. 61-70.

Nielsen, M. J., Madsen, M., Moller, H. J. and Moestrup, S. K. (2006) 'The macrophage scavenger receptor CD163: endocytic properties of cytoplasmic tail variants', *J Leukoc Biol*, 79(4), pp. 837-45.

Nin, J. W. M., Jorsal, A., Ferreira, I., Schalkwijk, C. G., Prins, M. H., Parving, H.-H., Tarnow, L., Rossing, P. and Stehouwer, C. D. A. (2010) 'Higher Plasma Soluble Receptor for Advanced Glycation End Products (sRAGE) Levels Are Associated With Incident Cardiovascular Disease and All-Cause Mortality in Type 1 Diabetes', *A 12-Year Follow-Up Study*, 59(8), pp. 2027-2032.

Nixon, A. E. and Wood, C. R. (2006) 'Engineered protein inhibitors of proteases', *Curr Opin Drug Discov Devel*, 9(2), pp. 261-8.

Nomura, J., Busso, N., Ives, A., Matsui, C., Tsujimoto, S., Shirakura, T., Tamura, M., Kobayashi, T., So, A. and Yamanaka, Y. (2014) 'Xanthine oxidase inhibition by febuxostat attenuates experimental atherosclerosis in mice', *Sci Rep*, 4, pp. 4554.

Nord, K., Nilsson, J., Nilsson, B., Uhlen, M. and Nygren, P. A. (1995) 'A combinatorial library of an alpha-helical bacterial receptor domain', *Protein Eng*, 8(6), pp. 601-8.

Ogura, S., Kakino, A., Sato, Y., Fujita, Y., Iwamoto, S., Otsui, K., Yoshimoto, R. and Sawamura, T. (2009) 'Lox-1: the multifunctional receptor underlying cardiovascular dysfunction', *Circ J*, 73(11), pp. 1993-9.

Ohta, K., Nagase, H., Suzukawa, M. and Ohta, S. (2017) 'Antibody therapy for the management of severe asthma with eosinophilic inflammation', *Int Immunol*, 29(7), pp. 337-343.

Ozturk, O., Colak, Y., Senates, E., Yilmaz, Y., Ulasoglu, C., Doganay, L., Ozkanli, S., Oltulu, Y. M., Coskunpinar, E. and Tuncer, I. (2015) 'Increased serum soluble lectin-like oxidized low-density lipoprotein receptor-1 levels in patients with biopsy-proven nonalcoholic fatty liver disease', *World journal of gastroenterology*, 21(26), pp. 8096-8102.

Pahk, K., Noh, H., Joung, C., Jang, M., Song, H. Y., Kim, K. W., Han, K., Hwang, J.-I., Kim, S. and Kim, W.-K. (2019) 'A novel CD147 inhibitor, SP-8356, reduces neointimal hyperplasia and arterial stiffness in a rat model of partial carotid artery ligation', *Journal of Translational Medicine*, 17(1), pp. 274.

Park, L., Raman, K. G., Lee, K. J., Lu, Y., Ferran, L. J., Chow, W. S., Stern, D. and Schmidt, A. M. (1998) 'Suppression of accelerated diabetic atherosclerosis by the soluble receptor for advanced glycation endproducts', *Nature Medicine*, 4(9), pp. 1025-1031.

Patetsios, P., Song, M., Shutze, W. P., Pappas, C., Rodino, W., Ramirez, J. A. and Panetta, T. F. (2001) 'Identification of uric acid and xanthine oxidase in atherosclerotic plaque', *Am J Cardiol*, 88(2), pp. 188-91, a6.

Pearce, S. F. A., Roy, P., Nicholson, A. C., Hajjar, D. P., Febbraio, M. and Silverstein, R. L. (1998) 'Recombinant Glutathione S-Transferase/CD36 Fusion Proteins Define an Oxidized Low Density Lipoprotein-binding Domain', *Journal of Biological Chemistry*, 273(52), pp. 34875-34881.

Percie du Sert, N., Ahluwalia, A., Alam, S., Avey, M. T., Baker, M., Browne, W. J., Clark, A., Cuthill, I. C., Dirnagl, U., Emerson, M., Garner, P., Holgate, S. T., Howells, D. W., Hurst, V., Karp, N. A., Lazic, S. E., Lidster, K., MacCallum, C. J., Macleod, M., Pearl, E. J., Petersen, O. H., Rawle, F., Reynolds, P., Rooney, K., Sena, E. S., Silberberg, S. D., Steckler, T. and Würbel, H. (2020) 'Reporting animal research: Explanation and elaboration for the ARRIVE guidelines 2.0', *PLOS Biology*, 18(7), pp. e3000411.

Plüddemann, A., Mukhopadhyay, S. and Gordon, S. (2011) 'Innate immunity to intracellular pathogens: macrophage receptors and responses to microbial entry', *Immunol Rev*, 240(1), pp. 11-24.

Plump, A. S., Smith, J. D., Hayek, T., Aalto-Setälä, K., Walsh, A., Verstuyft, J. G., Rubin, E. M. and Breslow, J. L. (1992) 'Severe hypercholesterolemia and atherosclerosis in apolipoprotein E-deficient mice created by homologous recombination in ES cells', *Cell*, 71(2), pp. 343-53.

Plüddemann, A., Neyen, C. and Gordon, S. (2007) 'Macrophage scavenger receptors and host-derived ligands', *Methods*, 43(3), pp. 207-17.

Politz, O., Gratchev, A., McCourt, P. A., Schledzewski, K., Guillot, P., Johansson, S., Svineng, G., Franke, P., Kannicht, C., Kzhyshkowska, J., Longati, P., Velten, F. W. and Goerdt, S. (2002) 'Stabilin-1 and -2 constitute a novel family of fasciclin-like hyaluronan receptor homologues', *Biochem J*, 362(Pt 1), pp. 155-64.

Prabhudas, M., Bowdish, D., Drickamer, K., Febbraio, M., Herz, J., Kobzik, L., Krieger, M., Loike, J., Means, T. K., Moestrup, S. K., Post, S., Sawamura, T.,

Silverstein, S., Wang, X. Y. and El Khoury, J. (2014) 'Standardizing scavenger receptor nomenclature', *J Immunol*, 192(5), pp. 1997-2006.

Puccetti, L., Pasqui, A. L., Bruni, F., Pastorelli, M., Ciani, F., Palazzuoli, A., Pontani, A., Ghezzi, A. and Auteri, A. (2007) 'Lectin-like oxidized-LDL receptor-1 (LOX-1) polymorphisms influence cardiovascular events rate during statin treatment', *International Journal of Cardiology*, 119(1), pp. 41-47.

Qin, L., Kim, E., Ratan, R., Lee, F. S. and Cho, S. (2011) 'Genetic Variant of BDNF (Val66Met) Polymorphism Attenuates Stroke-Induced Angiogenic Responses by Enhancing Anti-Angiogenic Mediator CD36 Expression', *The Journal of Neuroscience*, 31(2), pp. 775.

Rafiq, N. and Younossi, Z. M. (2009) 'Nonalcoholic fatty liver disease: a practical approach to evaluation and management', *Clin Liver Dis*, 13(2), pp. 249-66.

Raggi, P., Genest, J., Giles, J. T., Rayner, K. J., Dwivedi, G., Beanlands, R. S. and Gupta, M. (2018) 'Role of inflammation in the pathogenesis of atherosclerosis and therapeutic interventions', *Atherosclerosis*, 276, pp. 98-108.

Ramasamy, R., Yan, S. F. and Schmidt, A. M. (2005) 'The RAGE axis and endothelial dysfunction: maladaptive roles in the diabetic vasculature and beyond', *Trends Cardiovasc Med*, 15(7), pp. 237-43.

Ramasamy, R., Yan, S. F. and Schmidt, A. M. (2009) 'RAGE: therapeutic target and biomarker of the inflammatory response--the evidence mounts', *J Leukoc Biol*, 86(3), pp. 505-12.

Rasouli, N., Yao-Borengasser, A., Varma, V., Spencer, H. J., McGehee, R. E., Jr., Peterson, C. A., Mehta, J. L. and Kern, P. A. (2009) 'Association of scavenger receptors in adipose tissue with insulin resistance in nondiabetic humans', *Arterioscler Thromb Vasc Biol*, 29(9), pp. 1328-35.

Rayner, K. J. (2017) 'Cell Death in the Vessel Wall: The Good, the Bad, the Ugly', *Arterioscler Thromb Vasc Biol*, 37(7), pp. e75-e81.

Ribbens, C., Martin y Porras, M., Franchimont, N., Kaiser, M. J., Jaspar, J. M., Damas, P., Houssiau, F. A. and Malaise, M. G. (2002) 'Increased matrix metalloproteinase-3 serum levels in rheumatic diseases: relationship with synovitis and steroid treatment', *Ann Rheum Dis*, 61(2), pp. 161-6.

Rosano, G. L. and Ceccarelli, E. A. (2014) 'Recombinant protein expression in *Escherichia coli*: advances and challenges', *Frontiers in microbiology*, 5, pp. 172-172.

Ryoo, S., Bhunia, A., Chang, F., Shoukas, A., Berkowitz, D. E. and Romer, L. H. (2011) 'OxLDL-dependent activation of arginase II is dependent on the LOX-1 receptor and downstream RhoA signaling', *Atherosclerosis*, 214(2), pp. 279-87.

Santilli, F., Bucciarelli, L., Noto, D., Cefalù, A. B., Davì, V., Ferrante, E., Pettinella, C., Averna, M. R., Ciabattini, G. and Davì, G. (2007) 'Decreased plasma soluble RAGE in patients with hypercholesterolemia: Effects of statins', *Free Radical Biology and Medicine*, 43(9), pp. 1255-1262.

Sawamura, T., Kume, N., Aoyama, T., Moriwaki, H., Hoshikawa, H., Aiba, Y., Tanaka, T., Miwa, S., Katsura, Y., Kita, T. and Masaki, T. (1997) 'An endothelial receptor for oxidized low-density lipoprotein', *Nature*, 386(6620), pp. 73-7.

Schaeffer, D. F., Riazzy, M., Parhar, K. S., Chen, J. H., Duronio, V., Sawamura, T. and Steinbrecher, U. P. (2009) 'LOX-1 augments oxLDL uptake by lysoPC-stimulated murine macrophages but is not required for oxLDL clearance from plasma', *Journal of lipid research*, 50(8), pp. 1676-1684.

Schlehuber, S. and Skerra, A. (2005) 'Anticalins as an alternative to antibody technology', *Expert Opin Biol Ther*, 5(11), pp. 1453-62.

Seizer, P., Schiemann, S., Merz, T., Daub, K., Bigalke, B., Stellos, K., Muller, I., Stockle, C., Muller, K., Gawaz, M. and May, A. E. (2010) 'CD36 and macrophage scavenger receptors modulate foam cell formation via inhibition of lipid-laden platelet phagocytosis', *Semin Thromb Hemost*, 36(2), pp. 157-62.

Shah, A. S. V., Anand, A., Strachan, F. E., Ferry, A. V., Lee, K. K., Chapman, A. R., Sandeman, D., Stables, C. L., Adamson, P. D., Andrews, J. P. M., Anwar, M.

S., Hung, J., Moss, A. J., O'Brien, R., Berry, C., Findlay, I., Walker, S., Cruickshank, A., Reid, A., Gray, A., Collinson, P. O., Apple, F. S., McAllister, D. A., Maguire, D., Fox, K. A. A., Newby, D. E., Tuck, C., Harkess, R., Parker, R. A., Keerie, C., Weir, C. J., Mills, N. L., Marshall, L., Stewart, S. D., Fujisawa, T., Vallejos, C. A., Tsanas, A., Hautvast, M., McPherson, J., McKinlay, L., Malo, J., Fischbacher, C. M., Croal, B. L., Leslie, S. J., Walker, A., Wackett, T., Armstrong, R., Stirling, L., MacDonald, C., Sadat, I., Finlay, F., Charles, H., Linksted, P., Young, S., Alexander, B. and Duncan, C. (2018) 'High-sensitivity troponin in the evaluation of patients with suspected acute coronary syndrome: a stepped-wedge, cluster-randomised controlled trial', *The Lancet*, 392(10151), pp. 919-928.

Sheedy, F. J., Grebe, A., Rayner, K. J., Kalantari, P., Ramkhalawon, B., Carpenter, S. B., Becker, C. E., Ediriweera, H. N., Mullick, A. E., Golenbock, D. T., Stuart, L. M., Latz, E., Fitzgerald, K. A. and Moore, K. J. (2013) 'CD36 coordinates NLRP3 inflammasome activation by facilitating intracellular nucleation of soluble ligands into particulate ligands in sterile inflammation', *Nat Immunol*, 14(8), pp. 812-20.

Shi, X., Niimi, S., Ohtani, T. and Machida, S. (2001) 'Characterization of residues and sequences of the carbohydrate recognition domain required for cell surface localization and ligand binding of human lectin-like oxidized LDL receptor', *J Cell Sci*, 114(Pt 7), pp. 1273-82.

Shi, Y., Cosentino, F., Camici, G. G., Akhmedov, A., Vanhoutte, P. M., Tanner, F. C. and Luscher, T. F. (2011) 'Oxidized low-density lipoprotein activates p66Shc via lectin-like oxidized low-density lipoprotein receptor-1, protein kinase C-beta, and c-Jun N-terminal kinase kinase in human endothelial cells', *Arterioscler Thromb Vasc Biol*, 31(9), pp. 2090-7.

Singh, T. D., Park, S. Y., Bae, J. S., Yun, Y., Bae, Y. C., Park, R. W. and Kim, I. S. (2010) 'MEGF10 functions as a receptor for the uptake of amyloid-beta', *FEBS Lett*, 584(18), pp. 3936-42.

Skalen, K., Gustafsson, M., Rydberg, E. K., Hulten, L. M., Wiklund, O., Innerarity, T. L. and Boren, J. (2002) 'Subendothelial retention of atherogenic lipoproteins in early atherosclerosis', *Nature*, 417(6890), pp. 750-4.

Skerra, A. (2007) 'Alternative non-antibody scaffolds for molecular recognition', *Current Opinion in Biotechnology*, 18(4), pp. 295-304.

Smith, J. D. and Breslow, J. L. (1997) 'The emergence of mouse models of atherosclerosis and their relevance to clinical research', *Journal of Internal Medicine*, 242(2), pp. 99-109.

Smolina, K., Wright, F. L., Rayner, M. and Goldacre, M. J. (2012) 'Determinants of the decline in mortality from acute myocardial infarction in England between 2002 and 2010: linked national database study', *Bmj*, 344, pp. d8059.

Song, G., Tian, H., Liu, J., Zhang, H., Sun, X. and Qin, S. (2011) 'H2 inhibits TNF- α -induced lectin-like oxidized LDL receptor-1 expression by inhibiting nuclear factor κ B activation in endothelial cells', *Biotechnology Letters*, 33(9), pp. 1715-1722.

Song, L., Lee, C. and Schindler, C. (2011) 'Deletion of the murine scavenger receptor CD68', *Journal of lipid research*, 52(8), pp. 1542-1550.

Sorenson, A. E., Askin, S. P. and Schaeffer, P. M. (2015) 'In-gel detection of biotin-protein conjugates with a green fluorescent streptavidin probe', *Analytical Methods*, 7(5), pp. 2087-2092.

Soro-Paavonen, A., Watson, A. M. D., Li, J., Paavonen, K., Koitka, A., Calkin, A. C., Barit, D., Coughlan, M. T., Drew, B. G., Lancaster, G. I., Thomas, M., Forbes, J. M., Nawroth, P. P., Bierhaus, A., Cooper, M. E. and Jandeleit-Dahm, K. A. (2008) 'Receptor for advanced glycation end products (RAGE) deficiency attenuates the development of atherosclerosis in diabetes', *Diabetes*, 57(9), pp. 2461-2469.

Stamler, J., Wentworth, D. and Neaton, J. D. (1986) 'Is relationship between serum cholesterol and risk of premature death from coronary heart disease

continuous and graded? Findings in 356,222 primary screenees of the Multiple Risk Factor Intervention Trial (MRFIT)', *Jama*, 256(20), pp. 2823-8.

Sternke, M., Tripp, K. W. and Barrick, D. (2019) 'Consensus sequence design as a general strategy to create hyperstable, biologically active proteins', *Proceedings of the National Academy of Sciences*, 116(23), pp. 11275.

Stewart, C. R., Stuart, L. M., Wilkinson, K., van Gils, J. M., Deng, J., Halle, A., Rayner, K. J., Boyer, L., Zhong, R., Frazier, W. A., Lacy-Hulbert, A., El Khoury, J., Golenbock, D. T. and Moore, K. J. (2010) 'CD36 ligands promote sterile inflammation through assembly of a Toll-like receptor 4 and 6 heterodimer', *Nat Immunol*, 11(2), pp. 155-61.

Subbotin, V. M. (2007) 'Analysis of arterial intimal hyperplasia: review and hypothesis', *Theoretical Biology and Medical Modelling*, 4(1), pp. 41.

Sugimoto, K., Ishibashi, T., Sawamura, T., Inoue, N., Kamioka, M., Uekita, H., Ohkawara, H., Sakamoto, T., Sakamoto, N., Okamoto, Y., Takawa, Y., Kakino, A., Fujita, Y., Tanaka, T., Teramoto, T., Maruyama, Y. and Takeishi, Y. (2009) 'LOX-1-MT1-MMP axis is crucial for RhoA and Rac1 activation induced by oxidized low-density lipoprotein in endothelial cells', *Cardiovasc Res*, 84(1), pp. 127-36.

Suzuki, E. and Nakayama, M. (2007) 'The mammalian Ced-1 ortholog MEGF10/KIAA1780 displays a novel adhesion pattern', *Exp Cell Res*, 313(11), pp. 2451-64.

Tabas, I. and Lichtman, A. H. (2017) 'Monocyte-Macrophages and T Cells in Atherosclerosis', *Immunity*, 47(4), pp. 621-634.

Takanabe-Mori, R., Ono, K., Sowa, N., Wada, H., Takaya, T., Horie, T., Satoh-Asahara, N., Shimatsu, A., Fujita, M., Sawamura, T. and Hasegawa, K. (2010) 'Lectin-like oxidized low-density lipoprotein receptor-1 is required for the adipose tissue expression of proinflammatory cytokines in high-fat diet-induced obese mice', *Biochem Biophys Res Commun*, 398(3), pp. 576-80.

Talle, M. A., Rao, P. E., Westberg, E., Allegar, N., Makowski, M., Mittler, R. S. and Goldstein, G. (1983) 'Patterns of antigenic expression on human monocytes as defined by monoclonal antibodies', *Cell Immunol*, 78(1), pp. 83-99.

Tan, K. C., Shiu, S. W., Wong, Y., Leng, L. and Bucala, R. (2008) 'Soluble lectin-like oxidized low density lipoprotein receptor-1 in type 2 diabetes mellitus', *J Lipid Res*, 49(7), pp. 1438-44.

Taye, A., Sawamura, T. and Morawietz, H. (2010) 'Aldosterone augments LOX-1-mediated low-density lipoprotein uptake in human umbilical artery endothelial cells', *Pharmacological Reports*, 62(2), pp. 311-318.

Teupser, D., Mueller, M. A., Koglin, J., Wilfert, W., Ernst, J., von Scheidt, W., Steinbeck, G., Seidel, D. and Thiery, J. (2008) 'CD36 mRNA expression is increased in CD14+ monocytes of patients with coronary heart disease', *Clin Exp Pharmacol Physiol*, 35(5-6), pp. 552-6.

Thakkar, S., Wang, X., Khaidakov, M., Dai, Y., Gokulan, K., Mehta, J. L. and Varughese, K. I. (2015) 'Structure-based Design Targeted at LOX-1, a Receptor for Oxidized Low-Density Lipoprotein', *Scientific reports*, 5, pp. 16740-16740.

Thomas, H., Senkel, S., Erdmann, S., Arndt, T., Turan, G., Klein-Hitpass, L. and Ryffel, G. U. (2004) 'Pattern of genes influenced by conditional expression of the transcription factors HNF6, HNF4alpha and HNF1beta in a pancreatic beta-cell line', *Nucleic acids research*, 32(19), pp. e150-e150.

Tiede, C., Bedford, R., Heseltine, S. J., Smith, G., Wijetunga, I., Ross, R., AlQallaf, D., Roberts, A. P., Balls, A., Curd, A., Hughes, R. E., Martin, H., Needham, S. R., Zanetti-Domingues, L. C., Sadigh, Y., Peacock, T. P., Tang, A. A., Gibson, N., Kyle, H., Platt, G. W., Ingram, N., Taylor, T., Coletta, L. P., Manfield, I., Knowles, M., Bell, S., Esteves, F., Maqbool, A., Prasad, R. K., Drinkhill, M., Bon, R. S., Patel, V., Goodchild, S. A., Martin-Fernandez, M., Owens, R. J., Nettleship, J. E., Webb, M. E., Harrison, M., Lippiat, J. D., Ponnambalam, S., Peckham, M., Smith, A., Ferrigno, P. K., Johnson, M., McPherson, M. J. and Tomlinson, D. C. (2017) 'Affimer proteins are versatile and renewable affinity reagents', *eLife*, 6, pp. e24903.

Tiede, C., Tang, A. A. S., Deacon, S. E., Mandal, U., Nettleship, J. E., Owen, R. L., George, S. E., Harrison, D. J., Owens, R. J., Tomlinson, D. C. and McPherson, M. J. (2014) 'Adhiron: a stable and versatile peptide display scaffold for molecular recognition applications', *Protein engineering, design & selection : PEDS*, 27(5), pp. 145-155.

Tsai, J. Y., Su, K. H., Shyue, S. K., Kou, Y. R., Yu, Y. B., Hsiao, S. H., Chiang, A. N., Wu, Y. L., Ching, L. C. and Lee, T. S. (2010) 'EGb761 ameliorates the formation of foam cells by regulating the expression of SR-A and ABCA1: role of haem oxygenase-1', *Cardiovasc Res*, 88(3), pp. 415-23.

Unal, B., Critchley Julia, A. and Capewell, S. (2004) 'Explaining the Decline in Coronary Heart Disease Mortality in England and Wales Between 1981 and 2000', *Circulation*, 109(9), pp. 1101-1107.

Usui, H. K., Shikata, K., Sasaki, M., Okada, S., Matsuda, M., Shikata, Y., Ogawa, D., Kido, Y., Nagase, R., Yozai, K., Ohga, S., Tone, A., Wada, J., Takeya, M., Horiuchi, S., Kodama, T. and Makino, H. (2007) 'Macrophage Scavenger Receptor-A–Deficient Mice Are Resistant Against Diabetic Nephropathy Through Amelioration of Microinflammation', *Diabetes*, 56(2), pp. 363-372.

VanderLaan Paul, A., Reardon Catherine, A. and Getz Godfrey, S. (2004) 'Site Specificity of Atherosclerosis', *Arteriosclerosis, Thrombosis, and Vascular Biology*, 24(1), pp. 12-22.

Virmani, R., Burke, A. P., Kolodgie, F. D. and Farb, A. (2002) 'Vulnerable plaque: the pathology of unstable coronary lesions', *J Interv Cardiol*, 15(6), pp. 439-46.

von Scheidt, M., Zhao, Y., Kurt, Z., Pan, C., Zeng, L., Yang, X., Schunkert, H. and Lusis, A. J. (2017) 'Applications and Limitations of Mouse Models for Understanding Human Atherosclerosis', *Cell Metab*, 25(2), pp. 248-261.

Walenbergh, S. M. A., Koek, G. H., Bieghe, V. and Shiri-Sverdlov, R. (2013) 'Non-alcoholic steatohepatitis: The role of oxidized low-density lipoproteins', *Journal of Hepatology*, 58(4), pp. 801-810.

Wang, S. Y. and Weiner, G. (2008) 'Complement and cellular cytotoxicity in antibody therapy of cancer', *Expert Opin Biol Ther*, 8(6), pp. 759-68.

Wang, Y. and Liu, Z. P. (2019) 'PCSK9 Inhibitors: Novel Therapeutic Strategies for Lowering LDLCholesterol', *Mini Rev Med Chem*, 19(2), pp. 165-176.

White, C. R., Darley-Usmar, V., Berrington, W. R., McAdams, M., Gore, J. Z., Thompson, J. A., Parks, D. A., Tarpey, M. M. and Freeman, B. A. (1996) 'Circulating plasma xanthine oxidase contributes to vascular dysfunction in hypercholesterolemic rabbits', *Proceedings of the National Academy of Sciences of the United States of America*, 93(16), pp. 8745-8749.

White, S. J., Sala-Newby, G. B. and Newby, A. C. (2011) 'Overexpression of scavenger receptor LOX-1 in endothelial cells promotes atherogenesis in the ApoE^{-/-} mouse model', *Cardiovascular Pathology*, 20(6), pp. 369-373.

Wilkinson, K. and El Khoury, J. (2012) 'Microglial scavenger receptors and their roles in the pathogenesis of Alzheimer's disease', *Int J Alzheimers Dis*, 2012, pp. 489456.

Wohlfart, P., Xu, H., Endlich, A., Habermeier, A., Closs, E. I., Hubschle, T., Mang, C., Strobel, H., Suzuki, T., Kleinert, H., Forstermann, U., Ruetten, H. and Li, H. (2008) 'Antiatherosclerotic effects of small-molecular-weight compounds enhancing endothelial nitric-oxide synthase (eNOS) expression and preventing eNOS uncoupling', *J Pharmacol Exp Ther*, 325(2), pp. 370-9.

Wu, Z., Sawamura, T., Kurdowska, A. K., Ji, H.-L., Idell, S. and Fu, J. (2011) 'LOX-1 deletion improves neutrophil responses, enhances bacterial clearance, and reduces lung injury in a murine polymicrobial sepsis model', *Infection and immunity*, 79(7), pp. 2865-2870.

Wågsäter, D., Olofsson, P. S., Norgren, L., Stenberg, B. and Sirsjö, A. (2004) 'The chemokine and scavenger receptor CXCL16/SR-PSOX is expressed in human vascular smooth muscle cells and is induced by interferon gamma', *Biochem Biophys Res Commun*, 325(4), pp. 1187-93.

Xia, N., Daiber, A., Habermeier, A., Closs, E. I., Thum, T., Spanier, G., Lu, Q., Oelze, M., Torzewski, M., Lackner, K. J., Munzel, T., Forstermann, U. and Li, H. (2010) 'Resveratrol reverses endothelial nitric-oxide synthase uncoupling in apolipoprotein E knockout mice', *J Pharmacol Exp Ther*, 335(1), pp. 149-54.

Xie, C., Kang, J., Chen, J. R., Lazarenko, O. P., Ferguson, M. E., Badger, T. M., Nagarajan, S. and Wu, X. (2011) 'Lowbush blueberries inhibit scavenger receptors CD36 and SR-A expression and attenuate foam cell formation in ApoE-deficient mice', *Food Funct*, 2(10), pp. 588-94.

Xu, L., Wang, Y.-R., Li, P.-C. and Feng, B. (2016) 'Advanced glycation end products increase lipids accumulation in macrophages through upregulation of receptor of advanced glycation end products: increasing uptake, esterification and decreasing efflux of cholesterol', *Lipids in health and disease*, 15(1), pp. 161-161.

Xu, S., Ogura, S., Chen, J., Little, P. J., Moss, J. and Liu, P. (2013) 'LOX-1 in atherosclerosis: biological functions and pharmacological modifiers', *Cellular and molecular life sciences : CMLS*, 70(16), pp. 2859-2872.

Xu, X., Gao, X., Potter Barry, J., Cao, J.-M. and Zhang, C. (2007) 'Anti-LOX-1 Rescues Endothelial Function in Coronary Arterioles in Atherosclerotic ApoE Knockout Mice', *Arteriosclerosis, Thrombosis, and Vascular Biology*, 27(4), pp. 871-877.

Yamanaka, S., Zhang, X. Y., Miura, K., Kim, S. and Iwao, H. (1998) 'The human gene encoding the lectin-type oxidized LDL receptor (OLR1) is a novel member of the natural killer gene complex with a unique expression profile', *Genomics*, 54(2), pp. 191-9.

Yang, H., Chen, S., Tang, Y. and Dai, Y. (2011) 'Interleukin-10 down-regulates oxLDL induced expression of scavenger receptor A and Bak-1 in macrophages derived from THP-1 cells', *Archives of Biochemistry and Biophysics*, 512(1), pp. 30-37.

Yasaka, M., Yamaguchi, T. and Shichiri, M. (1993) 'Distribution of atherosclerosis and risk factors in atherothrombotic occlusion', *Stroke*, 24(2), pp. 206-11.

Yokoi, H. and Yanagita, M. (2016) 'Targeting the fatty acid transport protein CD36, a class B scavenger receptor, in the treatment of renal disease', *Kidney Int*, 89(4), pp. 740-2.

Yoshida, H., Kondratenko, N., Green, S., Steinberg, D. and Quehenberger, O. (1998a) 'Identification of the lectin-like receptor for oxidized low-density lipoprotein in human macrophages and its potential role as a scavenger receptor', *Biochem J*, 334 (Pt 1), pp. 9-13.

Yoshida, H., Quehenberger, O., Kondratenko, N., Green, S. and Steinberg, D. (1998b) 'Minimally oxidized low-density lipoprotein increases expression of scavenger receptor A, CD36, and macroscialin in resident mouse peritoneal macrophages', *Arterioscler Thromb Vasc Biol*, 18(5), pp. 794-802.

Yue, H., Febbraio, M., Klenotic Philip, A., Kennedy David, J., Wu, Y., Chen, S., Gohara Amira, F., Li, O., Belcher, A., Kuang, B., McIntyre Thomas, M., Silverstein Roy, L. and Li, W. (2019) 'CD36 Enhances Vascular Smooth Muscle Cell Proliferation and Development of Neointimal Hyperplasia', *Arteriosclerosis, Thrombosis, and Vascular Biology*, 39(2), pp. 263-275.

Zani, I. A., Stephen, S. L., Mughal, N. A., Russell, D., Homer-Vanniasinkam, S., Wheatcroft, S. B. and Ponnambalam, S. (2015) 'Scavenger receptor structure and function in health and disease', *Cells*, 4(2), pp. 178-201.

Zhou, B., Weigel, J. A., Fauss, L. and Weigel, P. H. (2000) 'Identification of the hyaluronan receptor for endocytosis (HARE)', *J Biol Chem*, 275(48), pp. 37733-41.

Zhou, F., Wang, J., Wang, K., Zhu, X., Pang, R., Li, X., Zhu, G. and Pan, X. (2016) 'Serum CXCL16 as a Novel Biomarker of Coronary Artery Disease in Type 2 Diabetes Mellitus: a Pilot Study', *Ann Clin Lab Sci*, 46(2), pp. 184-9.

Zhou, J., Bai, W., Liu, Q., Cui, J. and Zhang, W. (2018) 'Intermittent Hypoxia Enhances THP-1 Monocyte Adhesion and Chemotaxis and Promotes M1

Macrophage Polarization via RAGE', *BioMed research international*, 2018, pp. 1650456-1650456.

Zhu, G. Y., Zhu, W., Pan, L. Y., Ma, X. J., Yuan, H. T. and Yang, G. (2016) '[Effect of Ginkgo biloba Tablet on the Expression of Scavenger Receptor A of the Aortic Wall in Atherosclerotic Rats]', *Zhongguo Zhong Xi Yi Jie He Za Zhi*, 36(4), pp. 449-53.

Zhu, G. Y., Zhu, X. L., Li, R. T., Liu, T. B., Shang, D. Y. and Zhang, Y. (2007) '[Atorvastatin inhibits scavenger receptor A and monocyte chemoattractant protein-1 expressions in foam cell]', *Zhonghua Xin Xue Guan Bing Za Zhi*, 35(7), pp. 666-9.

Zhu, X., Li, Z., Li, C., Zhang, J., Zou, Z. and Wang, J. (2013) 'Ginkgo biloba extract and Aspirin synergistically attenuate activated platelet-induced ROS production and LOX-1 expression in human coronary artery endothelial cells', *Phytomedicine*, 20(2), pp. 114-119.

Cardiovascular disease statistics 2017. 2017. British Heart Foundation.

Škrlec, K., Štrukelj, B. and Berlec, A. (2015) 'Non-immunoglobulin scaffolds: a focus on their targets', *Trends in Biotechnology*, 33(7), pp. 408-418.

Appendix A: Publications and conference proceedings

Manuscripts in preparation (1):

Gary A Cuthbert, Faheem Shaik, Nadira Yuldasheva, Sreenivasan Ponnambalam, Shervanthi Homer-Vanniasinkam. Scavenger receptors as biomarkers and therapeutic targets in atherosclerosis.

Poster presentations (2):

Gary A Cuthbert, Jonathan de Siqueira, Izma Abdul-Zani, Darren C. Tomlinson, Sreenivasan Ponnambalam, Shervanthi Homer-Vanniasinkam. LOX-1 specific proteins in atherosclerosis. Arteriosclerosis, thrombosis and vascular biology meeting, San Francisco, US. 9th May 2018.

Gary A Cuthbert, Jonathan de Siqueira, Izma Abdul-Zani, Darren C. Tomlinson, Sreenivasan Ponnambalam, Shervanthi Homer-Vanniasinkam. LOX-1 specific proteins in atherosclerosis. North of England Cell Biology meeting, University of Manchester, UK. 12th September 2019.

Oral presentations (1):

Gary A Cuthbert, Nadira Yuldasheva, Darren C Tomlinson, Sreenivasan Ponnambalam, Shervanthi Homer-Vanniasinkam. Targeting the LOX-1 scavenger receptor attenuates atherosclerosis and neointimal hyperplasia in APO-E null transgenic mice. Society of Academic Research Surgery meeting, Royal College of Surgeons Ireland, Dublin, Republic of Ireland. 20th March 2020.

Appendix B: Supplementary figures

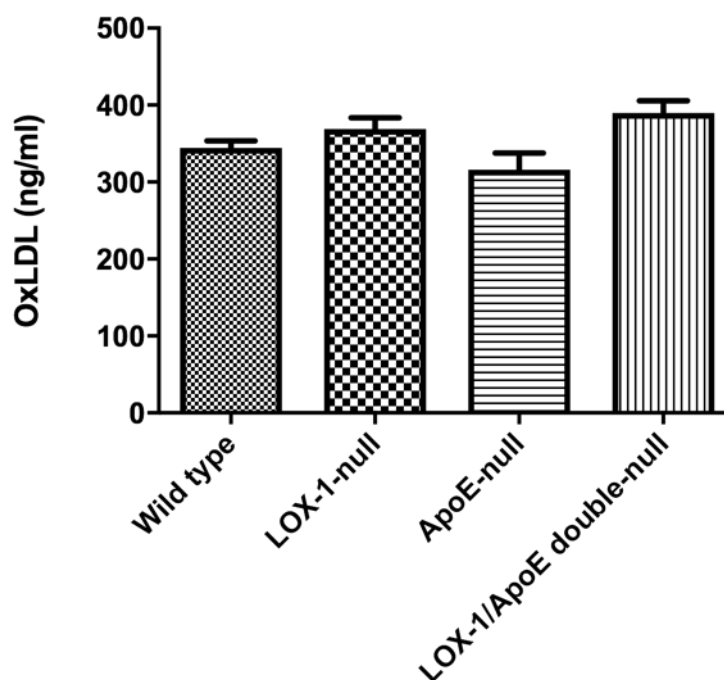


Figure B.1. Serum oxLDL concentrations in transgenic mice fed 12 weeks of WD. Serum oxLDL concentration was significantly raised in APO-E/LOX-1 null mice compared with APO-E null mice ($p= 0.016$). LOX-1 null mice maintained a high concentration of oxLDL, however this was not significantly raised compared with wild type.